NSF Grant ATM-9321361

National Science Foundation

CLIMATOLOGICAL CHARACTERISTICS OF CLOUD-TO-GROUND LIGHTNING ACTIVITY IN THE CONTIGUOUS UNITED STATES

by Bard A. Zajac
Steven A. Rutledge

Colorado State University

DEPARTMENT OF ATMOSPHERIC SCIENCE

PAPER NO. 652

CLIMATOLOGICAL CHARACTERISTICS OF CLOUD-TO-GROUND LIGHTNING ACTIVITY IN THE CONTIGUOUS UNITED STATES

by

Bard A. Zajac

Steven A. Rutledge

Department of Atmospheric Science

Colorado State University

Fort Collins, CO 80523

Research Supported by

National Science Foundation

under Grant ATM-9321361

April 1998

Atmospheric Science Paper No. 652

ABSTRACT

CLIMATOLOGICAL CHARACTERISTICS OF
CLOUD-TO-GROUND LIGHTNING ACTIVITY
IN THE CONTIGUOUS UNITED STATES

We present a national climatology of cloud-to-ground (CG) lightning in the contiguous United States from 1995–97 using data from the National Lightning Detection Network. Annual statistics, cumulative frequency distributions, and annual and daily variations are documented with a series of maps with 100 km spatial resolution. We also identify characteristics of convective events which produced positive CG lightning over two case study areas located in the north-central U.S. and along the Gulf coast. Characteristics of convective events were identified by comparing plots of CG strike locations with national radar summaries.

Surface features such as elevated and depressed terrain, coastlines, and the Gulf Stream appear to control the location, magnitude, daily frequency, and timing of CG lightning activity. Cumulative frequency distributions of daily CG flash count show a similar degree of skewness throughout the contiguous U.S. The majority of cloud-to-ground lightning is produced during summer over all areas in the contiguous U.S. with the exception of the south-central U.S. and the Pacific Coast. Summertime CG lightning

activity over the western and eastern U.S. exhibits a diurnal cycle with a well-defined time of maximum frequency occurring in the afternoon or early evening. Over the central U.S., summertime CG lightning activity is complex with significant longitudinal variations in daily activity.

The production of positive cloud-to-ground lightning over the north-central U.S. is dominated by convective events which occur during summer and during the late afternoon and evening hours. These events comprise thunderstorms, some of which produce predominantly positive CG lightning and are likely severe. Over the Gulf coast, positive CG lightning is produced throughout the year, by diurnally-forced convection during the warm season and by mesoscale convective systems with areally-extensive stratiform regions during the cold season.

ACKNOWLEDGMENTS

We acknowledge Dr. Clara Deser (NCAR) for her assistance in our analysis of diurnal variations and Dr. Thomas McKee for insightful discussion regarding climatological methods. Constructive comments from Dr. Richard Johnson and Stefan Tulich greatly improved the clarity of the text. We are grateful to Paul Hein for his assistance in software development. We thank Larry Carey and Dr. Walt Petersen for stimulating conversations about atmospheric electricity. We also thank Richard Wohlman and Sherry Harrison at the National Aeronautics and Space Administration Global Hydrology Resource Center (NASA-GHRC) for assisting us in obtaining lightning and radar data. This research was supported by the National Science Foundation under grant ATM-93213461.

TABLE OF CONTENTS

LIST OF TABLES

LIST OF FIGURES

CHAPTER 1

INTRODUCTION

1.1 Overview

Convective storms play an important role in human society. In addition to producing beneficial rainfall, convective storms can also produce excessive rainfall and flooding, severe weather (e.g., tornadoes, hail, strong winds), lightning, and thunder. It is important to know how these weather phenomena are distributed in space and time in order to plan for both the beneficial and destructive effects of convective storms. The spatial and temporal distributions of these weather phenomena can also be used to 1) understand what physical processes control the frequency of occurrence of convective storms, 2) forecast for convective storms, and 3) verify output from numerical model which resolve the effects of convective storms. For these reasons, national climatologies of precipitation (e.g., Baldwin 1973; Wallace 1975; Winkler et al. 1988), flash floods (e.g., Maddox et al. 1979), tornadoes (e.g., Kelly et al. 1978), hail and strong winds (e.g., Kelly et al. 1985), cloud-to-ground lightning (e.g., Orville 1991a, 1994; Orville and Silver 1997), and thunder (e.g., Rasmusson 1971; Baldwin 1973; Wallace 1975; Court and Griffiths 1981; Easterling and Robinson 1985) have been developed. These national climatologies have documented significant spatial, annual, and diurnal variations in convective activity over the contiguous U.S. Interestingly, the diurnal variations in cloud-

to-ground (CG) lightning activity have not been documented over the contiguous U.S. For this reason, the goal of this study is to extend the national climatology of cloud-to-ground lightning and document the spatial, annual, *and diurnal variations* in CG lightning activity over the contiguous U.S. Our national climatology of cloud-to-ground lightning will compliment other climatologies of convective activity in the contiguous U.S. and will help to refine our knowledge of convective storms.

We also examine the spatial, annual, and diurnal variations in positive cloud-to-ground lightning activity over the contiguous U.S. Case studies of convective storms have shown that positive CG lightning tends to be produced by 1) dissipating ordinary thunderstorms (i.e., nonsevere thunderstorms; e.g., Pierce 1955, Fuquay 1982), 2) dissipating severe storms (e.g., Orville et al. 1983; Kane 1991), 3) positive strike dominated storms — which are usually severe (PSD storms - Knapp 1994; e.g., Rust et al. 1985; Curran and Rust 1992; Branick and Doswell 1992; Seimon 1993; MacGorman and Burgess 1994; Stolzenburg 1994; Perez et al. 1997; Carey et al. 1997; Carey and Rutledge 1997), and 4) convective and stratiform regions of mesoscale convective systems (MCSs; e.g., Orville et al. 1988; Rutledge and MacGorman 1988; Engholm et al. 1990; Rutledge et al. 1990, Schuur et al. 1991; Holle et al. 1994). Our documentation of the spatial, annual, and diurnal variations in positive CG lightning activity over the contiguous U.S. will provide a national-scale, climatological context for these case studies.

We extend our national analysis of positive cloud-to-ground lightning activity and examine positive CG lightning activity over two areas located in the north-central U.S.

and along the Gulf Coast (i.e., the KFSD and KEOX case study areas, respectively; Fig. 1.1). These two case study areas were chosen for specific reasons. The KFSD case study area was chosen because it is located within a region characterized by a high percentage of positive polarity lightning (Orville 1994; Orville and Silver 1997; Fig. 3.12) and by high positive peak current values (Lyons 1996; Fig. 3.15). Lyons (1996) speculated that the correlation between the percentage of positive polarity lightning and positive peak current may be related to the production of positive CG lightning by stratiform regions of MCSs or to the production of positive CG lightning by PSD storms. We attempt to resolve this issue in our study. The KEOX case study area was chosen because it is located within a region where diurnally-forced convection tends to occur during the warm season and baroclinically-forced convection tends to occur during the cold season (Geertz 1997). We compare positive CG lightning activity over the Gulf Coast between the warm season and the cold season. In our two case studies, we document the annual and diurnal variations in positive CG lightning activity. We also identify characteristics of convective events which produce positive CG lightning over the two case study areas by comparing plots of CG strike locations with national radar summaries.

This study is organized in the following manner. We review climatologies of convective activity in the contiguous U.S. in Sec. 1.2 and discuss the production of positive CG lightning in Sec. 1.3. Data sets and methods used in this study are described in Chapter 2. Our national climatology of cloud-to-ground lightning and our case studies are presented in Chapters 3 and 4, respectively. Conclusions and recommendations for future research are presented in Chapter 5.

1.2 Climatologies of Convective Activity

In this section, we review national and regional climatologies of thunderstorms, precipitation, severe weather, MCSs, and cloud-to-ground lightning.

Baldwin (1973) and Court and Griffiths (1981) examined the daily frequency of thunderstorms over the contiguous U.S. Maps of the annual number of days with thunder show a strong west-to-east gradient in the daily frequency of thunder over the western U.S. and a strong north-to-south gradient in the daily frequency of thunder over the central and eastern U.S.. Maps also show that maxima in the daily frequency of thunder are located over geographical features including the Florida peninsula, the Gulf Coast, and elevated terrain in the western U.S. Court and Griffiths (1981) also examined the annual variations in thunderstorm activity over the contiguous U.S. and found that thunderstorms are most frequent during the warm season (April–September) over most areas in the contiguous U.S. During the cold season (October–March), thunderstorm activity is isolated to the south-central and southeastern U.S.

Rasmusson (1971), Wallace (1975), Easterling and Robinson (1985), and Winkler et al. (1988) examined the diurnal variations in thunderstorm activity during summer (June–August) over the contiguous U.S. Maps of the diurnal cycle of thunderstorm frequency show that thunderstorms are most frequent during the afternoon over the western and eastern U.S. Over the central U.S., thunderstorms occur throughout the day but are more likely to occur at night. Wallace (1975) also examined the diurnal variations

in precipitation and severe weather frequency in the central U.S. Wallace (1975) found that the maximum frequency in severe weather and precipitation occurs in the early evening and in the early morning, respectively.

Kelly et al. (1978) examined the spatial and temporal distributions of tornado reports over the contiguous U.S. and found that tornadoes occur most frequently in the central U.S. during late spring and early summer and during late afternoon and early evening. Kelly et al. (1985) examined the spatial and temporal distributions of large hail (> 19 mm) and strong wind reports over the contiguous U.S. and found that the spatial and temporal distributions of tornadoes, large hail, and strong winds are similar.

Mesoscale convective systems are prolific producers of cloud-to-ground lightning, precipitation, and severe weather in the central U.S. (e.g., Goodman and MacGorman 1986; Fritsch et al. 1986; Houze et al. 1990). For this reason, it has been suggested that MCSs dominate the convective and precipitation climatologies in the central U.S. (Maddox 1980). We review studies of MCSs, beginning with studies of mesoscale convective complexes (MCCs; Maddox 1980). McAnelly and Cotton (1989) examined 122 MCCs and found that MCCs are predominantly nocturnal, west-to-east propagating convective systems; the "average" MCC initiates around 2030 CST (Central Standard Time) over eastern Nebraska, reaches its maximum areal extent around 0145 CST over western Iowa, and terminates around 0700 CST over eastern Iowa. With respect to MCC lifecycle, most severe weather occurs prior to initiation (e.g., Maddox 1980; Goodman and MacGorman 1986; Maddox et al. 1986), CG lightning activity is maximized roughly

two hours after initiation (e.g., Goodman and MacGorman 1986), and the production of precipitation is maximized around the time of maximum areal extent (e.g., McAnelly and Cotton 1989). The timing, propagation, and production of lightning, precipitation, and severe weather by MCCs is consistent with the spatial and diurnal variations in these weather phenomena over the central U.S. (McAnelly and Cotton 1989).

Radar studies have shown that mesoscale convective systems with linear organization are a common mode of convection in the central U.S. (e.g., Bluestein and Jain 1985; Bluestein et al. 1987, Houze et al. 1990; Blanchard 1990). Frequently these systems persist in time such that stratiform regions form behind the line as it propagates; systems with this type of organization are called leading-line/trailing stratiform squall lines (Houze et al. 1990). Convective systems exhibiting no linear organization (with and without stratiform regions) are also observed (Blanchard 1990).

In another radar study, Geertz (1997) developed a climatology of mesoscale convective systems over the southeastern U.S. and found significant differences in the timing of MCSs between the warm season and cold season. The occurrence of MCSs is modulated by the diurnal cycle of solar insolation during the warm season but is not modulated by the diurnal cycle of solar insolation during the cold season. Geertz (1997) also found significant differences in the organization of MCSs between the warm season and cold season. Most cold season MCSs exhibited leading-line/trailing stratiform structure. In contrast, roughly half of the warm season MCSs exhibited leading-line/trailing stratiform structure; the other half exhibited a two-stage lifecycle consisting of

a convective growth phase followed by a stratiform expansion and decay phase. Geertz (1997) attributed these differences to seasonal variations in convective forcing, diurnal-forcing during the warm season and baroclinic-forcing during the cold season.

During the 1970s and 1980s, regional lightning location networks were placed in operation over the contiguous U.S., culminating in the establishment of the National Lightning Detection Network in 1989 (Orville 1991a). Observations from lightning location networks have been analyzed on the regional-scale and on the national-scale. We begin by reviewing regional studies of CG lightning activity. Regional studies have examined the spatial, annual, and/or diurnal variations of CG lightning activity throughout the contiguous U.S. (e.g., Maier et al. 1994, Florida; Lopez and Holle 1986, Colorado and Florida; Reap 1986, western U.S.; Orville et al. 1987, northeastern U.S.; Reap and MacGorman 1989, Oklahoma and Kansas; Biswas and Hobbs 1990, Gulf Stream; Orville 1990b, Gulf Stream; Reap and Orville 1990, northeastern U.S.; Reap 1994, Florida; Watson et al. 1994a,b, Arizona; Clodman and Chisholm 1996, Great Lakes). These studies have shown that variations in elevation, surface type (e.g., land versus water), and surface temperature (e.g., the Gulf Stream) consistently influence the location, magnitude, timing, and daily frequency of CG lightning activity. These studies have also shown that most cloud-to-ground lightning is produced during summer and during the afternoon and early evening.

Reap and MacGorman (1989) examined the relationships between positive CG lightning activity and severe weather over Oklahoma and Kansas and found a significant

correlation between elevated positive flash densities and the occurrence of severe weather. This result has been supported by observations of severe storms which produce predominately positive polarity lightning (e.g., Rust et al. 1985) and by Carey et al. (1997). Carey et al. (1997) examined reports of tornadoes and large hail in the central U.S. during the 1994 and 1995 warm seasons and found that 24% of these reports were accompanied by greater than 50% positive polarity lightning.

National studies of cloud-to-ground lightning activity (e.g., Orville 1991a, 1994; Orville and Silver 1997) have examined spatial and annual variations in CG lightning activity. These national studies, like regional studies, have documented significant spatial variations in CG lightning activity and have shown that most cloud-to-ground lightning is produced during summer.

1.3 Positive Cloud-to-Ground Lightning

Positive cloud-to-ground lightning has been a topic of study for decades primarily because of its anomalous behavior. Positive CG lightning accounts for less than 10% of the total population of CG flashes (Orville 1994; Orville and Silver 1997). In addition, case studies of convective storms have shown that positive CG lightning tends to occur in specific situations which depend upon the type, organization (e.g., convective regions versus stratiform regions), and evolution of convective activity. In this section, we review case studies of positive CG lightning in convective storms. Our review is organized by convective type; we discuss the production of positive CG lightning in ordinary

thunderstorms, severe storms, and in mesoscale convective systems. We do not discuss winter thunderstorms.

Positive cloud-to-ground lightning in ordinary thunderstorms is most frequent during storm dissipation (e.g., Pierce 1955; Fuquay 1982) and is observed to emanate from stratiform regions (or thunderstorm anvil; e.g., Lopez et al. 1990). In addition, positive CG lightning activity tends to lag negative CG lightning activity in time (Petersen et al. 1995). Two hypotheses have been offered to explain these observations: tilted dipole and precipitation unshielding. The tilted dipole hypothesis assumes a normal polarity dipole (positive charge located above negative charge; e.g., Wilson 1920) and states that vertical wind shear causes the positive charge region aloft to be displaced horizontally from the negative charge region below (Brook et al. 1982). This charge structure, called a tilted dipole, increases the likelihood of a positive CG flash because the positive charge region is not shielded from the earth's surface by the lower negative charge center. The precipitation unshielding hypothesis assumes a normal polarity dipole and states that the positive charge region is less shielded from the earth's surface when the negative charge region, associated with convective precipitation, falls out of the storm and is neutralized at the earth's surface (Carey and Rutledge 1997).

The production of positive cloud-to-ground lightning by most severe storms appears to be similar in nature to the production of positive cloud-to-ground lightning by ordinary thunderstorms. Observations have shown that positive flashes emanate from the thunderstorm anvil (e.g., Rust et al. 1981) and that the percentage of positive flashes

increases during storm dissipation (e.g., Orville et al. 1983; Kane 1991). However, recent studies have shown that some hailstorms and some tornadic storms produce predominantly positive polarity lightning for extended periods of time (> 30 minutes) during the mature phase (e.g., Rust et al. 1985; Curran and Rust 1992; Branick and Doswell 1992; Seimon 1993; Knapp 1994, MacGorman and Burgess 1994; Stolzenburg 1994; Perez et al. 1997; Carey et al. 1997; Carey and Rutledge 1997). The studies listed above have shown that positive strike dominated storms 1) tend to form in the afternoon or in the early evening, 2) exhibit positive flash rates greater than 0.01 flashes km^{-2} hr^{-1} for extended periods of time (> 2 hours; Stolzenburg 1994), and 3) frequently switch from producing predominately positive polarity lightning to predominantly negative polarity lightning during the mature phase. In addition, positive strike dominated storms are associated with severe weather outbreaks (MacGorman and Burgess 1994), long track tornadoes (Perez et al. 1997), and F5 tornadoes (Seimon 1993).

Three hypotheses have been proposed to explain the production of positive cloud-to-ground lightning in positive strike dominated storms: tripole, tilted dipole, and precipitation unshielding. The tripole hypothesis assumes that noninductive charging occurs in thunderstorms and states that riming hailstones in wet growth acquire positive charge under specific conditions; these conditions occur in the lower levels of thunderstorms where temperatures are greater than the charge reversal temperature (Williams et al. 1991). The positive charging of hailstones at lower levels produces a lower positive charge region beneath the main negative charge region, or a tripole charge structure. The existence of a lower positive charge region may explain observations of

positive CG strike locations collocated with regions of high radar reflectivity values (> 50 dBZ; e.g., Curran and Rust 1992; Seimon 1993). In contrast to the tripole hypothesis, the tilted dipole hypothesis, as discussed above, predicts that positive flashes will emanate from the upper levels of the thunderstorm. The tilted-dipole hypothesis is consistent with observations of positive CG flashes emanating from the upper levels of severe storms (e.g., Rust et al. 1981). The precipitation unshielding hypothesis, also discussed above, has been used to explain the temporal and spatial negative-correlation between positive CG lightning and convective precipitation in severe storms (e.g., Carey and Rutledge 1997).

Positive cloud-to-ground lightning is produced by convective and stratiform regions in mesoscale convective systems. Positive CG lightning associated with convection regions is often spatially clustered and collocated with intensely convective cells (e.g., Rutledge et al. 1990). This behavior may be associated with the production of positive CG lightning by severe storms within the system (e.g., Nielsen et al. 1994; Toracinta et al. 1996). In contrast, positive CG lightning associated with stratiform regions is not spatially clustered; positive flash densities for stratiform regions are generally less than 0.01 flashes km^{-2} hr^{-1} (Stolzenburg 1994). We should note that stratiform regions tend to produce predominantly positive CG lightning (e.g., Rutledge and MacGorman 1988). This behavior is opposite of what is commonly observed in convective regions; convective regions tend to produce predominantly negative CG lightning (e.g., Holle et al. 1994).

Two signals are associated with the tendency for stratiform regions to produce predominantly positive CG lightning and for convective regions to produce predominantly negative CG lightning. First, the strike locations of positive CG flashes tend to be separated over mesoscale distances (> 50 km) from the strike locations of negative CG flashes. The resulting pattern is called bipolar lightning (Orville et al. 1988). Second, positive CG lightning activity tends to lag negative CG lightning activity in time due to the persistence of stratiform regions relative to convective regions (Rutledge and MacGorman (1988). However, positive CG lightning is not always observed to lag negative CG lightning. The production of positive and negative CG lightning is in phase when significant amounts of positive CG lightning are produced by convective regions (e.g., Rutledge et al. 1990).

Two hypotheses have been offered to explain observations of positive cloud-to-ground lightning in stratiform regions of mesoscale convective systems: charge advection and in-situ charging. The charge advection hypothesis can be considered the steady-state case of the tilted dipole; positive charge aloft, produced by convection, is continually advected into the stratiform region (Rutledge and MacGorman 1988). The in-situ charging hypothesis states that noninductive charging occurs within stratiform regions and produces an inverted-dipole (negative charge located above positive charge) which favors the occurrence of positive CG lightning relative to negative CG lightning (Rutledge et al. 1990). An inverted-dipole is predicted in stratiform regions because ice collisions occur at temperatures above the charge reversal temperature and positive charge is imparted to the

more massive particle. In-situ charging is invoked to explain the occurrence of both positive and negative CG lightning in stratiform regions of MCSs. In a modeling study of MCS electrification, Schuur (1997) showed the importance of both charge advection and in-situ charging.

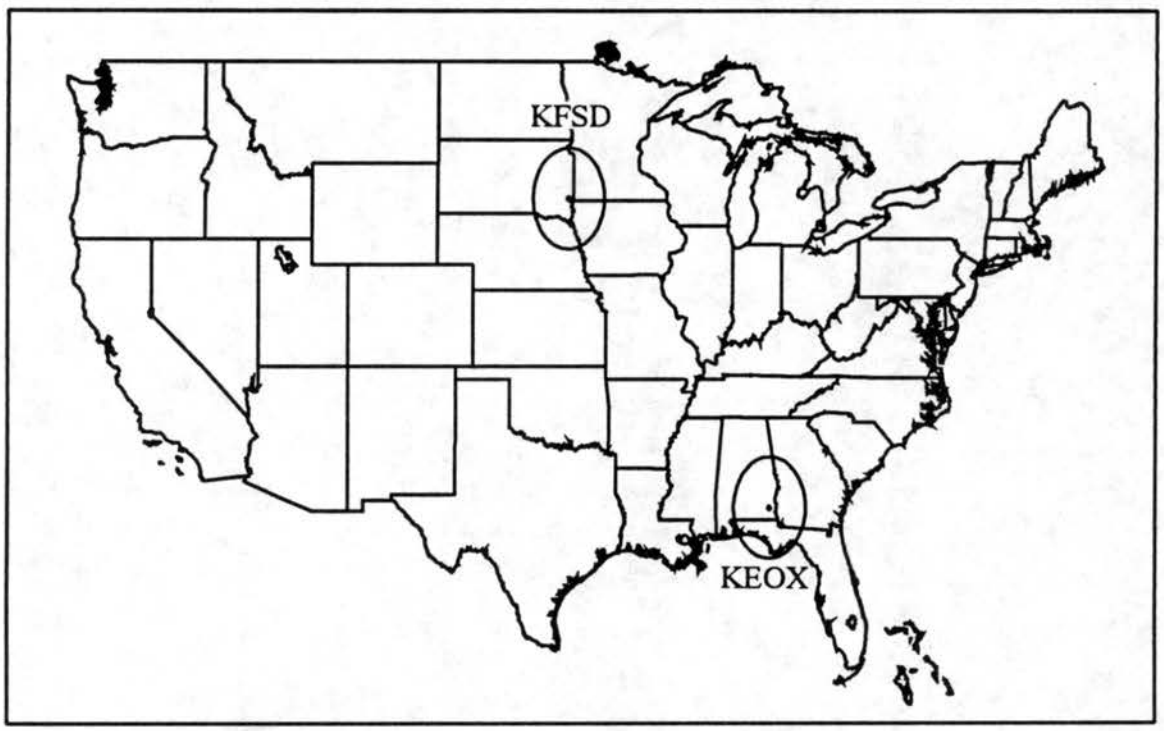

Figure 1.1 Locations of the KFSD and KEOX case study areas. Case study areas are 200–km radius areas centered on WSR-88D radars located in Sioux Falls, South Dakota (designation KFSD) and at Fort Rucker, Alabama (designation KEOX).

CHAPTER 2

DATA AND METHOD

2.1 Overview

In this chapter we discuss the data sets and methods used in this study. We describe the lightning data and radar data used in this study in Secs. 2.2 and 2.3, respectively. Methods used in our national climatology of cloud-to-ground lightning and in our case studies are discussed in Secs. 2.4 and 2.5, respectively.

2.2 Lightning Data

The lightning data used in this study is produced by the National Lightning Detection Network (NLDN). The NLDN is a lightning location network which records the time, location, polarity, peak signal strength, and multiplicity (number of return strokes per CG flash) of CG flashes detected over the contiguous U.S. (Cummins et al. 1995, 1996). The NLDN comprises a network of 105 electromagnetic sensors (Fig. 2.1), a satellite communication system, and a central processor. Sensors are antennae and microprocessor systems with sufficient signal processing capability to identify electromagnetic waveforms associated with cloud-to-ground lightning. The NLDN uses two types of sensors: time-of-arrival sensors (LPATS sensors) and time-of-arrival and

direction-finding sensors (IMPACT sensors). LPATS sensors provide timing information while IMPACT sensors provide timing and azimuth information. The number of LPATS sensors and the number of IMPACT sensors are roughly equal (Fig. 2.1). Salient information from each sensor is transmitted to a central processor via a two-way satellite communication system. The central processor uses a lightning location method to compute the time and location of each CG flash. This method requires that there are more independent observations of time and/or azimuth than there are variables to estimate (i.e., time, latitude, longitude; Cummins et al. 1995, 1996). Thus, a CG flash must be identified by a minimum of two sensors (i.e., two IMPACT sensors) for it to be located by the network. The central processor also computes the polarity, peak signal strength, and multiplicity of CG flashes.

Peak signal strength is an estimate of the range-normalized peak signal strength of the first return stroke of a CG flash. Peak signal strength is determined from measurements of peak signal strength from all sensors detecting a CG flash. These measurements, along with the location of the CG flash, are used to calculate the peak signal strength normalized to a distance of 100 km (Lopez et al. 1991). This range-normalized signal strength is expressed in uncalibrated units of magnetic radiation called LLP units. We converted peak signal strength to peak current using the following equation published in Orville (1991b):

$$I_{cur} = 0.2 \bullet I_{sig} \tag{2.1}$$

where I_{cur} is peak current in units of kiloamps (kA) and I_{sig} is peak signal strength in LLP units.

The National Lightning Detection Network has undergone a series of upgrades since it became operational in 1989. The most recent network upgrade was performed in 1995 in order to 1) increase the location accuracy of CG flashes and 2) increase the detection efficiency of low peak current CG flashes, down to 5 kA (see Cummins et al. 1995 for a detailed discussion). The 1995 NLDN upgrade consisted of a network reconfiguration, sensor modifications, and central processing modifications. The upgrade improved network performance. Location accuracy increased by a factor of 4 to 8, resulting in an average accuracy of 500 meters, and network-wide detection efficiency increased from 65–80% to 80–90% (Cummins et al. 1995). Figure 2.2 shows that network detection efficiency after the upgrade is greater than 80% over most areas in the contiguous U.S. However, detection efficiency decreases rapidly towards the continental borders. Note that no distinction is made between the detection efficiency of positive CG lightning and negative CG lightning.

While it appears that the 1995 NLDN upgrade improved network performance, results from our research suggest that the 1995 NLDN upgrade may have introduced problems with observations of positive CG lightning. Our results indicate that a large number of low peak current positive CG flashes are now being detected over localized areas in the southeastern U.S. We suspect that these positive CG flashes may be false

detections of intracloud lightning based on previous research of postive CG lightning (e.g., MacGorman and Taylor 1989; Lopez et al. 1991). Fortunately, the main results of this study are not affected by the detection of low peak current positive CG flashes. We discuss the topics of the 1995 NLDN upgrade, low peak current positive CG lightning, and the false detection of intracloud lightning in Appendix A.

Data from 1995–97 was analyzed as a part of our national climatology of cloud-to-ground lightning (data from June–August 1994–96 was analyzed as a part of our national analysis of diurnal variations); data from 1994–96 was analyzed as a part of our case studies.

2.3 Radar Data

Radar data used in this study are national radar summaries produced by the WSI Corporation (summaries are a NOWrad™ product). National radar summaries are composites of low-level reflectivity scans collected by National Weather Service radars which are currently operational in the contiguous U.S.: 10–cm WSR-88D and WSR-57S radars and 5–cm WSR-74C radars. (Most reflectivity data is collected by the NEXRAD WSR-88D radar system). The WSI Corporation maintains the quality of national radar summaries by using algorithms to remove ground clutter and other spurious reflectivity echoes. Summaries are produced every 15 minutes and are stored in Graphical Interchange Format (GIF) file format with 8 km × 8 km spatial resolution. We examined national radar summaries from 1996 as part of our case studies.

2.4 Method: National Climatology of Cloud-to-Ground Lightning

We document the spatial and temporal variations of cloud-to-ground lightning activity with a series of maps. Maps were created from gridded lightning data. The grid spacing used in this study is 0.900° × 1.152° in latitude and longitude (roughly 100 km ×100 km). This grid spacing was chosen because we wanted to emphasize regional-scale patterns; maps based on a grid with shorter spacing (e.g., 50 km × 50 km) were found to be too granular. Because our grid spacing is based on fixed angular displacements, grid element area increases from north to south. For example, grid element area increases by a factor of 1.4 from 25° N to 49° N. The north-to-south gradient in grid element area is accounted for in all maps with the exception of the map of annual CG lightning days (Fig. 3.3).

We now describe the method used to produce the map of the normalized amplitude and phase of the diurnal cycle of CG lightning frequency (Fig. 3.9). Lightning data from June–August 1994–96 was first converted to LMT-time (local mean solar-time, Kelly et al. 1978) in order to eliminate the effects caused by time zones. LMT-time is a function of longitude such that the sun crosses the local meridian at 12 LMT. Lightning data was then gridded (as described above) and filtered into hourly time bins. The amplitude and phase of the diurnal cycle of CG lightning frequency was obtained by decomposing the daily march of hourly CG flash count into twelve harmonics. The first harmonic is the diurnal cycle and the second harmonic is the semidiurnal cycle. The

semidiurnal cycle is not examined in this study because studies of the diurnal cycles of thunderstorm and precipitation frequency (e.g., Rasmusson 1971; Wallace 1975) have shown that the semidiurnal cycle generally acts to reinforce the diurnal cycle. Normalized amplitude values were calculated by dividing the amplitude of the diurnal cycle by the daily mean and multiplying this value by 100 (following Wallace 1975). Amplitude and phase information is plotted in the following manner. Normalized amplitude values are contoured. The time of maximum frequency of the diurnal cycle is indicated with harmonic dials. Harmonic dials behave like a 24–hour clock and point to the time of maximum frequency: an arrow pointing to the north indicates a maximum of the diurnal cycle at 0000 LMT; an arrow pointing to the east indicates a maximum at 0600 LMT; etc.

The map of the time lag between the diurnal cycles of positive and negative CG lightning frequency (Fig. 3.14) was produced in similar manner as Fig. 3.9. Again lightning data from June–August 1994–96 was converted to LMT-time. Lightning data was then gridded and filtered into 5–minute bins so that time lag between the diurnal cycles of positive and negative CG lightning frequency could be resolved to 10 minutes. The daily marches of 5–minute positive and negative CG flash count were decomposed into 288 harmonics; the first harmonic is the diurnal cycle. We calculated the time lag between the diurnal cycles of positive and negative CG lightning frequency using the following convention: time lag values greater than zero indicate that the time of maximum positive CG lightning frequency occurred after the time of maximum negative CG lightning frequency.

The Fourier analysis technique used in this study was applied to all gridded lightning data because an examination of the map of total (positive) flash density for June–August 1994–96 (not shown) indicates that almost all grid elements in the contiguous U.S. contain 1000 (100) or more CG flashes over this time period. We believe that this sample is sufficiently large to produce results which are statistically significant.

2.5 Method: Case Studies

We examined cloud-to-ground lightning activity over two 200–km radius areas centered on WSR-88D radars located in Sioux Falls, South Dakota and at Fort Rucker, Alabama (designations KFSD and KEOX, respectively; Fig. 1.1). As mentioned in Sec. 1.1, the KFSD case study area was chosen because it is located in a region characterized by a high percentage of positive polarity flashes and high mean positive peak current values. The KEOX case study area was chosen because it is located within a region where diurnally-forced convection tends to occur during the warm season and baroclinically-forced convection tends to occur during the cold season. The KEOX area was also chosen because it is located over a local maximum of mean positive peak current (Fig. 3.15) and over a local minimum of percentage of positive CG flashes with peak current values less than 7 kA (Fig. A1). The choice of this location reduces the number of low peak current positive CG flashes sampled and may reduce the number of false detections of intracloud lightning sampled (Appendix A).

We centered our case study areas on WSR-88D radars so that radar reflectivity data shown in national radar summaries would represent observations from a single radar rather than a composite from multiple radars. We chose a 200–km radius areas because we wanted to sample roughly 10,000 positive CG flashes per month during summer and because radar reflectivity data within this range is deemed reliable. Both case study areas are located with the 80% detection efficiency contour (Fig. 2.2).

We identified characteristics of convective events which produced positive CG lightning over the KFSD and KEOX case study areas by comparing plots of CG strike locations for 15–minute periods (CG plots; e.g., Figs. 2.4 and 2.6) with national radar summaries (e.g., Fig. 2.3). This comparison was performed on 19 days for each case study area. The 19 days selected for each case study area were determined by sorting the time series of daily positive CG flash count for 1996 and identifying the largest 19 days. Using this method, we sampled 21 convective events over the KFSD area and 25 convective events over the KEOX area. The 21 convective events sampled over the KFSD area produced 75% of the positive CG lightning observed over the KFSD area during 1996 (Table 4.1); the 25 convective events sampled over the KEOX area produced 55% of the positive CG lightning observed over the KEOX area during 1996 (Table 4.3). The convective type and maximum level of organization (MLO; Rickenbach 1996) of these 46 convective events was determined using a radar echo classification scheme described below. We also identified positive strike dominated storms (Knapp 1994) and bipolar lightning patterns (Orville et al. 1988) in these 46 convective events. The lightning

statistics, radar echo characteristics, and positive CG lightning characteristics of convective events sampled over the KFSD and KEOX areas are listed in Tables B1 and B2, respectively.

Convective type was determined by classifying radar echoes associated with positive CG lightning production at the time of maximum positive CG lightning production. We identified the time of maximum positive CG lightning production by examining a 15–minute time series of CG lightning statistics produced for each case study area. Radar echoes were classified into the following eight convective types: isolated convective cells (e.g., Fig. 2.3; the corresponding CG plot is shown in Fig. 2.4), short-lived lines (lasting less than one hour; e.g., Figs. 2.5 and 2.6), cluster of cells (grouped cells with no linear organization; e.g., Figs. 2.7 and 2.8), line of cells (e.g., Figs. 2.9 and 2.10), broken line (Bluestein and Jain 1985; e.g., Figs. 2.11 and 2.12), contiguous line (e.g., Figs. 2.13 and 2.14), leading-line/trailing stratiform MCS (LL/TS MCS; e.g., Figs. 2.15 and 2.16), and MCS with no linear organization (MCS cluster; e.g., Figs. 2.17 and 2.18). We defined an MCS using the definition given by Cotton and Anthes (1991) with one additional qualification. Cotton and Anthes (1991) defined an MCS as:

> a deep convective system that is considerably larger than an individual thunderstorm and that is often marked by an extensive middle to upper tropospheric stratiform-anvil cloud of several hundred kilometers in horizontal dimension.

We extended this definition and required that an MCS comprise an area of deep convection and an areally-extensive stratiform region. The requirement of an areally-

extensive stratiform region was used to identify convective systems with well-developed mesoscale circulations. We realize that inconsistencies exist in our radar echo classification scheme. These inconsistencies are unavoidable due to the complex behavior of convective activity and the subjective classification scheme used in this study. Nevertheless, we feel that our classification scheme provides a reasonable description of the types of convection that occur over the north-central U.S. and Gulf Coast.

We determined the maximum level of organization of convective events by animating national radar summaries over the lifecycle of each convective event. We defined the MLO to be the convective type of a convective event at its largest areal extent using the radar echo classification scheme described above. Note that the maximum level of organization of a convective event may occur after the event has propagated over the case study area.

Positive strike dominated storms were identified by examining CG plots. Examples of PSD storms are shown in Figs. 2.4, 2.8, 2.10, and 2.14. Note that the positive CG clusters shown in these figures are associated with intense convective activity (Figs. 2.3, 2.7, 2.9, and 2.13, respectively). We believe that PSD storms can be used as a proxy for severe storms because studies have shown that most storms which produce predominately positive CG lightning over extended periods of time during the mature phase produce large hail and/or tornadoes. However, we should point out that most severe storms are not PSD storms (Carey et al. 1997). Thus, we underestimate the actual

number of severe storms occurring over a case study area by using PSD storms as a proxy for severe storms. Bipolar lightning patterns were identified by comparing CG plots with national radar summaries. Examples of bipolar lightning patterns are shown in Figs. 2.15 and 2.16 and in Figs. 2.17 and 2.18.

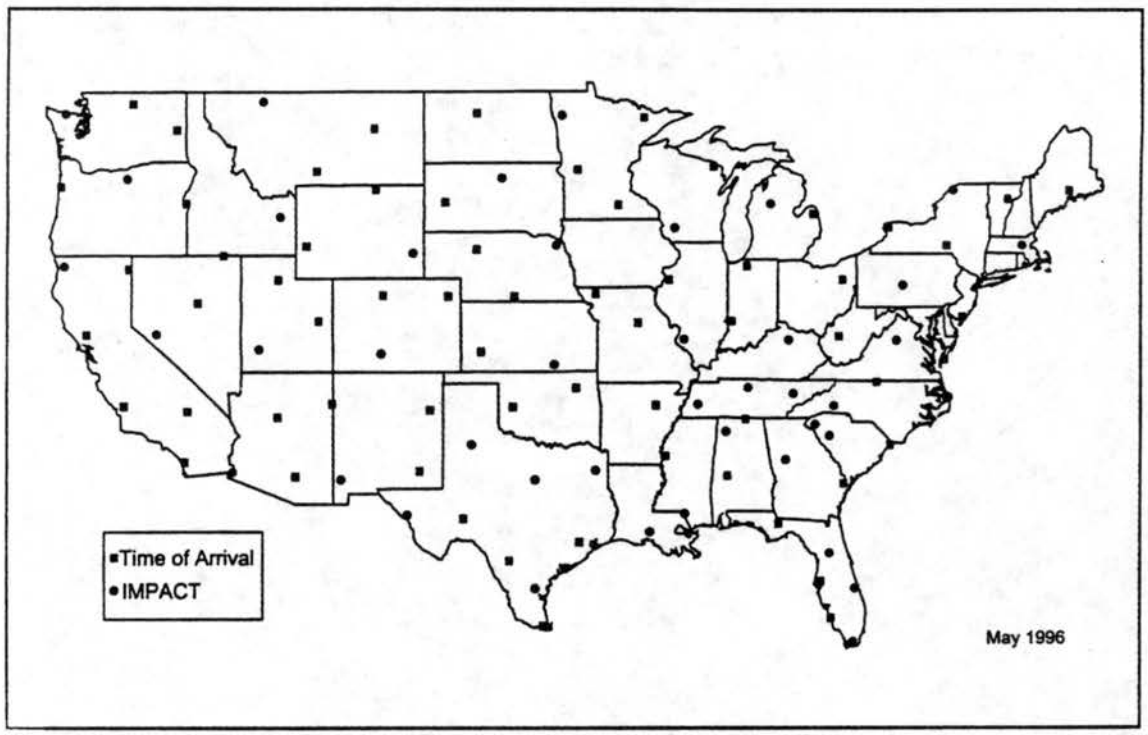

Figure 2.1 NLDN sensor types and locations after the 1995 NLDN upgrade (after Graham et al. 1997).

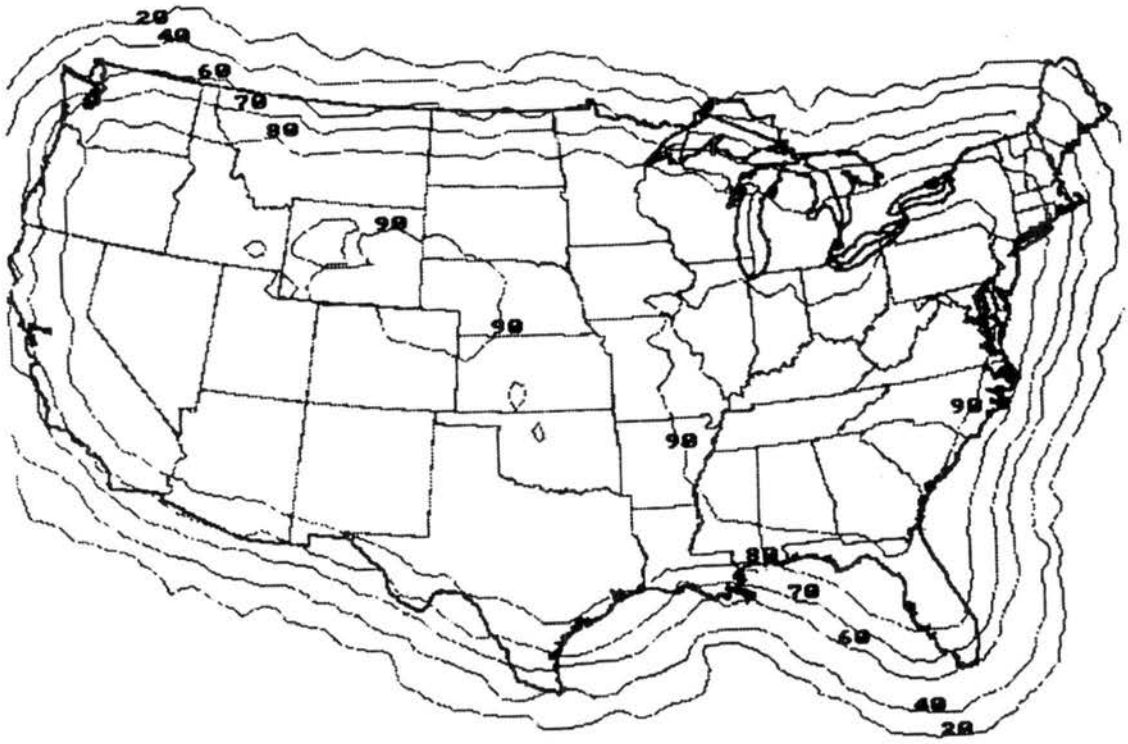

Figure 2.2 Projected NLDN detection efficiency after the 1995 NLDN upgrade (after Cummins et al., 1995).

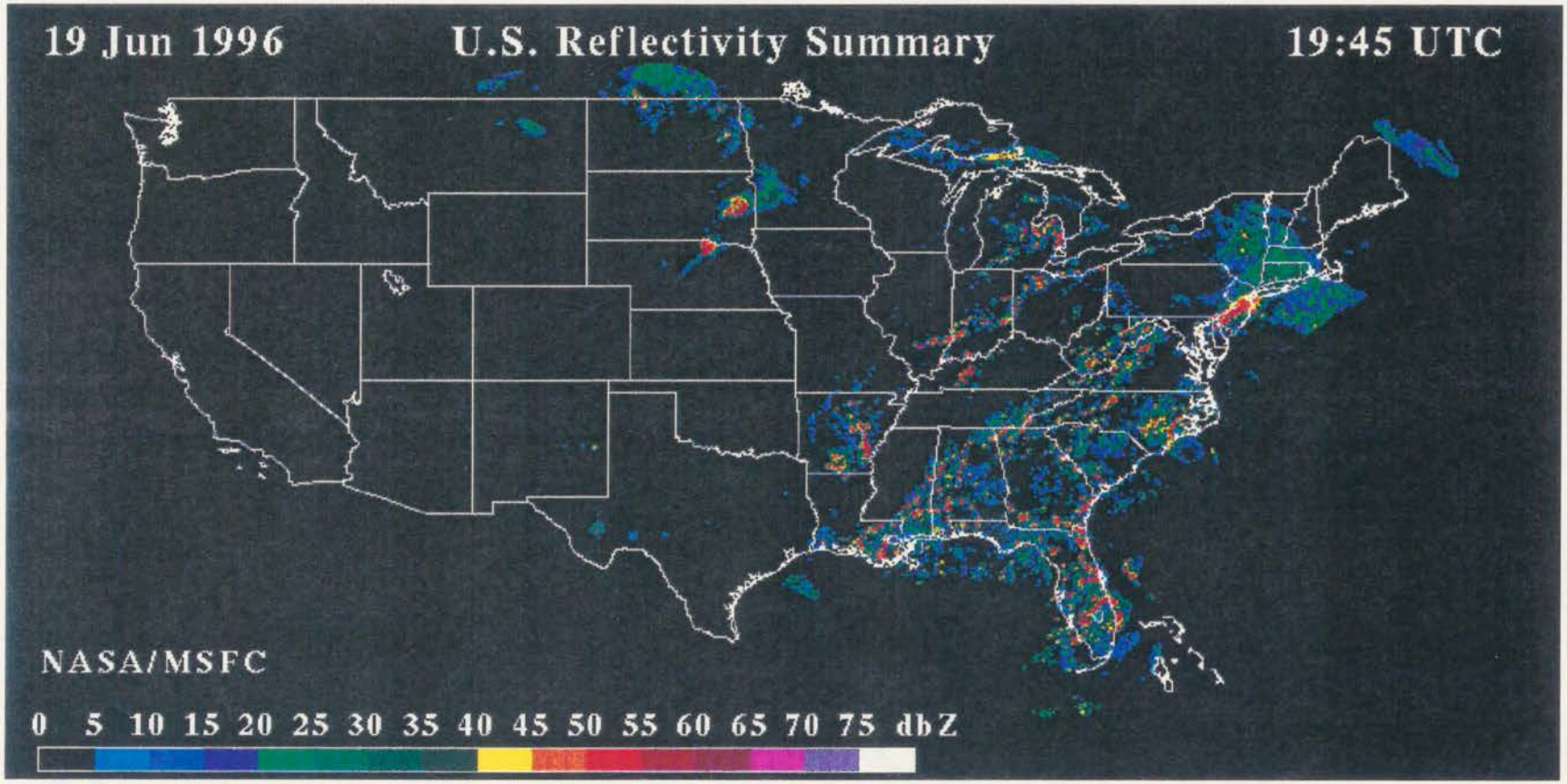

Figure 2.3 National radar summary for an "isolated convective cells" event over the KFSD area at 1945Z, 19 June 1996. This time is the time of maximum positive CG lightning production for this event.

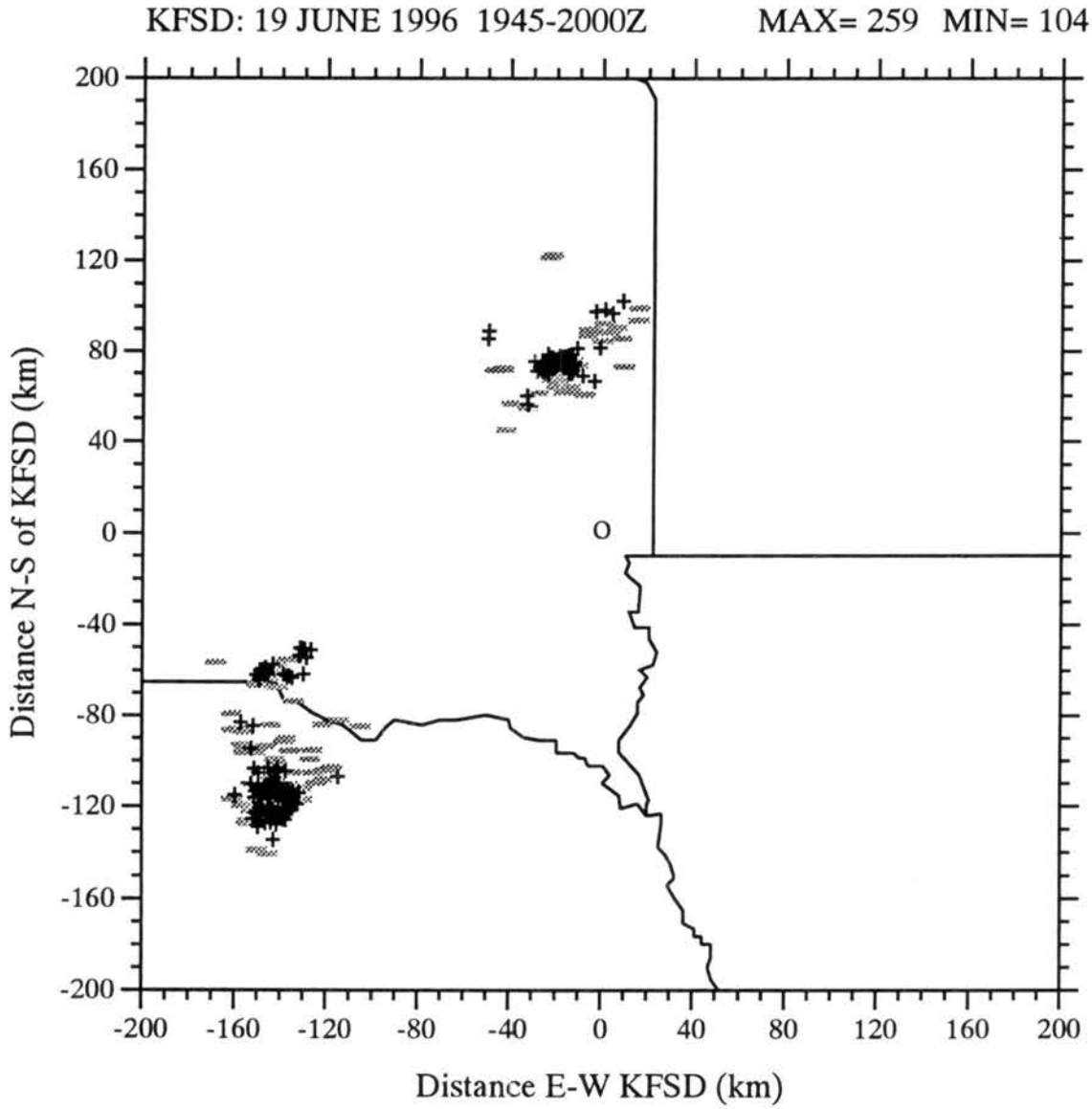

Figure 2.4 Plot of cloud-to-ground strike locations for an "isolated connective cells" event over the KFSD area for the 15–minute period 1945–2000Z on 19 June 1996. This time period is the 15–minute period of maximum positive CG lightning production for this event. Pluses (+) and minuses (-) indicate strike locations of positive and negative CG flashes, respectively. MAX and MIN indicate the number of positive and negative CG flashes plotted, respectively. Distances are relative to the WSR-88D radar located in Sioux Falls, South Dakota (designation KFSD). This plot corresponds to the national radar summary shown in Fig. 2.3.

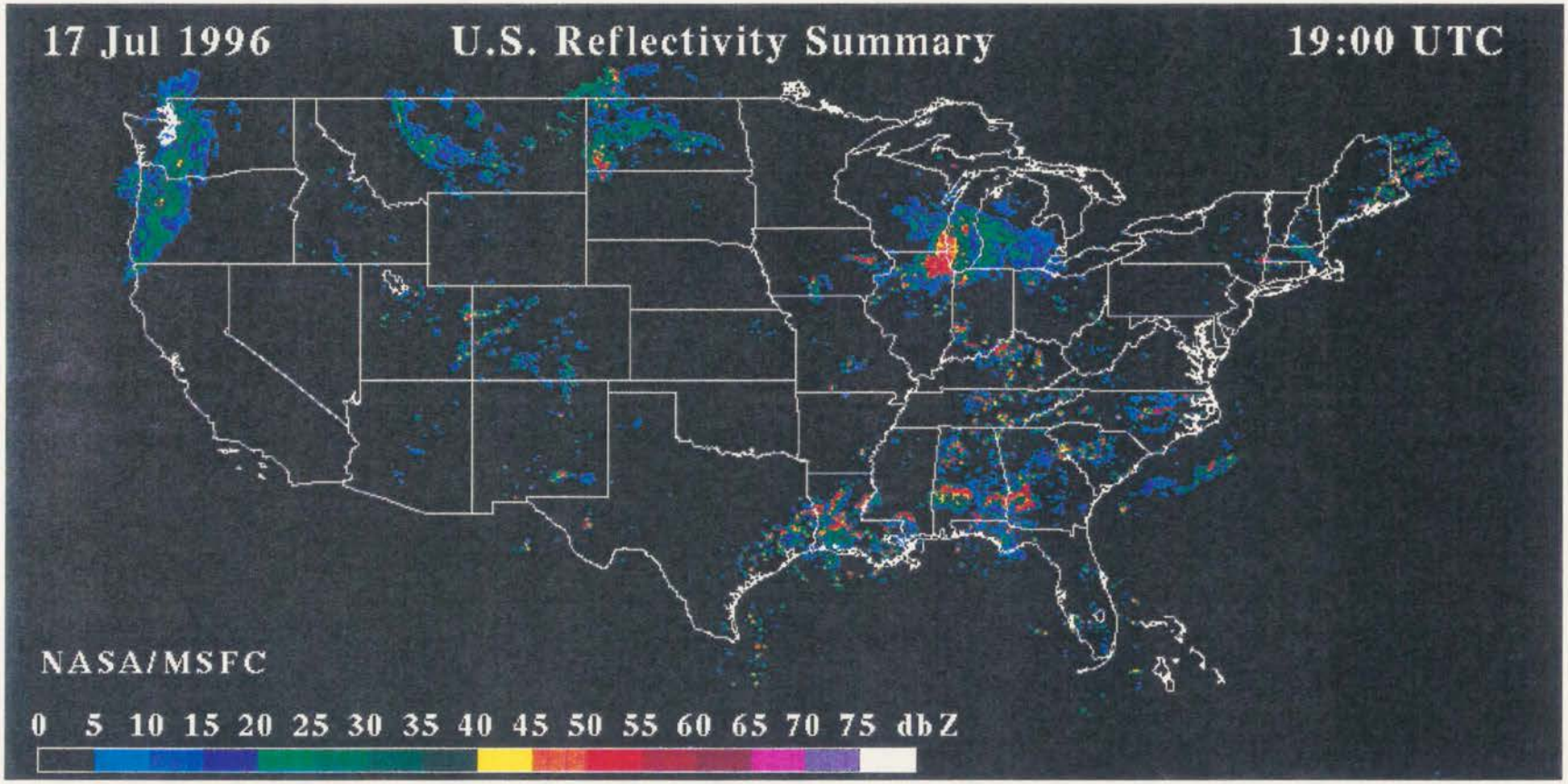

Figure 2.5 As in Fig. 3, but for a "short-lived line" event over the KEOX area at 1900Z, 17 July 1996.

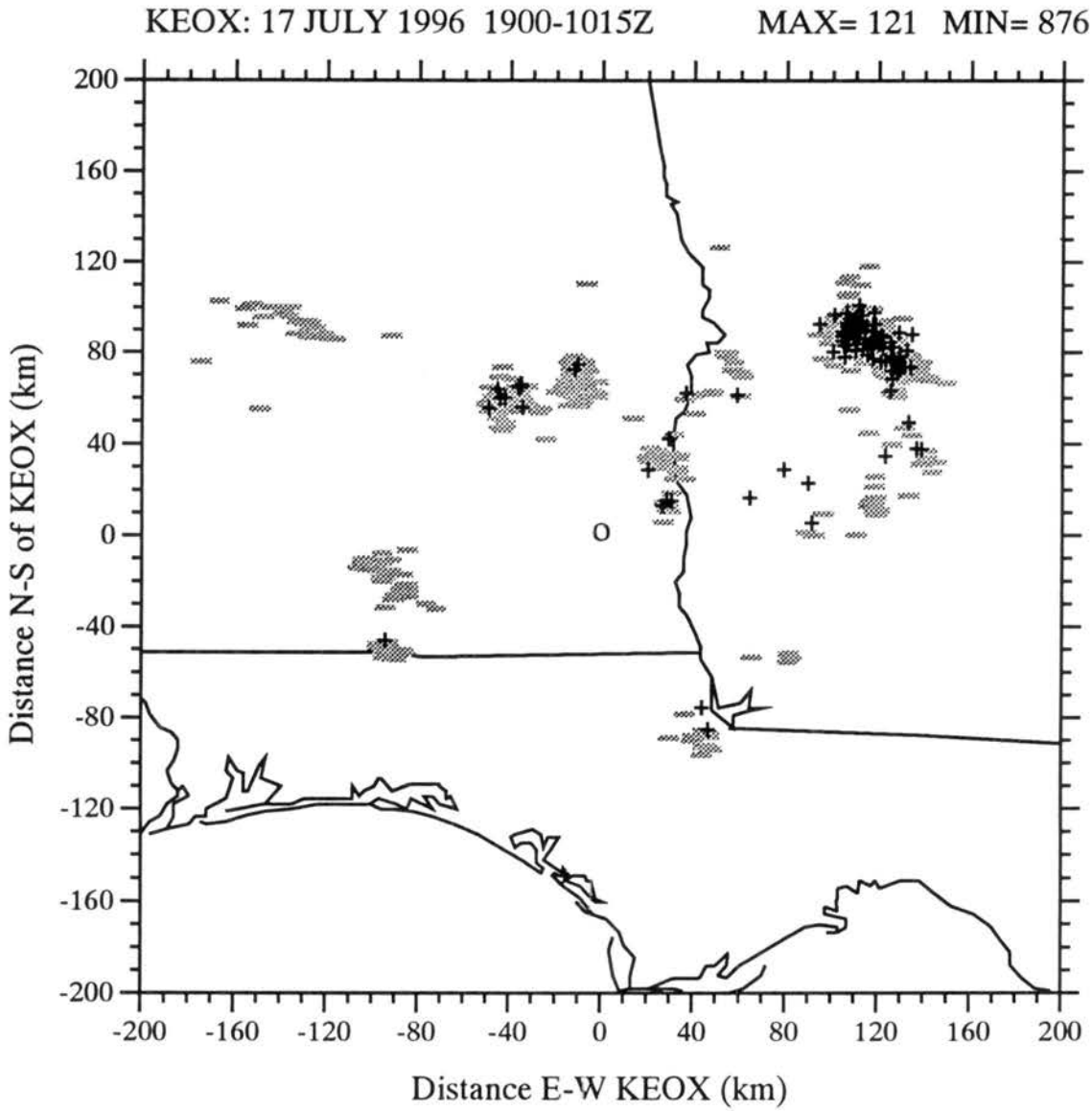

Figure 2.6 As in Fig. 2.4, but for a "short-lived line" event over the KEOX area for the 15–minute period 1900–1915Z on 17 July 1996. This plot corresponds to the national radar summary shown in Fig. 2.5.

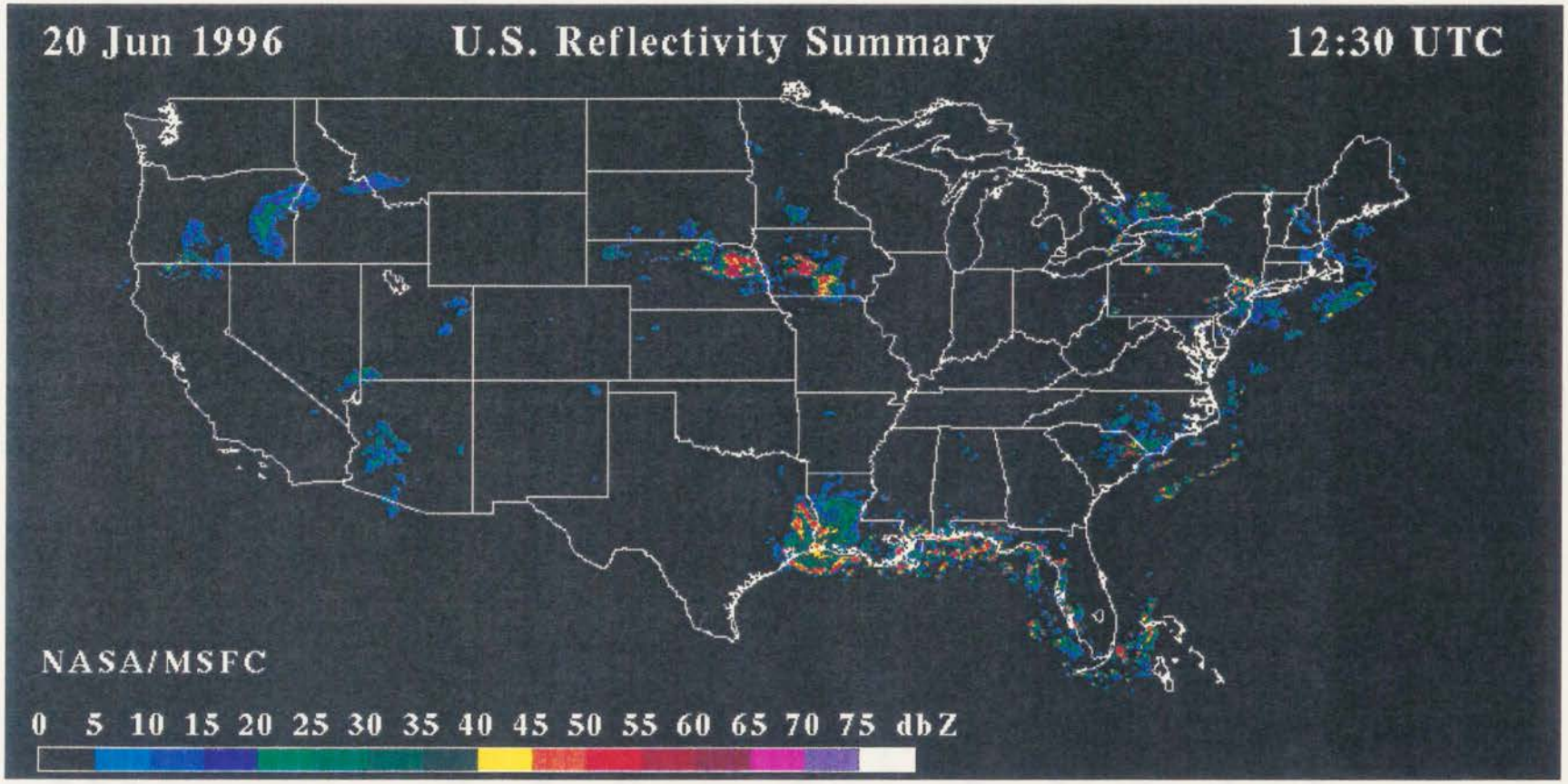

Figure 2.7 As in Fig. 3, but for a "cluster of cells" event over the KFSD area at 1230Z, 20 June 1996.

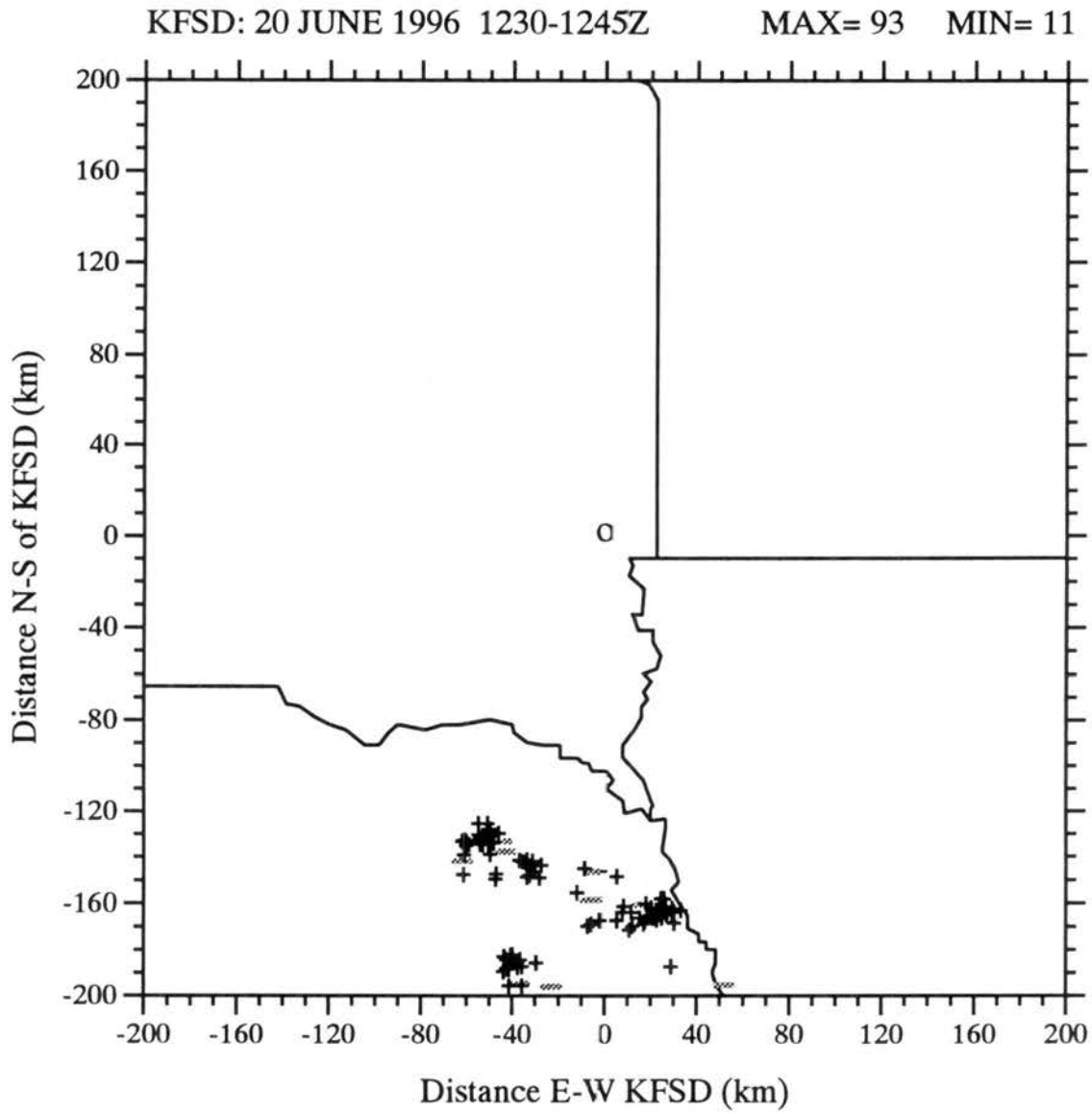

Figure 2.8 As in Fig. 2.4, but for a "cluster of cells" event over the KFSD area for the 15–minute period 1230–1245Z on 20 June 1996. This plot corresponds to the national radar summary shown in Fig. 2.7.

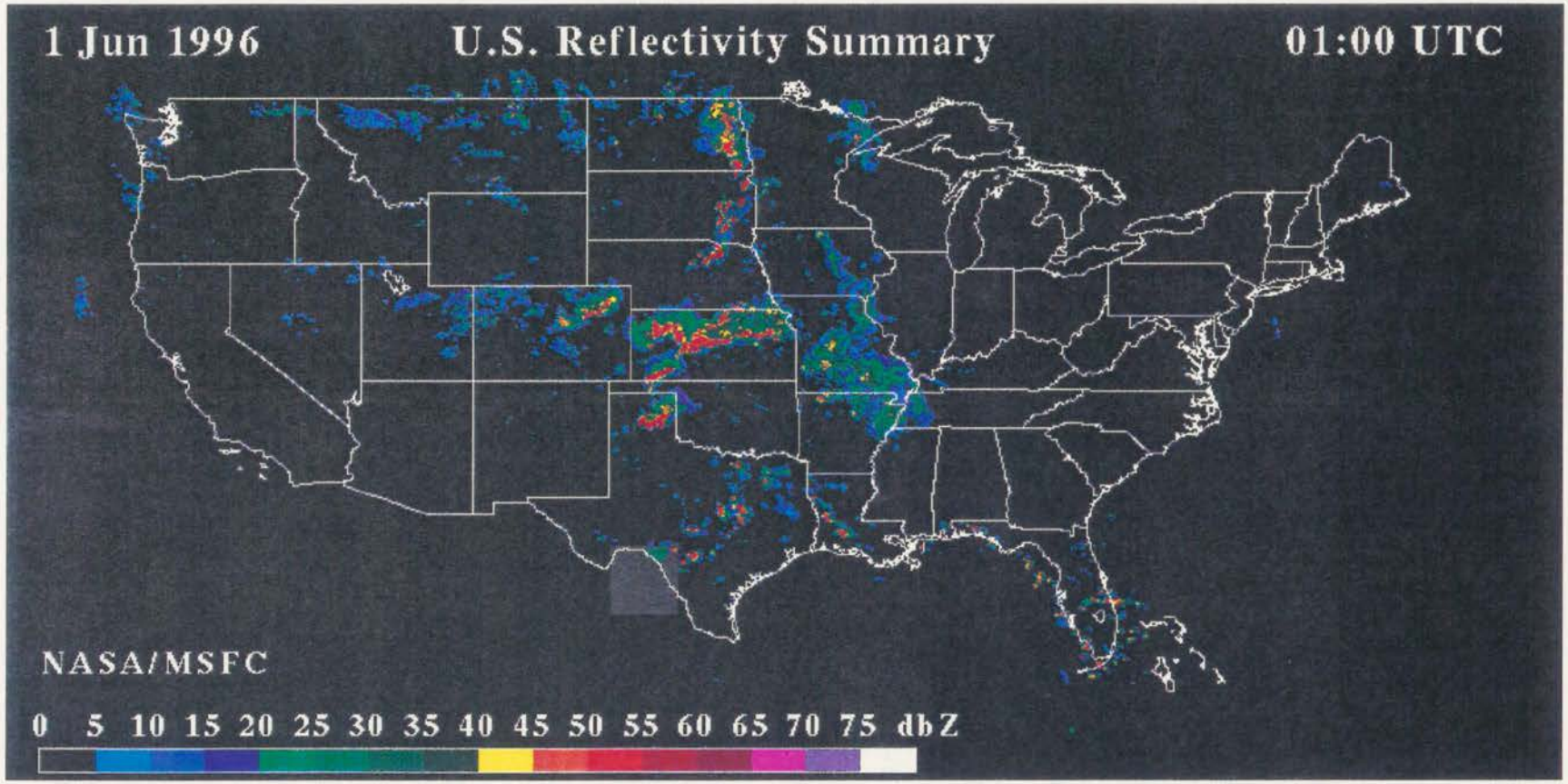

Figure 2.9 As in Fig. 3, but for a "line of cells" event over the KFSD area at 0100Z, 1 June 1996.

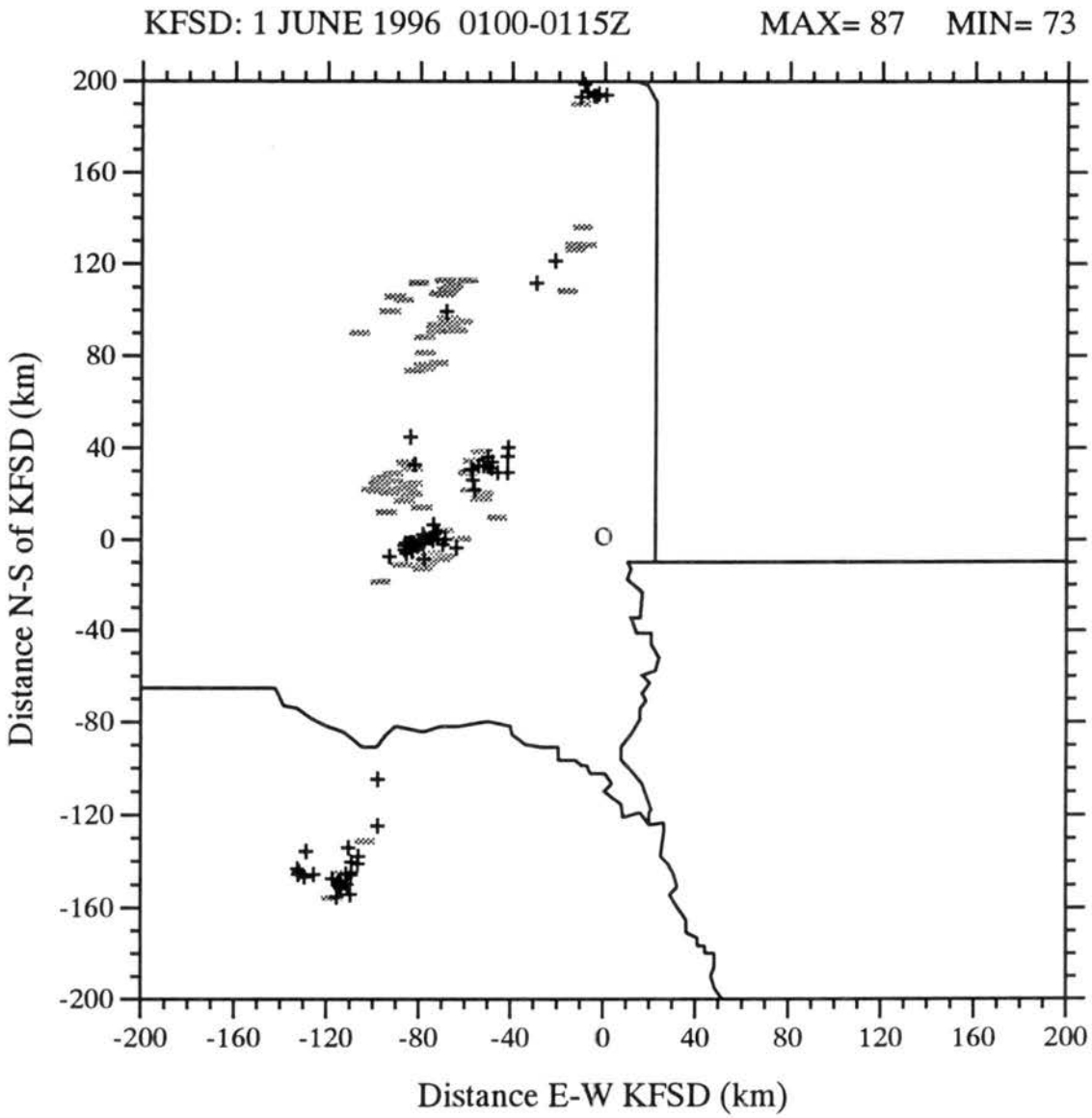

Figure 2.10 As in Fig. 2.4, but for a "line of cells" event over the KFSD area for the 15–minute period 0100–0115Z on 1 June 1996. This plot corresponds to the national radar summary shown in Fig. 2.9.

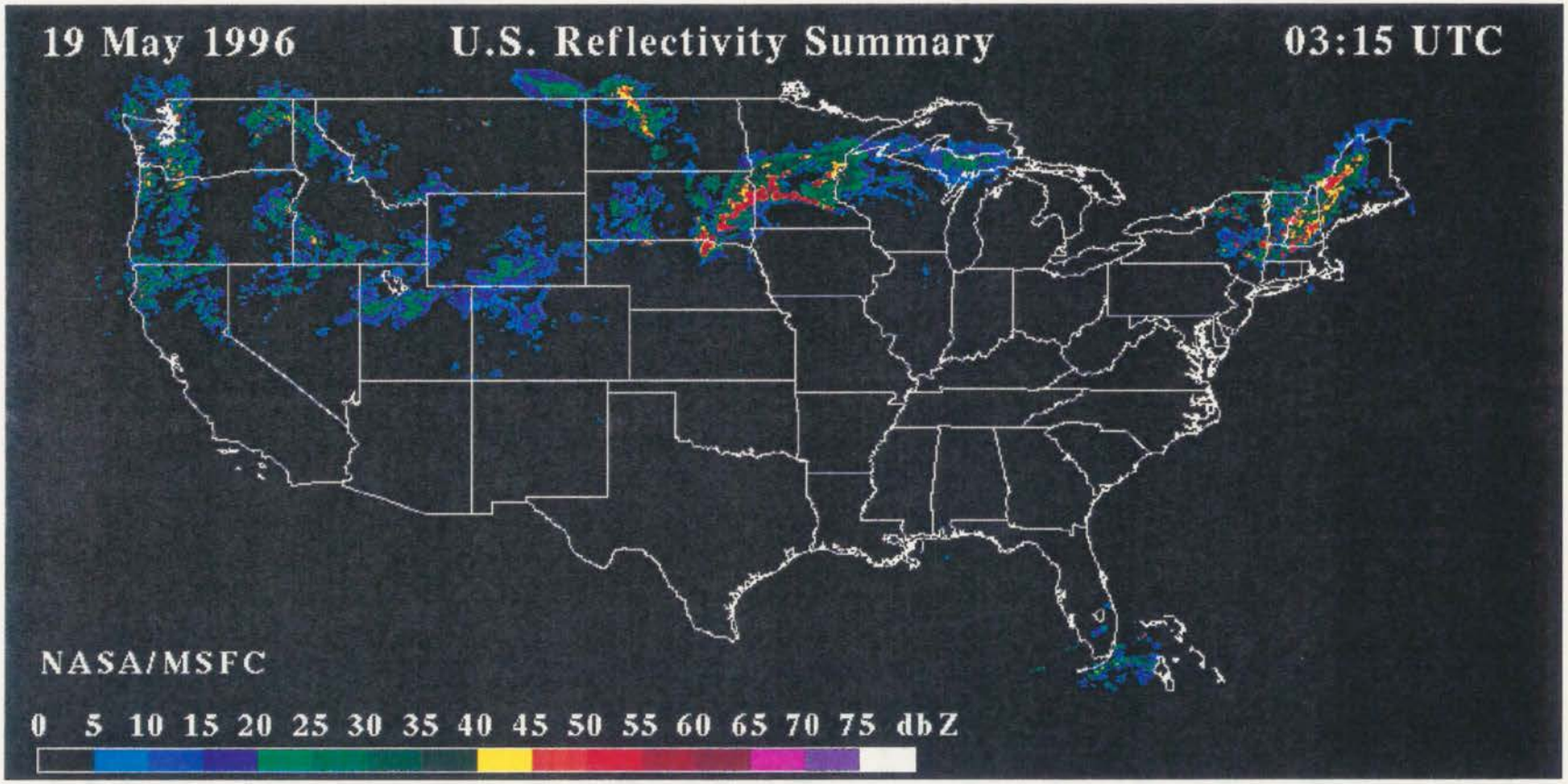

Figure 2.11 As in Fig. 3, but for a "broken line" event over the KFSD area at 0315Z, 19 May 1996.

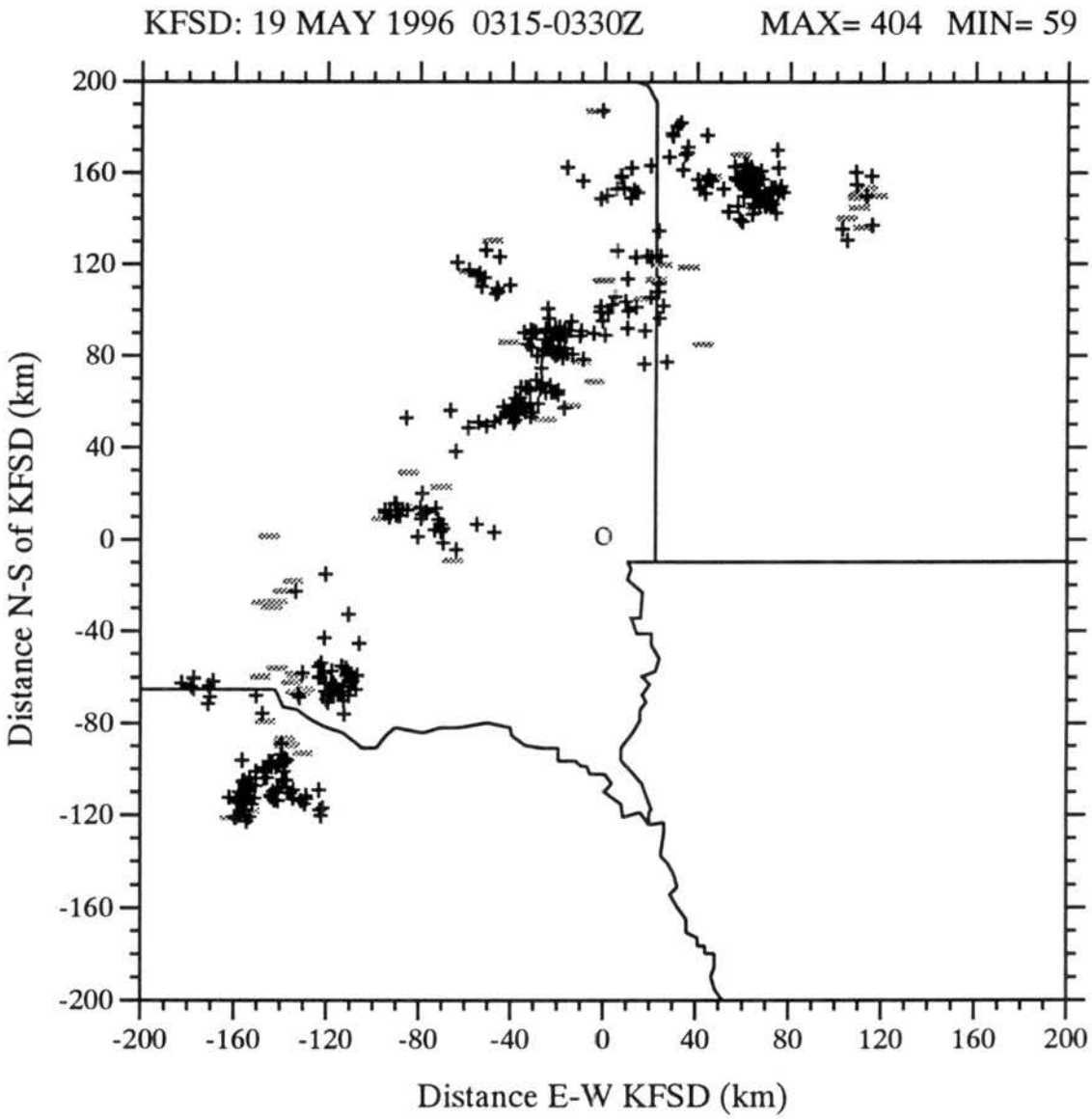

Figure 2.12 As in Fig. 2.4, but for a "broken line" event over the KFSD area for the 15–minute period 0315–0330Z on 19 May 1996. This plot corresponds to the national radar summary shown in Fig. 2.11.

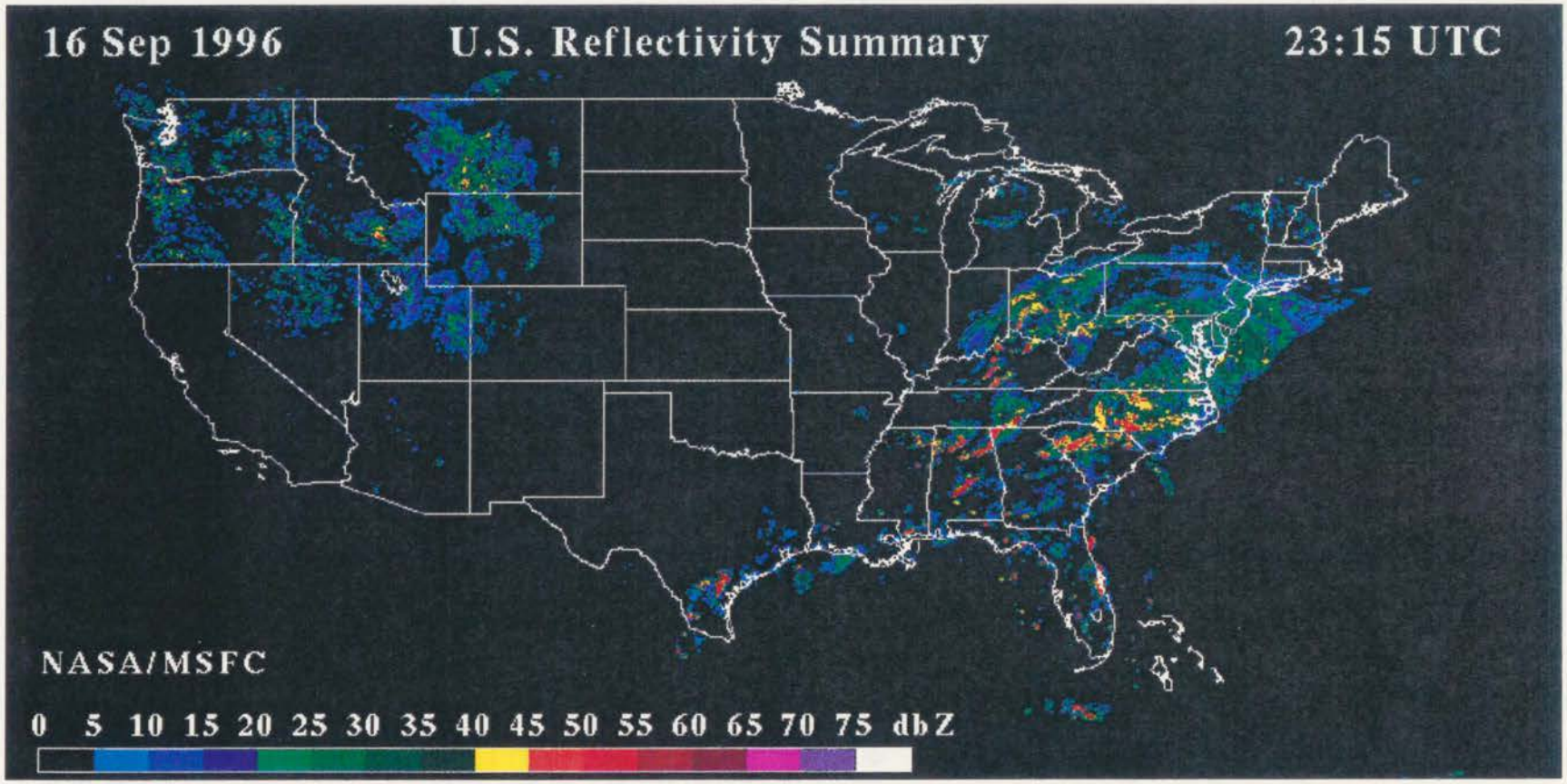

Figure 2.13 As in Fig. 3, but for a "contiguous line" event over the KEOX area at 2315Z, 16 September 1996.

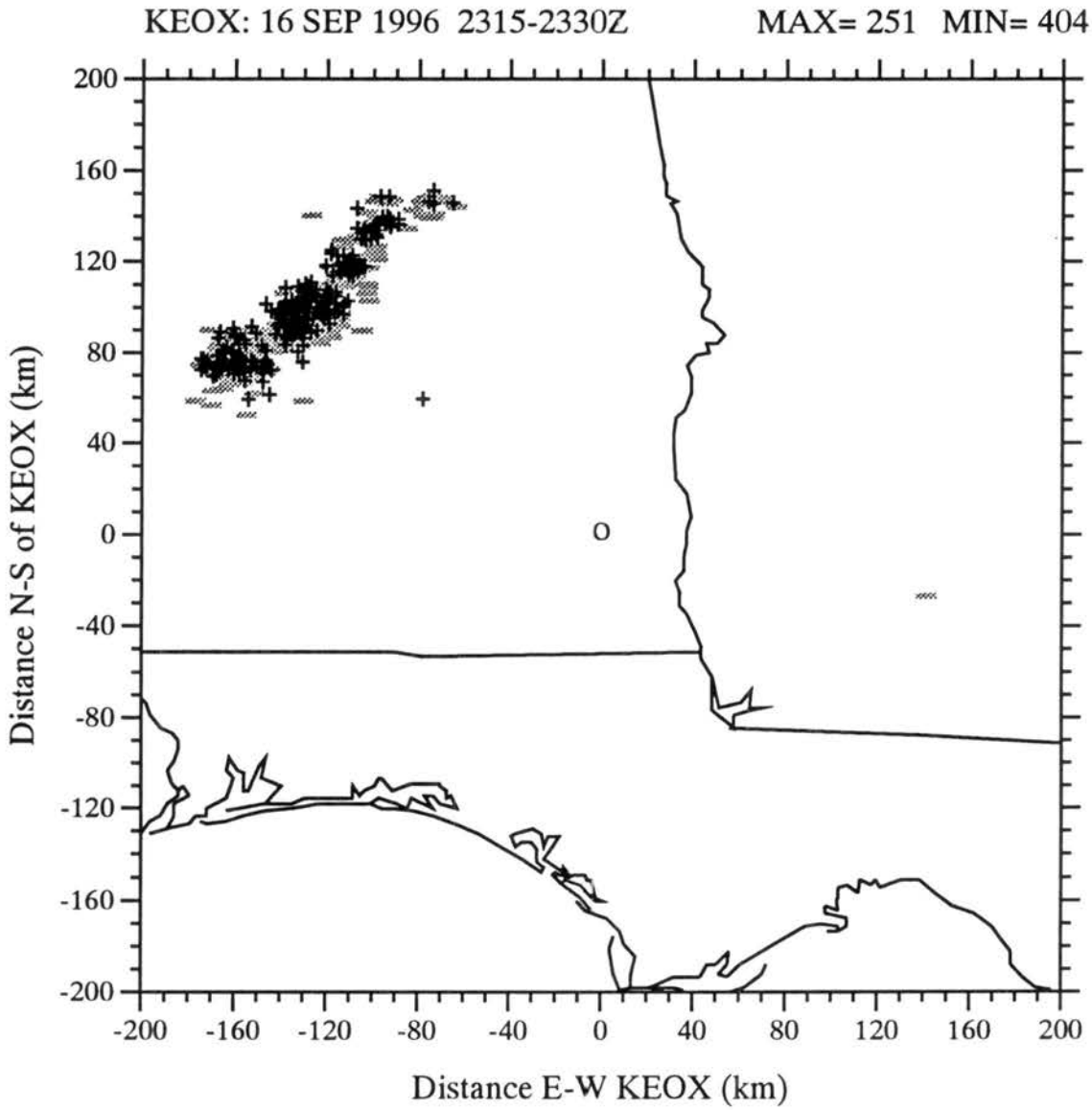

Figure 2.14 As in Fig. 2.4, but for a "contiguous line" event over the KEOX area for the 15–minute period 2315–2330Z on 16 September 1996. This plot corresponds to the national radar summary shown in Fig. 2.13.

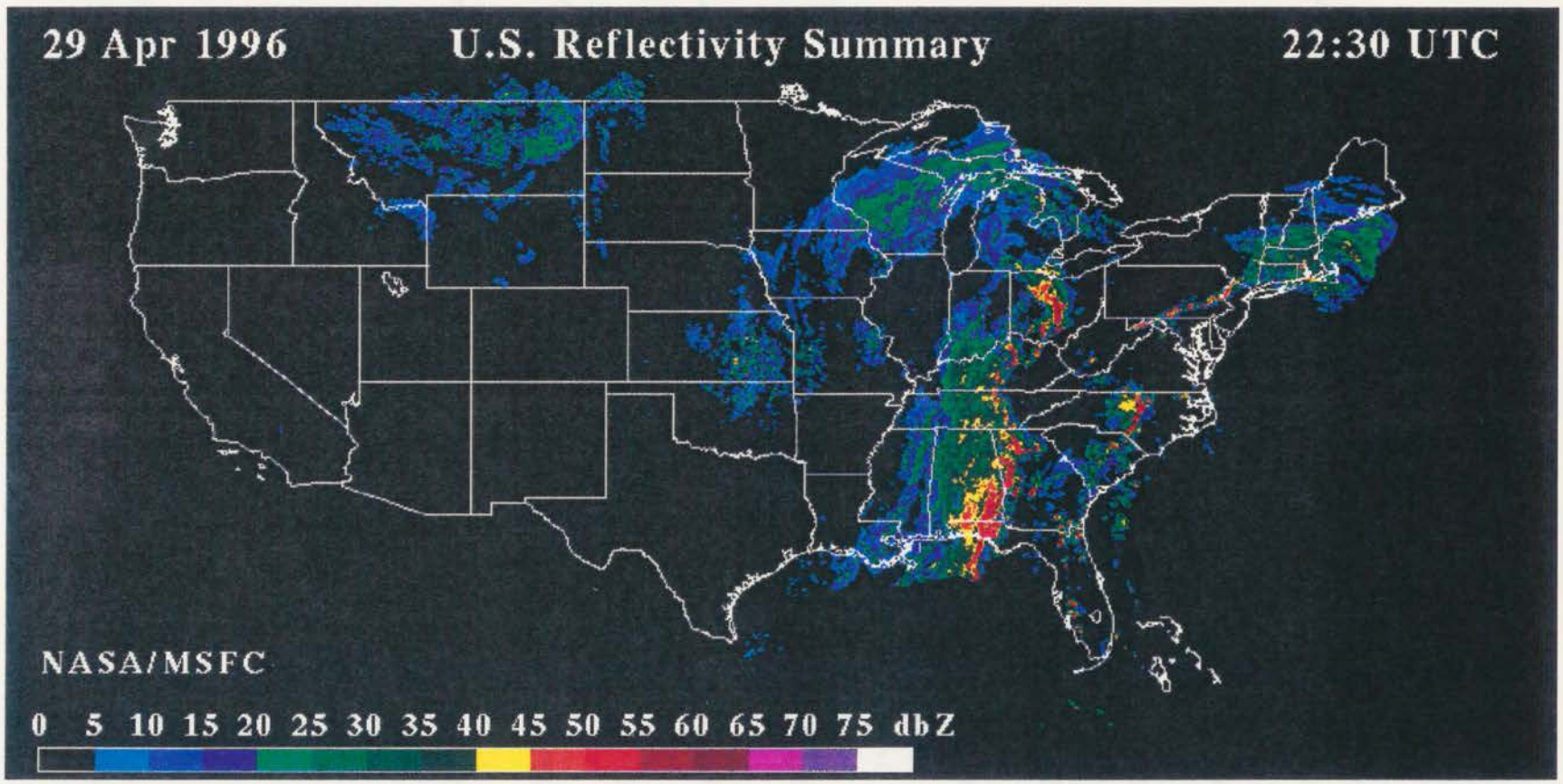

Figure 2.15 As in Fig. 3, but for a "LL/TS MCS" event over the KEOX area at 2230Z, 29 April 1996.

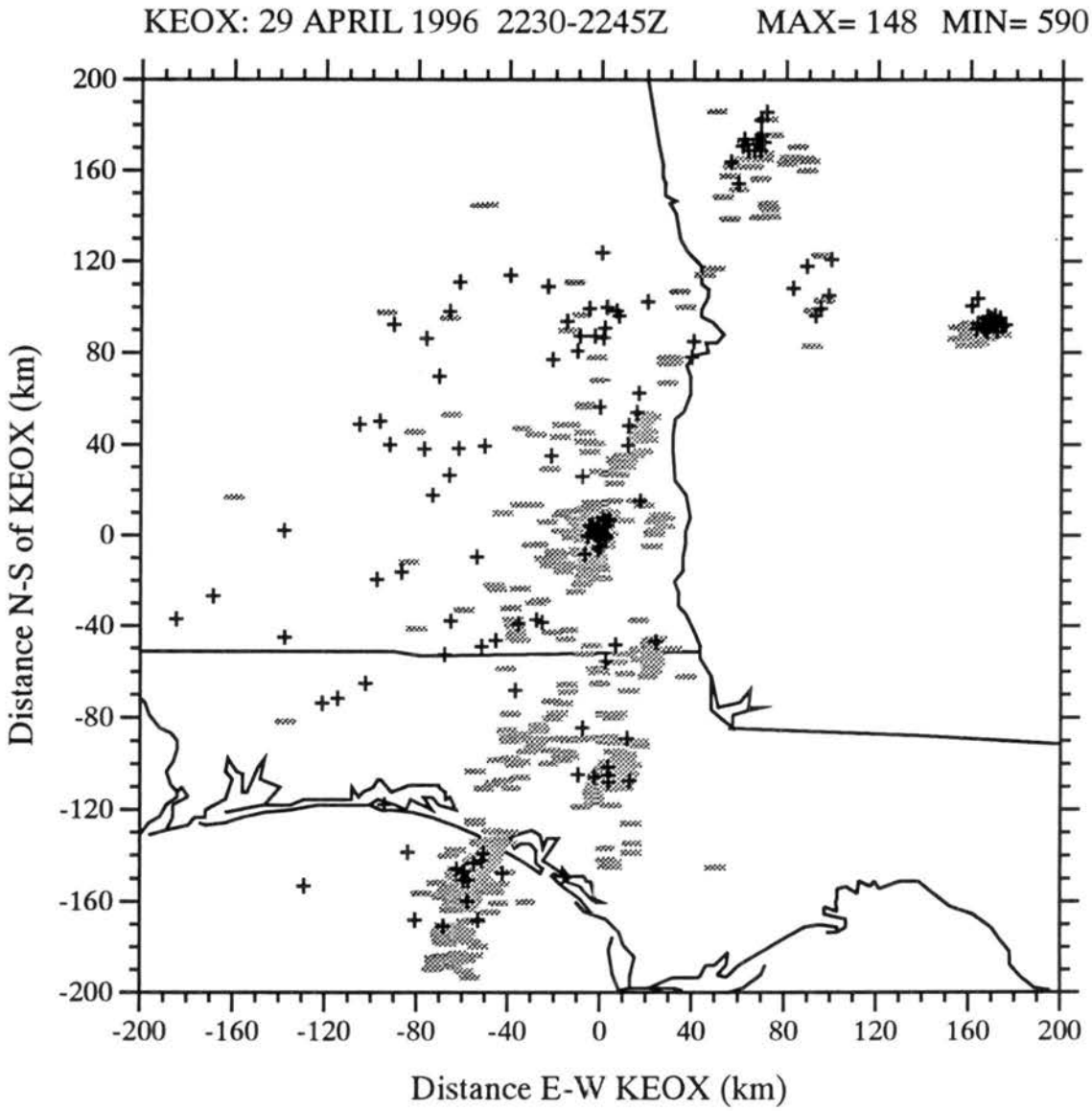

Figure 2.16 As in Fig. 2.4, but for a "LL/TS MCS" event over the KEOX area for the 15–minute period 2230–2245Z on 29 April 1996. This plot corresponds to the national radar summary shown in Fig. 2.15.

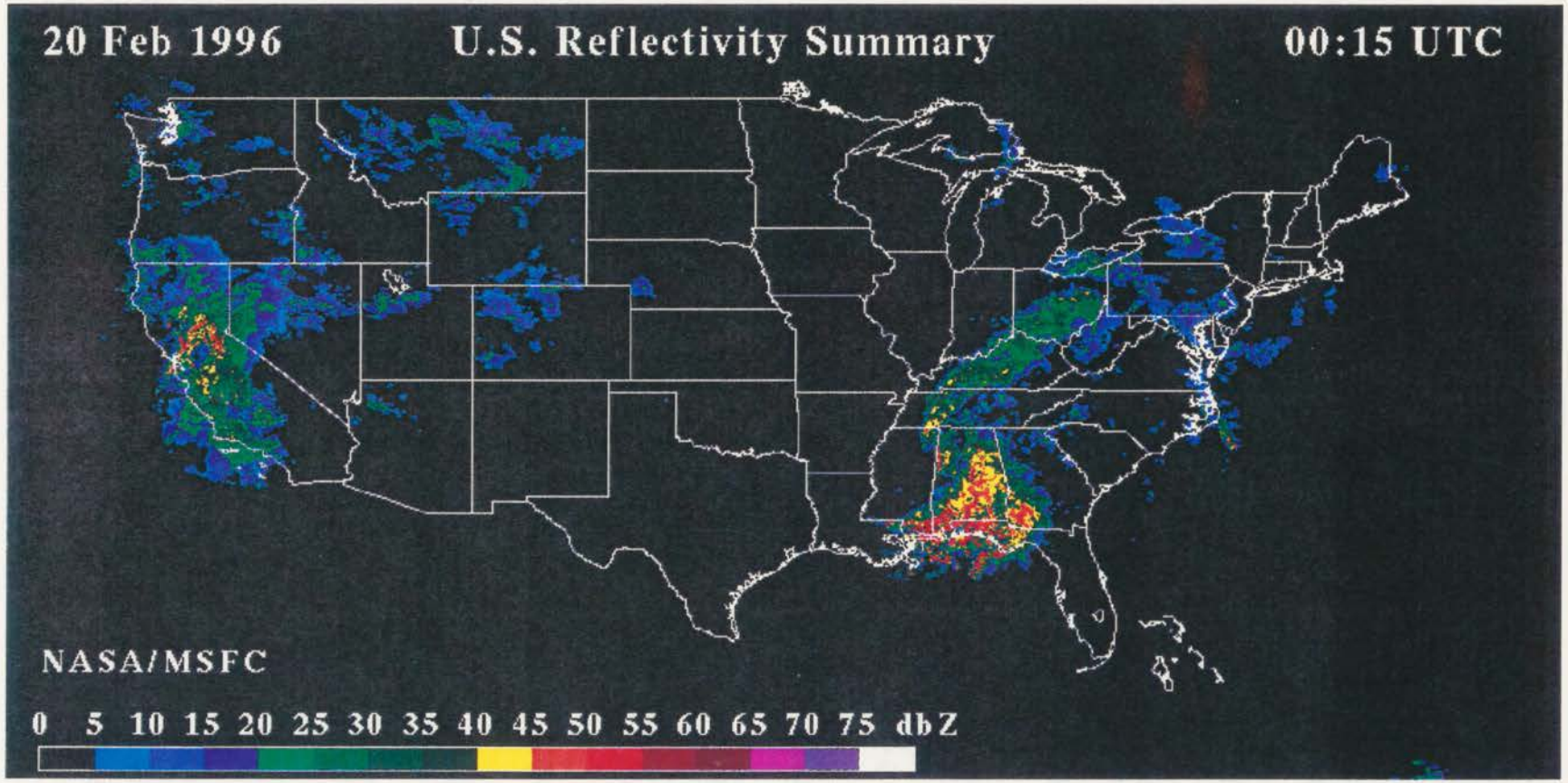

Figure 2.17 As in Fig. 3, but for a "MCS cluster" event over the KEOX area at 0015Z, February 20 1996.

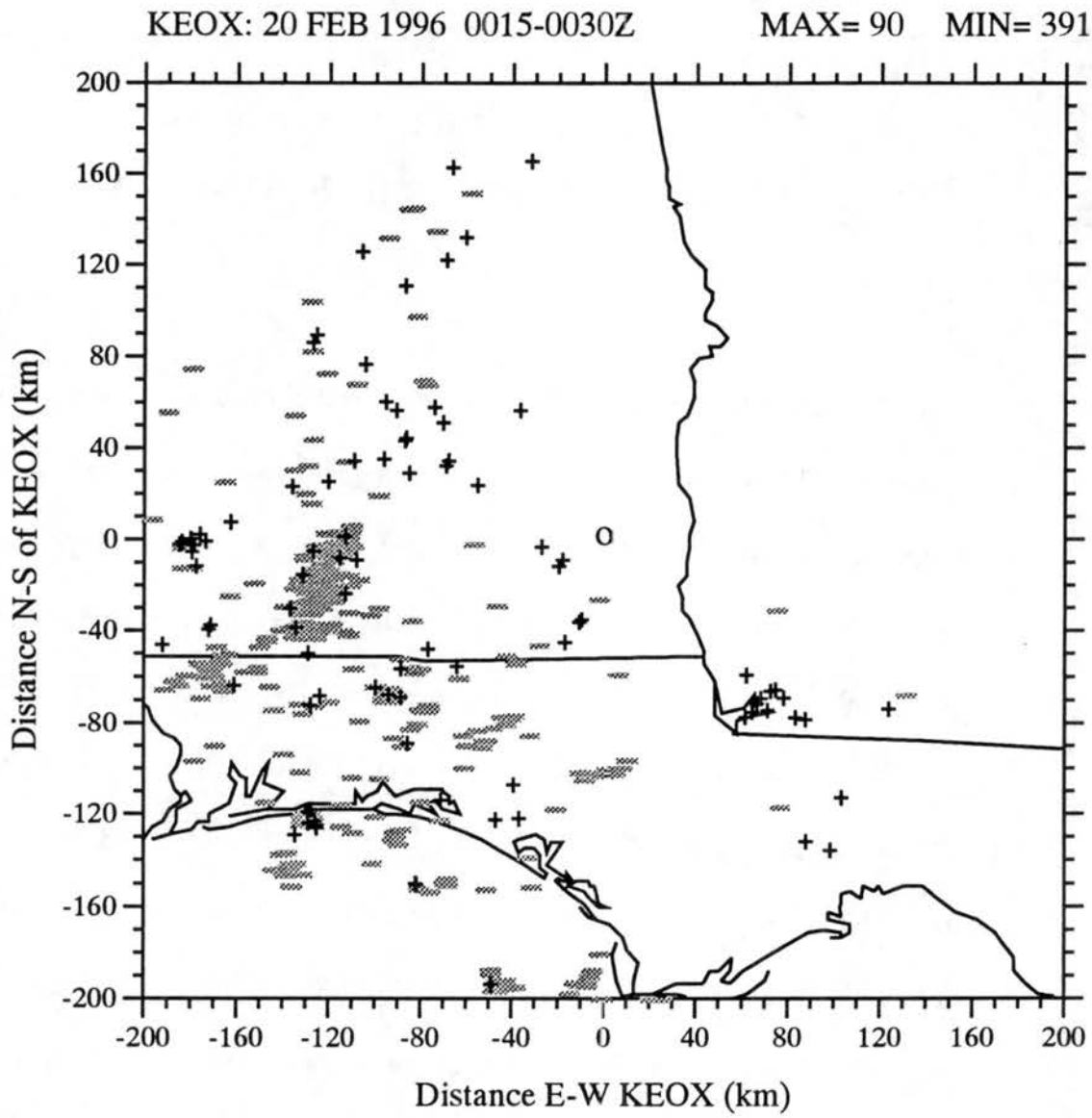

Figure 2.18 As in Fig. 2.4, but for a "MCS cluster" event over the KEOX area for the 15–minute period 0015–0030Z on 20 February 1996. This plot corresponds to the national radar summary shown in Fig. 2.17.

CHAPTER 3

NATIONAL CLIMATOLOGY OF CLOUD-TO-GROUND LIGHTNING

3.1 Overview

In this chapter, we present our three-year national climatology of cloud-to-ground lightning from 1995–97. Our climatology is separated into an examination of the spatial and temporal variations in total CG lightning activity (Sec. 3.2) and an examination of the spatial and temporal variations in positive and negative CG lightning activity (Sec. 3.3). The spatial and temporal variations in total, positive, and negative CG lightning activity are documented with a series of maps with 100 km spatial resolution. Spatial features observed in the maps are identified and discussed. We will generally focus on spatial features within the 80% detection efficiency contour (Fig. 2.2) because observations within this contour are deemed most reliable. A topographic map of the contiguous U.S. is shown in Fig. 3.1 because we will identify spatial features which are collocated with geographic features such as elevated and depressed terrain and coastlines. Annual lightning statistics for 1995–97 are listed in Table 3.1.

3.2 Total Cloud-to-Ground Lightning Activity

3.2.1 Annual CG Flash Density

Figure 3.2 shows annual CG flash density, averaged over 1995–97. Annual flash density values vary between 0.01 and 10.0 flashes km^{-2} over the contiguous U.S. Flash density values greater than 0.1 flashes km^{-2} cover all areas within the 80% detection efficiency (DE) contour. We observe a strong west-to-east gradient over the western U.S. and a strong north-to-south gradient over the central and eastern U.S. Over the western U.S., flash density values increase from 0.1 flashes km^{-2} over the Pacific Coast states (along the 80% DE contour) to 1.0 flashes km^{-2} over the southwestern U.S. and northern Great Plains. Over the central and eastern U.S., flash density values increase from 1.0 flashes km^{-2} over the northern tier states (along the 80% DE contour) to 4.0 flashes km^{-2} over the south-central and southeastern U.S. We believe that the west-to-east gradient observed over the western U.S. is caused by variations in continentality and that the north-to-south gradient observed over the central and eastern U.S. is caused by variations in latitude and by proximity to the Gulf of Mexico, the main source of moisture for convective activity over the central U.S.

Maximum observed and corrected flash density values are found over coastal areas and over elevated terrain, respectively. Maximum observed flash density values are found over the Florida peninsula and the Gulf Coast; flash density values range between 8.0 and 10.0 flashes km^{-2} over these areas. Maximum corrected flash density values are found outside the contiguous U.S. We estimate corrected flash density values between 20 and

30 flashes km^{-2} over the Sierra Madre Occidental (Mexico) using flash density values between 4.0 and 6.0 flashes km^{-2} and a detection efficiency value of 20%.

Other flash density maxima in Fig. 3.2 are found over elevated terrain and coastal areas. We observe maxima over the Mogollon Rim (Arizona), the Colorado Front Range (Rocky Mountains adjacent to the Great Plains), the Black Hills (Wyoming-South Dakota border), and Cuba. We also observe a maximum over the Gulf Stream and a minimum over the central and southern Appalachian Mountains. These observations indicate that surface features such as elevated terrain, coastlines, and the Gulf Stream can control the location and magnitude of CG lightning activity. Observations of flash density maxima and minima collocated with surface features have been reported in national studies of CG lightning activity (e.g., Orville 1991a, 1994; Orville and Silver 1997) and in regional studies of CG lightning activity (e.g., Maier et al. 1984; Reap 1986; Lopez and Holle 1986; Orville 1990b; Biswas and Hobbs 1990; Watson et al. 1994a; Clodman and Chisholm 1996).

We compared Fig. 3.2 with maps of annual CG flash density published in Orville (1991a, 1994) and in Orville and Silver (1997) for the individual years 1989–95 and found that all maps show similar spatial patterns and values (when our observed flash density values are corrected for an assumed network-wide 70% detection efficiency).

3.2.2 Annual CG Lightning Days

Figure 3.3 shows the annual number of days with one or more CG flashes, averaged over 1995–97. The annual number of days with CG lightning varies between 10 and 200 days per year over the contiguous U.S. Almost all areas within the 80% detection efficiency contour have 25 or more days with CG lightning per year. We observe a strong west-to-east gradient in the daily frequency of CG lightning activity over the western U.S. and a strong north-to-south gradient in the daily frequency of CG lightning activity over the central and eastern U.S. Over the western U.S., the annual number of days with CG lightning increases from 25 days over the Pacific Coast states (along the 80% DE contour) to 75 days over the southwestern U.S. and the northern Rocky Mountains. Over the central and eastern U.S., the annual number of days with CG lightning increases from 50 days over the northern tier states (along the 80% DE contour) to 125 days over the southeastern U.S. We believe that these two regional-scale gradients are related to the two regional-scale gradients observed in Fig. 3.2 and have the same causes. We discuss the relationship between Figs. 3.2 and 3.3 in Sec. 3.2.3.

The north-to-south gradient in grid element area may contribute to the north-to-south gradient observed over the central and eastern U.S. However, this contribution appears to be small. For example, over the latitude range from 48° N to 35° N, the annual number of days with CG lightning increases by a factor of 2.5 (from 50 days to 125 days) while grid element area increases by only a factor of 1.2. In addition, we believe that the annual number of days with CG lightning does not increase linearly with grid element area.

We observe a number of maxima in Fig. 3.3 which are collocated with surface features. We observe maxima over elevated terrain including the Sierra Madre Occidental, the Sierra Madre Oriental (Mexico), the Colorado plateau (the elevated region comprising most of New Mexico and Colorado and portions of Arizona, Utah, and Wyoming), and the central Rocky Mountains. We also observe maxima over coastal areas including the Florida peninsula, the Gulf Coast, and Cuba. In addition, we observe a maximum over the Gulf Stream and a minimum over the Columbia River basin (eastern Washington). These observations indicate that surface features such as elevated and depressed terrain, coastlines, and the Gulf Stream can control the daily frequency of CG lightning activity. Similar results have been reported in regional studies of CG lightning activity (e.g., Reap 1986; Clodman and Chisholm 1996).

We compared Fig. 3.3 with the national map of annual thunder days published in Baldwin (1973) and found that the two maps show similar spatial patterns but different values; the number of days with CG lightning is generally a factor of two greater than the number of days with thunderstorms. This difference can be attributed a number of factors (see Reap and Orville 1990 for a discussion) but is most likely due to the large grid spacing used in this study (i.e., 100 km) and the definition of a CG lightning day used in this study (i.e., one or more CG flashes). We note that Reap (1986), Reap and Orville (1990), and Clodman and Chisholm (1996) get good agreement between CG lightning

days and thunder days using ~50 km grid spacing and defining a CG lightning day as a day with two or more CG flashes.

3.2.3 Cumulative Frequency Distributions

Comparison of Figs. 3.2 and 3.3 reveals that both maps show similar spatial features. This similarity suggests that the distribution of daily CG flash count may be a constant in space and time when normalized. We investigate this hypothesis by examining cumulative frequency distributions (CDs) of daily CG flash count over the KFSD and KEOX case study areas and over the contiguous U.S. CDs of daily CG flash count were produced by sorting the time series of daily CG flash count (1994–96 for the case study areas and 1995–97 for the contiguous U.S.) in descending order and then summing daily CG flash count and the number of days with CG lightning on a cumulative basis. Cumulative subtotals of CG flash count and number of days with CG lightning were then normalized by the total CG flash count and the total number of days with CG lightning, respectively.

Cumulative frequency distributions of daily CG flash count for the KFSD and KEOX case study areas (Fig. 3.4) both show a similar degree of skewness. For example, over the KFSD (KEOX) area, 7% (9%) of the days with cloud-to-ground lightning produced 50% of the cloud-to-ground lightning. The similarity between the CDs of daily CG flash count over the two case study areas suggests that the normalized distribution of daily CG flash count may be independent of such climatic factors as latitude,

continentality, and elevation. Figure 3.5 substantiates this statement. Over the contiguous U.S., 2–15% of the days with cloud-to-ground lightning produced 50% of cloud-to-ground lightning. While some geographic variability is observed (i.e., maxima located over the Colorado plateau and the Florida peninsula), this variability does not change our main results: 1) a relatively few number of days with cloud-to-ground lightning produce a relatively large fraction of cloud-to-ground lightning and 2) this behavior is independent of climatic factors such as latitude, continentality, and elevation. Similar results have been published in studies of CG lightning activity (e.g., Lopez and Holle 1986) and rainfall (see Riehl 1954 for a review) but not with the spatial continuity shown here. CDs of daily rainfall show that 10–20% of the days with rain produce 50% of rainfall (Olascoaga 1950).

Our examination of the daily frequency of CG lightning activity and cumulative frequency distributions of daily CG flash count indicates that CG lightning activity is infrequent and episodic in nature. Figure 3.3 shows that, with the exception of the Florida peninsula, cloud-to-ground lightning occurs on less than half of days during the year. Comparison of Figs. 3.3 and 3.5 reveals that, for any locale in the contiguous U.S., the majority of cloud-to-ground lightning is produced on less than 30 days per year (less than 20 days per year if we exclude the Florida peninsula).

3.2.4 Annual Variations

National and regional studies of cloud-to-ground lightning activity have shown that the majority of cloud-to-ground lightning is produced during summer (June–August; national: Orville 1991a; Orville and Silver 1997; regional: Lopez and Holle 1986; Orville et al. 1987; Reap and MacGorman 1989; Reap and Orville 1990; Reap 1994; Watson et al. 1994a,b; Clodman and Chisholm 1996). For example, Orville (1991a) and Orville and Silver (1997) found that roughly 70% of all CG flashes detected over the contiguous U.S. are observed during summer. We extend the national analysis of summertime CG lightning activity and document the percentage of cloud-to-ground lightning produced during summer over the contiguous U.S. (Fig. 3.6). Figure 3.6 shows that the production of cloud-to-ground lightning is greater than 50% during summer over most areas in the contiguous U.S. with the exceptions of the southeastern U.S. and the Pacific Coast. Production of cloud-to-ground lightning is greater than 75% during summer over the eastern Rocky Mountains, the northern Great Plains, the upper Midwest, the northeastern U.S., the Atlantic Coast (excluding Florida), and over southern Oregon, northern California, and western Nevada.

We examine the south-to-north gradient of summertime CG lightning production over the central U.S. in greater detail by showing the annual marches of monthly CG flash density for five locations in the central U.S. separated by roughly 5° latitude (Fig. 3.7). Figure 3.7 shows a steady south-to-north increase in the fraction of cloud-to-ground lightning produced during summer from 15% in Brownsville to 82% in Bismark. Despite

the strong south-to-north gradient of summertime CG lightning production, the overwhelming majority of cloud-to-ground lightning (≥90%) is produced during the warm season (April–September) for all locations except Brownsville (68%). We believe that the south-to-north gradient of summertime CG lightning production is primarily a function of proximity to the Gulf of Mexico; locations closer to the Gulf of Mexico are more likely to experience convective activity throughout the year. This statement is supported by Fig. 3.8 which shows that CG lightning activity during the cold season (October–March) is confined to the south-central and southeastern U.S.

Examination of Fig. 3.7 indicates that CG lightning activity is modulated by the annual cycle with a summertime maximum when greater than 50% of cloud-to-ground lightning is produced during summer. This result suggests that CG lightning activity is modulated by the annual cycle with a summertime maximum over most of the contiguous U.S. with the exception of the south-central U.S. and the Pacific Coast. We should note that the annual march of monthly CG flash density for San Francisco (not shown) shows that most cloud-to-ground lightning is produced during the cold season. This behavior is likely representative of areas along the Pacific Coast where less than 25% of cloud-to-ground lightning is produced during summer.

3.2.5 Diurnal Variations

We document the diurnal variations in CG lightning activity over the contiguous U.S. during summer with a map of the normalized amplitude and phase of the diurnal

cycle of CG lightning frequency for June–August 1994–96 (Fig. 3.9). Before discussing Fig. 3.9, it is important to understand how the diurnal cycle represents diurnal variations since the amplitude and phase information plotted in Fig. 3.9 is based on diurnal marches of hourly CG flash count. We compared diurnal marches of hourly CG flash count with the normalized amplitude and phase of the diurnal cycle (Fig. 3.10) and found certain relationships between amplitude and phase information and diurnal variations. The relationship between the normalized amplitude of the diurnal cycle and diurnal variations has been described succinctly by Easterling and Robinson (1985):

> A normalized amplitude below [50] indicates a lack of a well-defined time of maximum, or a double maximum. Amplitudes between [50] and [100] suggest a definite diurnal trend with a clear time of maximum, but with storms likely at any hour, while a value over [100] represents conditions where there is very well-developed time of maximum activity, with few storms at other times.

Examination of Fig. 3.10 indicates that the accuracy of the time of maximum frequency of the diurnal cycle is a function of normalized amplitude; the time of maximum frequency is reasonably accurate when normalized amplitude values greater than 50. This statement is supported by examining Fig. 3.9 and noting that harmonic dials show spatial continuity over areas where normalized amplitude values are greater than 50. Finally, it is important to realize that CG lightning activity is infrequent and episodic in nature. Thus, the diurnal cycle of CG lightning frequency does not represent CG lightning activity on any given day during summer, rather it indicates the tendency for summertime CG lightning activity to occur at a specific time during the day.

Figure 3.9 shows that normalized amplitude values greater than 100 cover the western and eastern U.S. Over these areas, the time of maximum frequency occurs between 1300 and 1800 LMT. These results indicate that CG lightning activity over the western and eastern U.S. is modulated by the diurnal cycle with a well-defined time of maximum frequency occurring during the afternoon or early evening. Normalized amplitude values greater than 140 are found over the Florida peninsula, the Gulf Coast, the Atlantic Coast, the central and southern Rocky Mountains, and most of Arizona and Nevada. The collocation of these maxima with coastal areas and elevated terrain indicates the strong role surface features play in both forcing and suppressing convective activity during the day.

In contrast to the western and eastern U.S., cloud-to-ground lightning activity over the central U.S. is complex with significant latitudinal variations. We observe an east-to-west gradient of normalized amplitude values (from values greater than 140 to values less than 50) and a west-to-east gradient in time of maximum frequency (from 1800 LMT to 2100–0200 LMT) over the western Great Plains. Over the eastern Great Plains and upper Midwest, normalized amplitude values are less than 50 and harmonic dials shows little to no spatial continuity. Over the lower Midwest, middle and lower Mississippi Valley, and southern Texas, normalized amplitude values are greater than 50 and the time of maximum frequency occurs between 1500 and 1800 LMT.

We examine diurnal CG lightning activity over the central U.S. in greater detail by showing the diurnal marches of hourly CG flash count for five locations in the central U.S. separated by 2 to 4° longitude (Fig. 3.10). Figure 3.10 shows the transition from an afternoon regime (i.e., Denver) to an evening-nocturnal regime (i.e., North Platte) to an afternoon-nocturnal regime (i.e., Des Moines) and back to an afternoon regime (i.e., Peoria). We believe that these longitudinal variations have been accurately interpreted by McAnelly and Cotton (1989):

> Thunderstorms generally develop in the late afternoon east of the Rockies (or track off of the foothills), then track eastward into the nocturnal period, either decaying or persisting as long-lived MCSs. Further east in the regime (e.g., Iowa), thunderstorms are more variably associated with locally generated, late-afternoon convection, and with MCCs and MCSs at various nocturnal hours and stages of their lifecycle, including some that track all the way from the High Plains through the nocturnal period.

A number of physical mechanisms have been proposed to explain the tendency for convection to occur at night over the central U.S. including the nocturnal low-level jet (see Balling 1985 for a review).

Results from our examination of diurnal variations in cloud-to-ground lightning activity are consistent with results published in regional studies of cloud-to-ground lightning activity (e.g., Maier et al. 1984, Reap 1986; Lopez and Holle 1986; Reap and MacGorman 1989; Reap and Orville 1990; Reap 1994; Watson et al. 1994a). Our results are also consistent with results published in national studies of diurnal variations in thunderstorm frequency (e.g., Rasmusson 1971; Wallace 1975; Easterling and Robinson

1985). Results from our examination of annual and diurnal variations over the contiguous U.S. indicate that CG lightning activity is modulated by the annual and diurnal cycles of solar insolation over the most of the western and eastern U.S. Over the central U.S., CG lightning activity is generally modulated by the annual and diurnal cycles of solar insolation but significant portions of cloud-to-ground lightning are produced during the non-summer months over the south-central U.S. and during the nocturnal period over the eastern Great Plains and upper Midwest.

3.3. Positive and Negative Cloud-to-Ground Lightning Activity

3.3.1 Annual Positive CG Flash Density

Figure 3.11 shows annual positive CG flash density, averaged over 1995–97. Annual positive CG flash density values vary between 0.001 and 1.6 flashes km^{-2} over the contiguous U.S. Flash density values greater than 0.01 flashes km^{-2} cover almost all areas within the 80% detection efficiency contour. We observe a strong west-to-east gradient over the western Great Plains; flash density values increase from roughly 0.05 flashes km^{-2} over Rocky Mountains to 0.2 flashes km^{-2} over the Great Plains. We believe that this gradient is primarily due to the west-to-east gradient in the frequency of severe storms over the western Great Plains (Kelly et al. 1978; Kelly et al. 1985). The correlation between severe weather and elevated positive CG flash rates is well documented in climatological studies of severe weather (e.g., Reap and MacGorman 1989; Carey et al. 1997) and in case studies of severe storms (e.g., Curran and Rust 1992). Positive CG

flash density values are greater than 0.4 flashes km^{-2} over the southeastern U.S. and portions of the south-central U.S.

Maximum observed and corrected positive flash density values are found over southeastern U.S. Maximum observed flash density values are found over the Florida peninsula, the Gulf Coast, and the middle Mississippi Valley; flash density values range between 1.2 and 1.6 flashes km^{-2} over these areas. Maximum corrected flash density values are found along the Louisiana coast. We estimate corrected flash density values between 1.7 and 2.3 flashes km^{-2} using flash density values between 1.2 and 1.6 flashes km^{-2} and a detection efficiency value of 70%. Other flash density maxima in Fig. 3.11 are found over elevated terrain (e.g., Sierra Madre Occidental) and the Gulf Stream. We observe a minimum over the Columbia River basin. These observations indicate that surface features such as elevated and depressed terrain, coastlines, and the Gulf Stream can control the location and magnitude of positive CG lightning activity. Observations of positive flash density maxima and minima collocated with surface features have been reported in national studies of CG lightning activity (e.g., Orville 1994; Orville and Silver 1997).

We compared Fig. 3.11 with maps of annual positive CG flash density published in Orville (1994) and Orville and Silver (1997) for the individual years 1989–95 and found significant differences between maps for the years 1989–94 and maps for the years 1995–97. Maps for the years 1989–1994 show the national maximum to be located over the

central U.S. while maps for the years 1995–97 show the national maximum to be located over the southeastern U.S. We believe that this variation is due to the 1995 NLDN upgrade and may be related to the false detection of positive CG lightning. We discuss this topic in Appendix A.

3.3.2 Annual Percentage of Positive Polarity Lightning

Comparison of the map of positive CG flash density (Fig. 3.11) with the map of total CG flash density (Fig. 3.2) reveals that positive CG flash density values are generally an order of magnitude smaller than total flash density values (the national average is 9.6%; Table 3.1). The map of annual percentage of positive polarity lightning (Fig. 3.12) shows that percent positive polarity values vary between 0 and 25% over areas within the 80% detection efficiency contour. Percent positive polarity values range between 0 and 10% over the western and northeastern U.S. and between 10 and 25% over the central and southeastern U.S.

We observe a regional-scale maximum in the percentage of positive CG flashes over the north-central U.S. (values between 15 and 25%). This maximum has been observed in maps of annual percentage of positive polarity lightning since 1989 and has been attributed to the production of positive CG lightning by stratiform regions of MCSs or to the production of positive CG lightning by PSD storms (Orville 1994; Orville and Silver 1997). Results from our KFSD case study indicate that this maximum is due to the production of positive CG lightning by PSD storms.

We also observe maxima over localized areas in the southeastern U.S. (values greater than 15%). We believe that these maxima are due to the 1995 NLDN upgrade and may be related to the false detection of positive CG lightning. We note that the percentage of positive polarity lightning over the southeastern U.S. was less than 7% prior to the 1995 NLDN upgrade (Orville 1994; Orville and Silver 1997). This topic is discussed in Appendix A.

3.3.3 Annual Variations

We produced maps of the percentage of positive and negative CG lightning produced during June–August and compared these maps to the map of the percentage of total CG lightning produced during June–August (Fig. 3.6). The map of the percentage of negative CG lightning produced during June–August (not shown) and Fig. 3.6 show similar spatial patterns and values, indicating that the annual variations in negative CG lightning activity are similar to the annual variations in total CG lightning activity. In contrast, the map of the percentage of positive CG lightning produced during June–August (Fig. 3.13) and Fig. 3.6 shows similar spatial patterns but different values. A difference map of the fields plotted in Figs. 3.6 and 3.13 (not shown) shows that values plotted in Fig. 3.13 are 5 to 20% lower over the southwestern and south-central U.S., 5 to 35% lower over the southeastern U.S. (see Fig. 4.4 for an example), and 20 to 35% lower over the northeastern U.S.; values are similar in both maps over the northwestern and north-central U.S. (see Fig. 4.1 for an example). This difference map indicates that the

percentage of positive polarity lightning is a minimum during summer over most areas in the contiguous U.S. with the exceptions of the northwestern and north-central U.S. Other studies of CG lightning activity have shown that the percentage of positive polarity lightning reaches its minimum during summer (and its maximum during winter; e.g., Orville et al. 1987; Clodman and Chisholm 1996; Orville and Silver 1997). Clodman and Chisholm (1996) attributed the annual variation in the percentage of positive polarity lightning to increased vertical wind shear and lower cloud tops during winter, both of which enhance the production of positive CG lightning (Williams 1989; Engholm et al. 1990).

3.3.4 Diurnal Variations

We document the diurnal variations in positive and negative CG lightning activity with a map of the time lag between the diurnal cycles of positive and negative CG lightning frequency for June–August 1994–96 (Fig. 3.14). This map must be interpreted with care because time lag values are physically significant only if the diurnal cycle accurately describes the diurnal variations in positive and negative CG lightning activity. In our examination of Figs. 3.9 and 3.10, we found that the time of maximum frequency of the diurnal cycle is reasonably accurate over areas where normalized amplitude values are greater than 50. For this reason, we believe that time lag values are physically significant over most of the contiguous U.S. with the exception of the eastern Great Plains and upper Midwest (Fig. 3.9).

Figure 3.14 shows that positive CG lightning activity lags negative CG lightning activity by 0 to 2 hours over most of the contiguous U.S. with the exception of an area over the north-central U.S. where negative CG lightning activity lags positive CG lightning activity by 0 to 12 hours. The positive time lag observed over most of the contiguous U.S. (see Fig. 4.6 for an example) is consistent with observations of positive time lag in ordinary thunderstorms (e.g., Fuquay 1982), severe storms (e.g., Kane 1991), and in mesoscale convective systems (e.g., Rutledge and MacGorman 1988). The tendency for positive CG lightning activity to lag negative CG lightning activity has been explained using the tilted dipole (Brook et al. 1982), precipitation unshielding (Carey and Rutledge 1997), charge advection (Rutledge and MacGorman 1988), and in-situ charging (Rutledge et al. 1990) hypotheses. These hypotheses postulate physical processes which create a positive charge region and expose (or unshield) this positive charge region to ground.

Results from the KFSD case study show that the negative time lag observed over the north-central U.S. is real despite the low normalized amplitude values over this region (Fig. 3.9). The diurnal marches of hourly positive and negative CG flash count for the KFSD area (Fig. 4.2) show that the maximum frequency of positive CG lightning occurs five hours before the maximum frequency of negative CG lightning (i.e., 1800 LMT and 2300 LMT, respectively). Results from the KFSD case study indicate that the negative time lag observed over the north-central U.S. is due to the dominant production of positive (negative) CG lightning by late afternoon and evening PSD storms (nocturnal

storms). Note that the region of negative time lag is collocated with a maximum in the percentage of positive polarity lightning (Fig. 3.12).

3.2.5 Annual Mean Positive Peak Current

Figure 3.15 shows annual mean positive peak current, averaged over 1995–97. Annual mean positive peak current values vary between 10 and 50 kA over areas within the 80% detection efficiency contour (the national average is 25 kA; Table A1). Mean peak current values range between 10 and 30 kA over the southern U.S.. Over the northern U.S., mean peak current values range between 30 and 50 kA with the exceptions of the northern Rocky Mountains and the lower Midwest where mean peak current values range between 20 and 30 kA.

We observe a regional-scale maximum in mean positive peak current over the north-central U.S. (values between 40 and 50 kA). This maximum is collocated with a maximum in the percentage of positive polarity lightning (Fig. 3.12) and with a region characterized by negative time lag (Fig. 3.14). The correlation between the percentage of positive polarity lightning and positive peak current over the north-central U.S. has been noted previously by Lyons (1996). Lyons (1996) speculated that this correlation could be related to the production of positive CG lightning and sprites by stratiform regions of MCSs or to the production of positive CG lightning by PSD storms. Results from the KFSD case study indicate the correlation between the percentage of positive polarity

lightning and positive peak current over the north-central U.S. is due to the production of high peak current positive CG lightning by PSD storms.

We believe that the low mean positive peak current values observed over the southeastern U.S. (values between 10 and 20 kA) are due to the 1995 NLDN upgrade and may be related to the false detection of positive CG lightning. We note that mean annual positive peak current values ranged between 20 and 40 kA over these same areas in 1994 (map not shown). This topic is discussed in Appendix A.

The increase of mean positive current values towards the continental borders is likely due to the fact that low peak current CG flashes are not detected over these areas. Low peak current CG flashes emit weak signals and, thus, are not identified by enough sensors to be located by the NLDN central processor. The detection of fewer CG flashes towards the continental borders would explain the decrease of NLDN detection efficiency over these areas (Fig. 2.2).

We compared the information plotted in Figs. 3.15 with results from regional studies of CG lightning activity (e.g., Orville et al. 1987; Reap and MacGorman 1989; Orville 1990a; Lopez et al. 1991). Our comparison revealed an overall lack of agreement; the peak current values reported in this study were generally less than those reported in the studies listed above. We believe that this lack of agreement is due to the high

sensitivity of the NLDN relative to the lightning location networks utilized in the other studies.

Table 3.1 Annual lightning statistics for 1995–97. Statistics were calculated using all flashes detected by the NLDN. Peak current values are given in kiloamps.

Year	Total Count ($\times 10^3$)	Positive Count ($\times 10^3$)	Percent Positive Polarity
1995	19,273	1,642	8.5
1996	25,877	2,583	10.0
1997	26,817	2,729	10.2
Average 1995–97	23,865	2,297	9.6

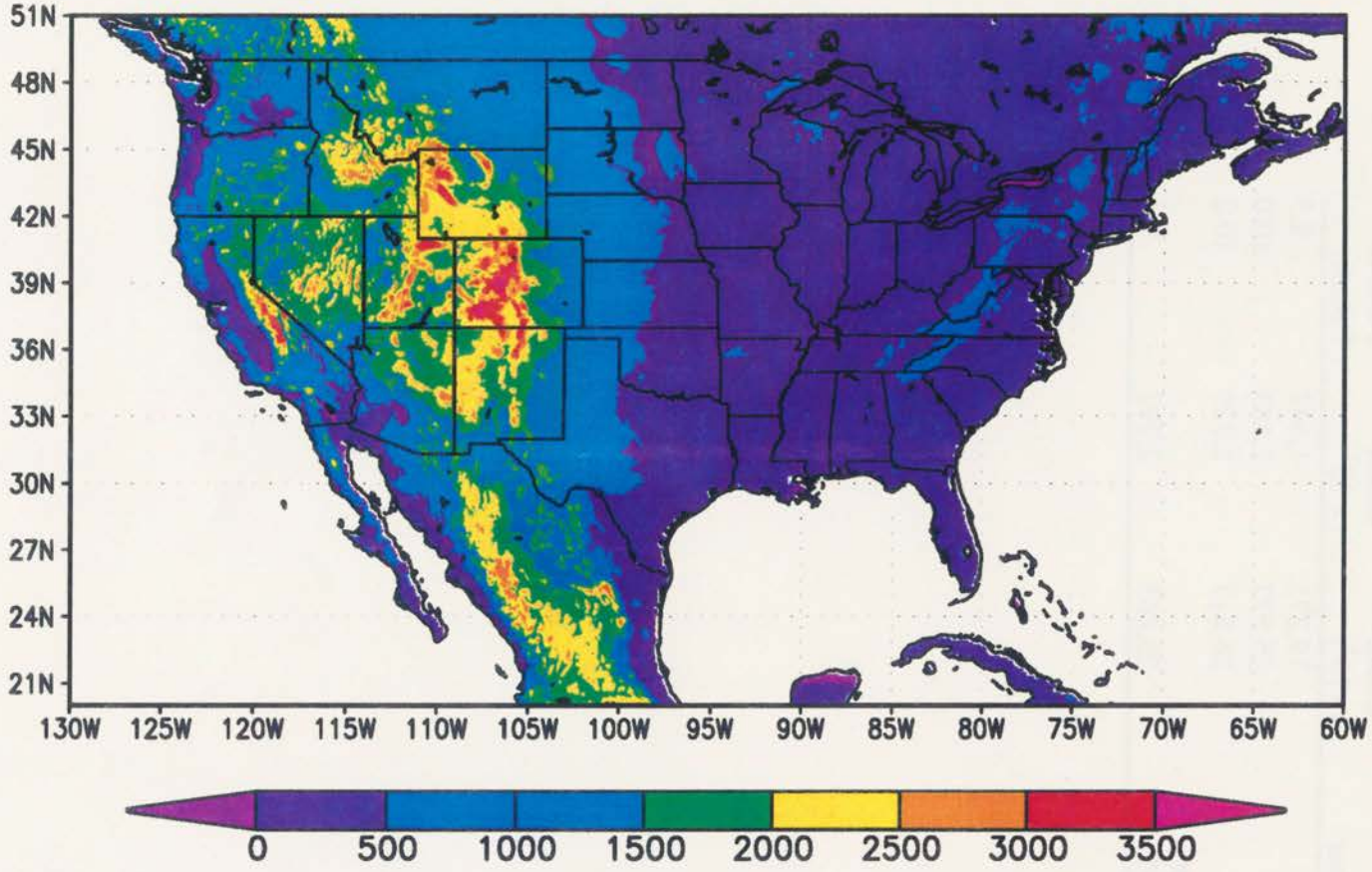

Figure 3.1 Topography of the contiguous United States. Elevation is given in meters above sea level.

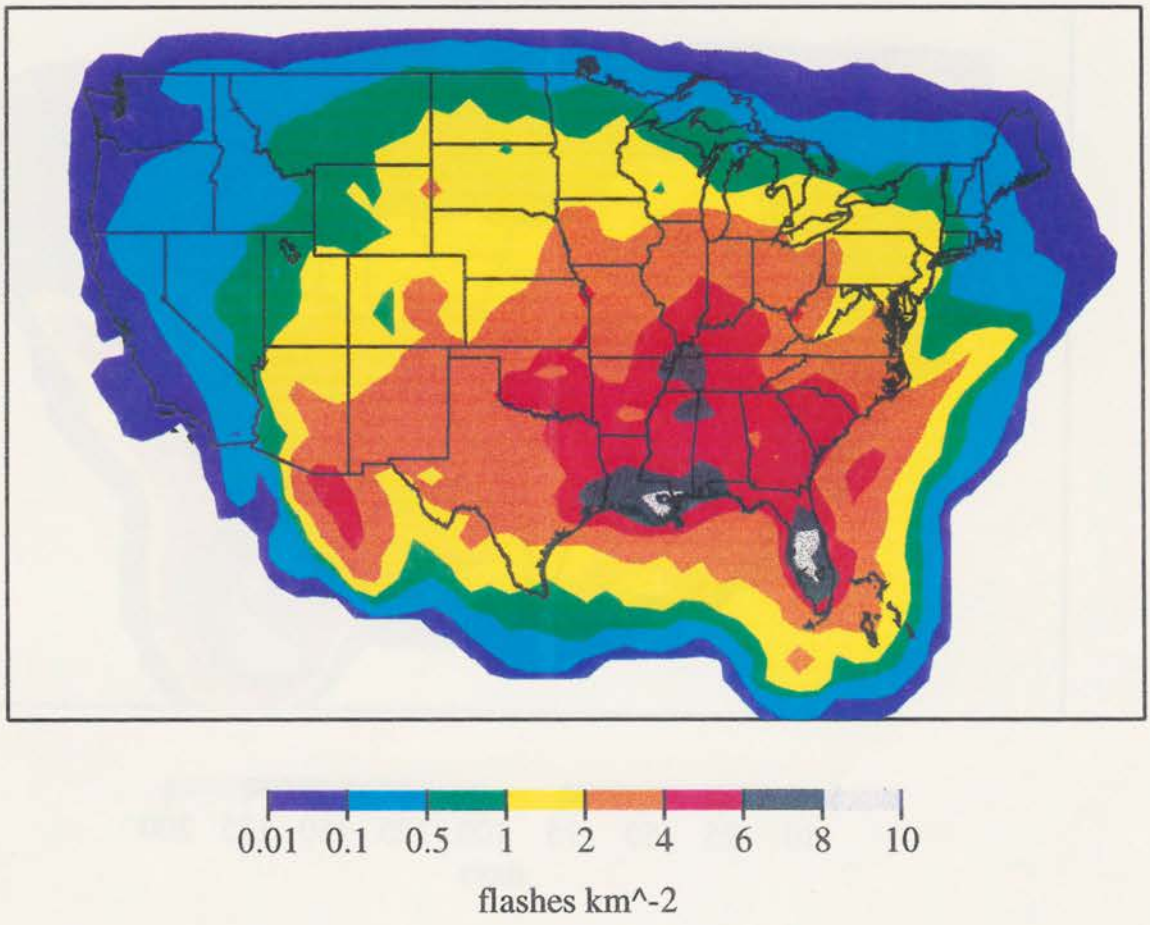

Figure 3.2 Annual CG flash density, averaged over 1995-97. Flash density values were not modified in order to account for detection efficiency values less than one.

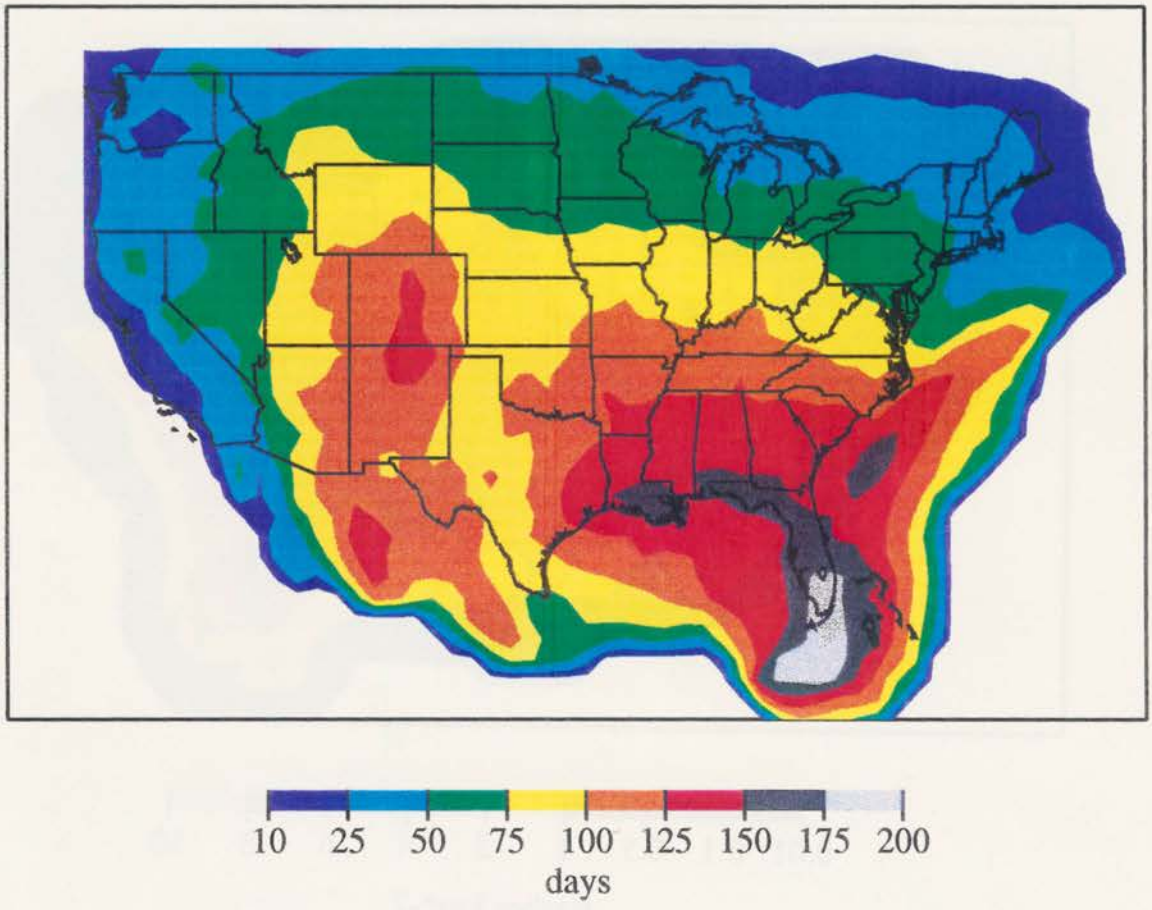

Figure 3.3 Annual number of days with one or more CG flashes, averaged over 1995-97.

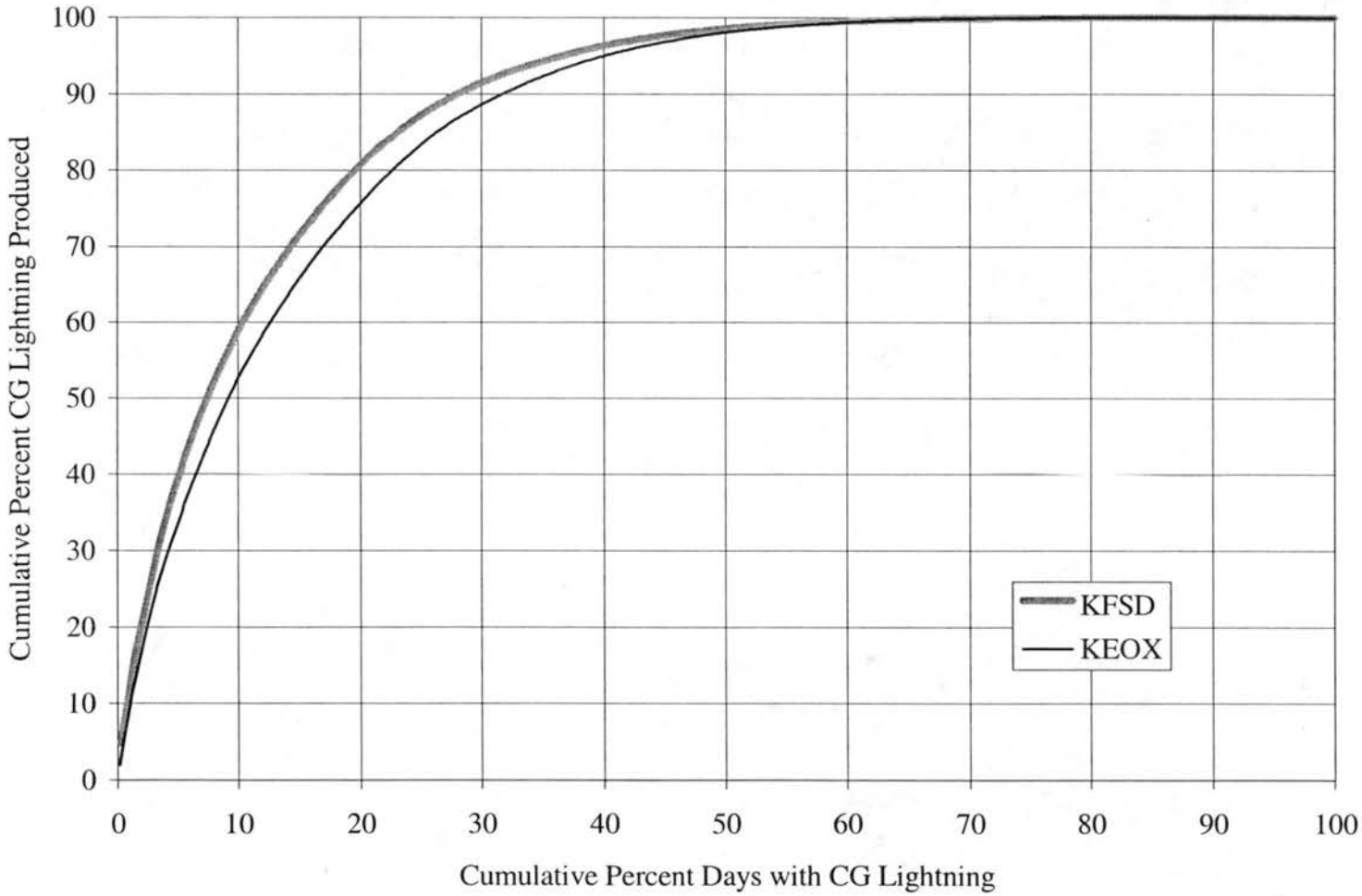

Figure 4.6 Cumulative frequency distributions of daily CG count for KFSD and KEOX, 1994–96.

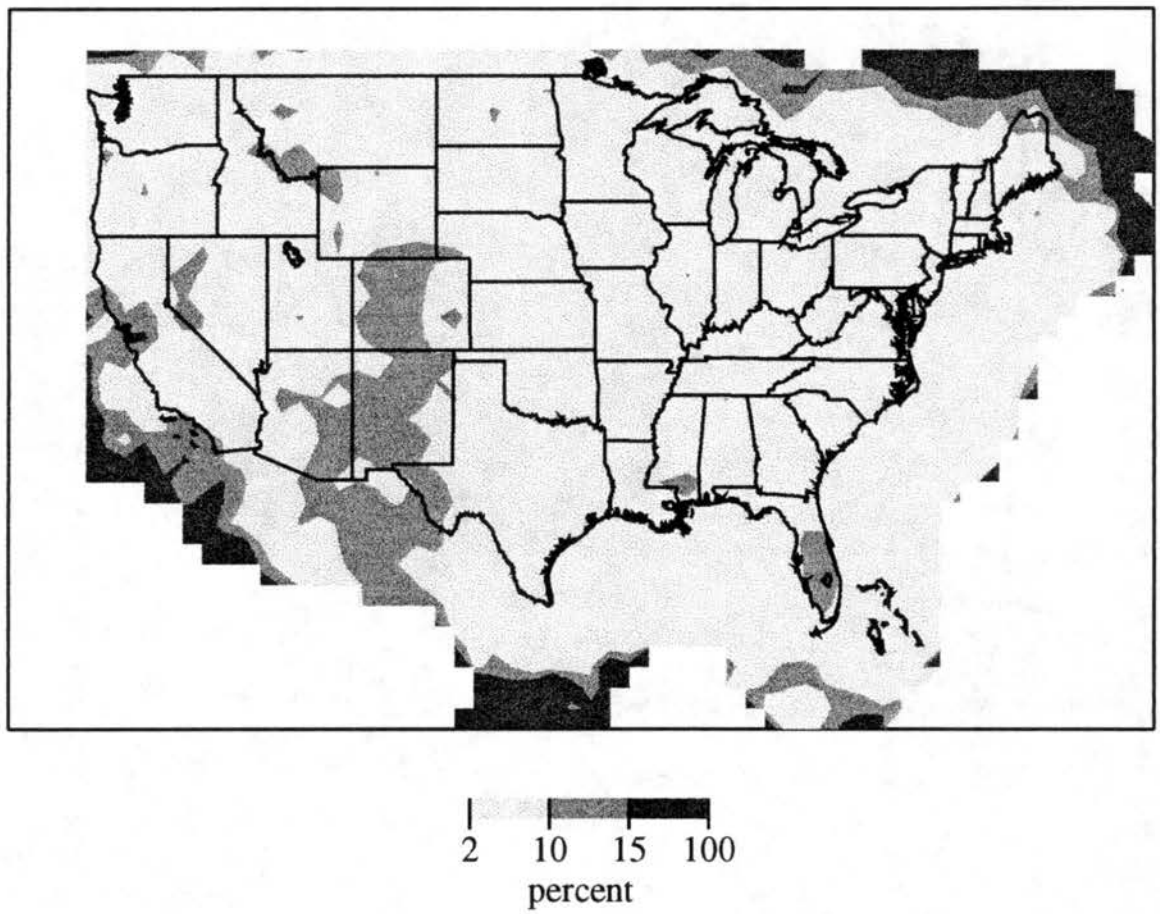

Figure 3.5 Percent cumulative number of days with cloud-to-ground lightning to produce 50% of cloud-to-ground lightning from 1995-97.

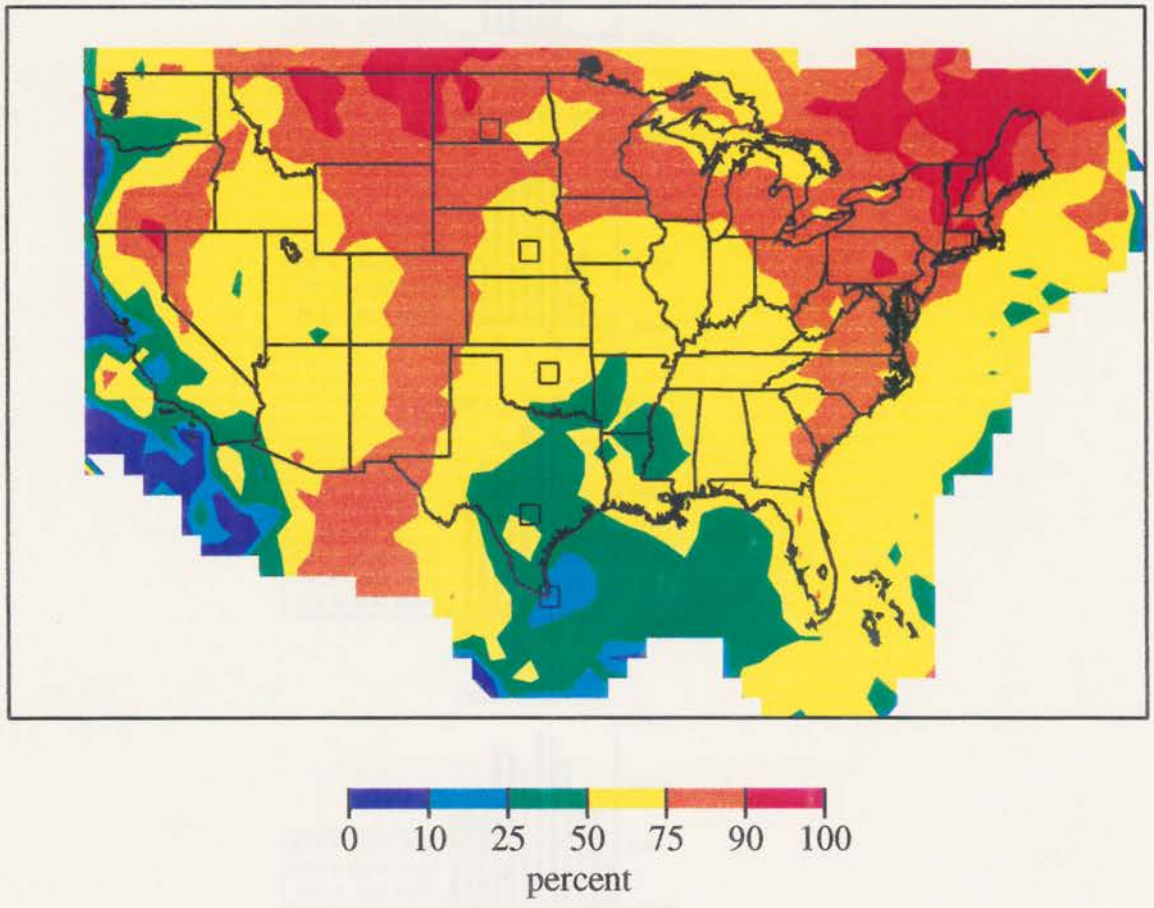

Figure 3.6 Percentage of cloud-to-ground lightning produced during June-August, averaged over 1995-97. Boxes show the locations of grid elements examined in Fig. 3.7.

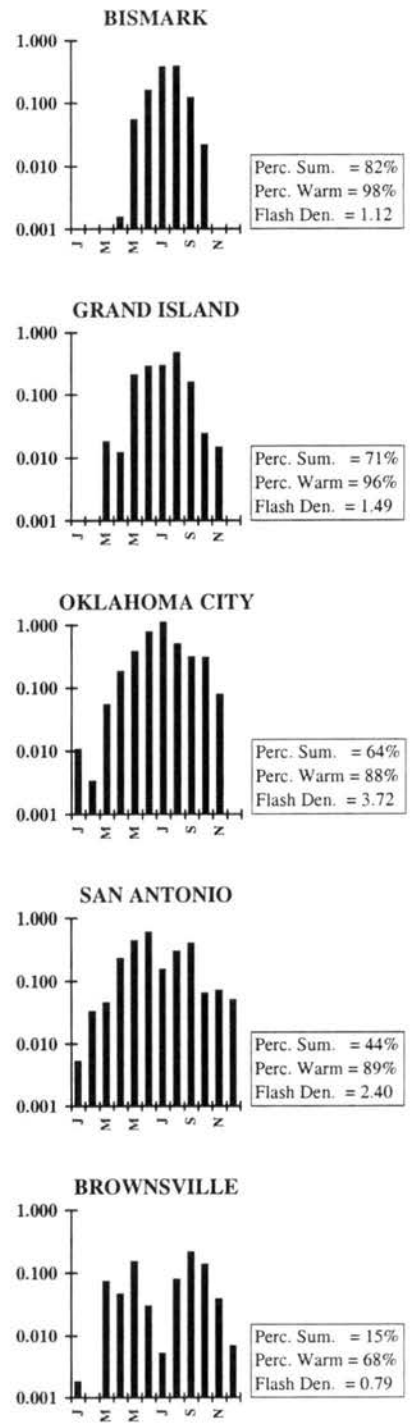

Figure 3.7 Annual marches of monthly CG flash density for select grid elements, averaged over 1995-97. Note the use of a logarithmic scale on the ordinate. The percentage of cloud-to-ground lightning produced during summer (June-August) and during the warm season (April-September) and the annual CG flash density for each grid element are listed. Locations of grid elements are shown in Fig. 3.6.

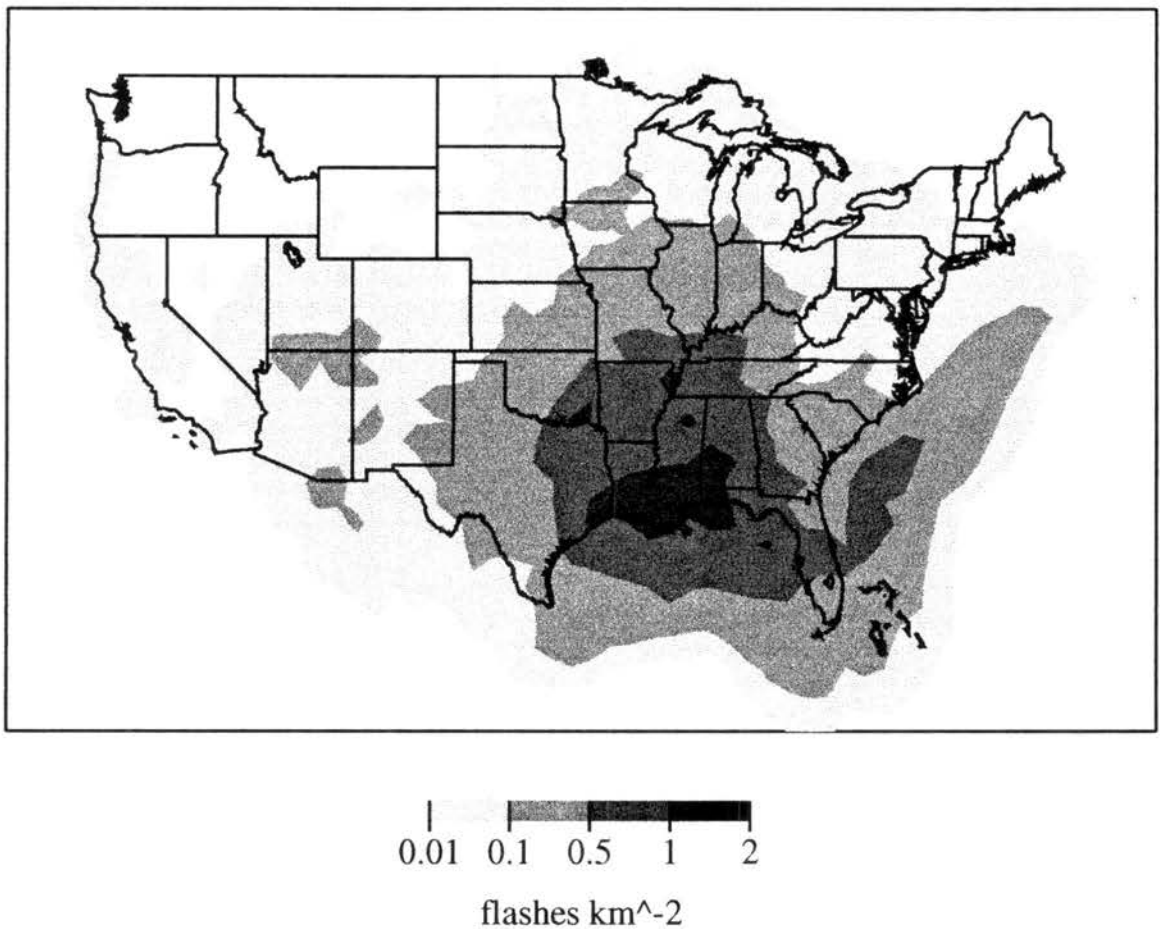

Figure 3.8 Cloud-to-ground flash density for October-March, averaged over 1995-97. Flash density values were not modified in order to account for detection efficiency values less than one.

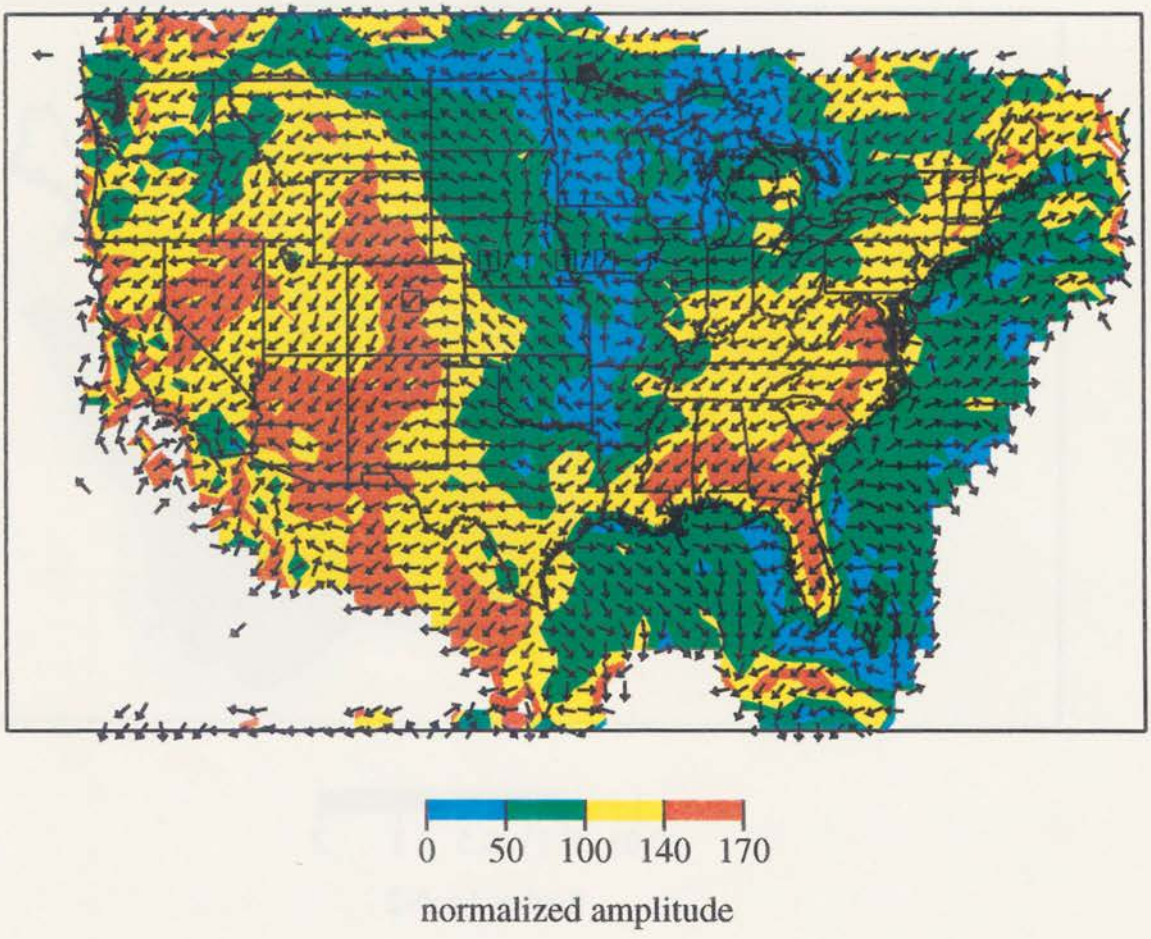

Figure 3.9 Normalized amplitude and phase of the diurnal cycle of CG lightning frequency for June-August 1994-96. Normalized amplitude values are contoured. The time of the maximum frequency of the diurnal cycle is indicated with harmonic dials. Harmonic dials behave like a 24-hour clock and point to the time of maximum frequency: an arrow pointing to the north indicates a maximum of the diurnal cycle at 0000 LMT (local mean solar time); an arrow pointing to the east indicates a maximum of the diurnal cycle at 0600 LMT; etc. Boxes show the locations of grid elements examined in Fig. 3.10.

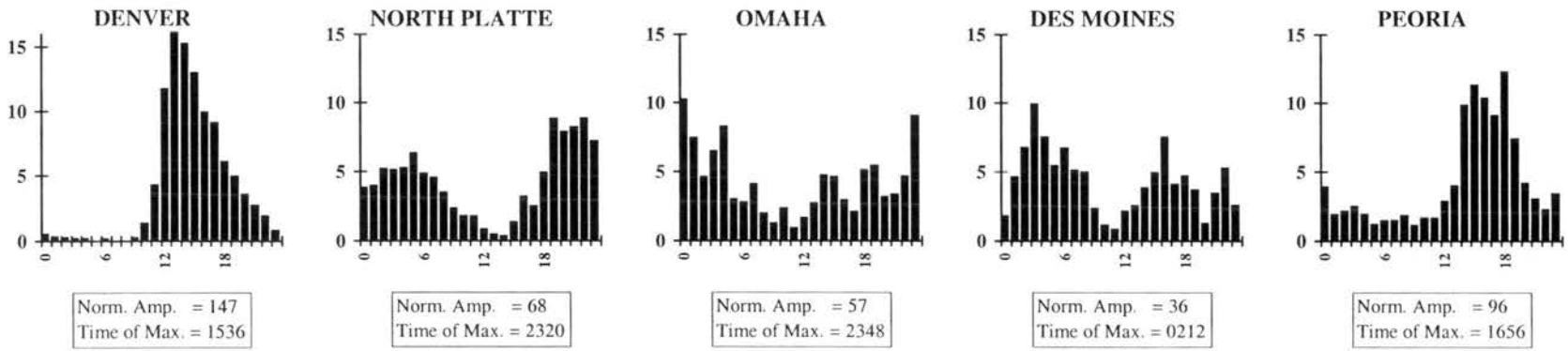

Figure 3.10 Diurnal marches of normalized hourly CG flash count for select grid elements, June-August 1994-96. The normalized amplitude and phase (i.e., the time of maximum frequency) of the diurnal cycle of CG lightning frequency for each grid element are listed. Locations of grid elements are shown in Fig. 3.9.

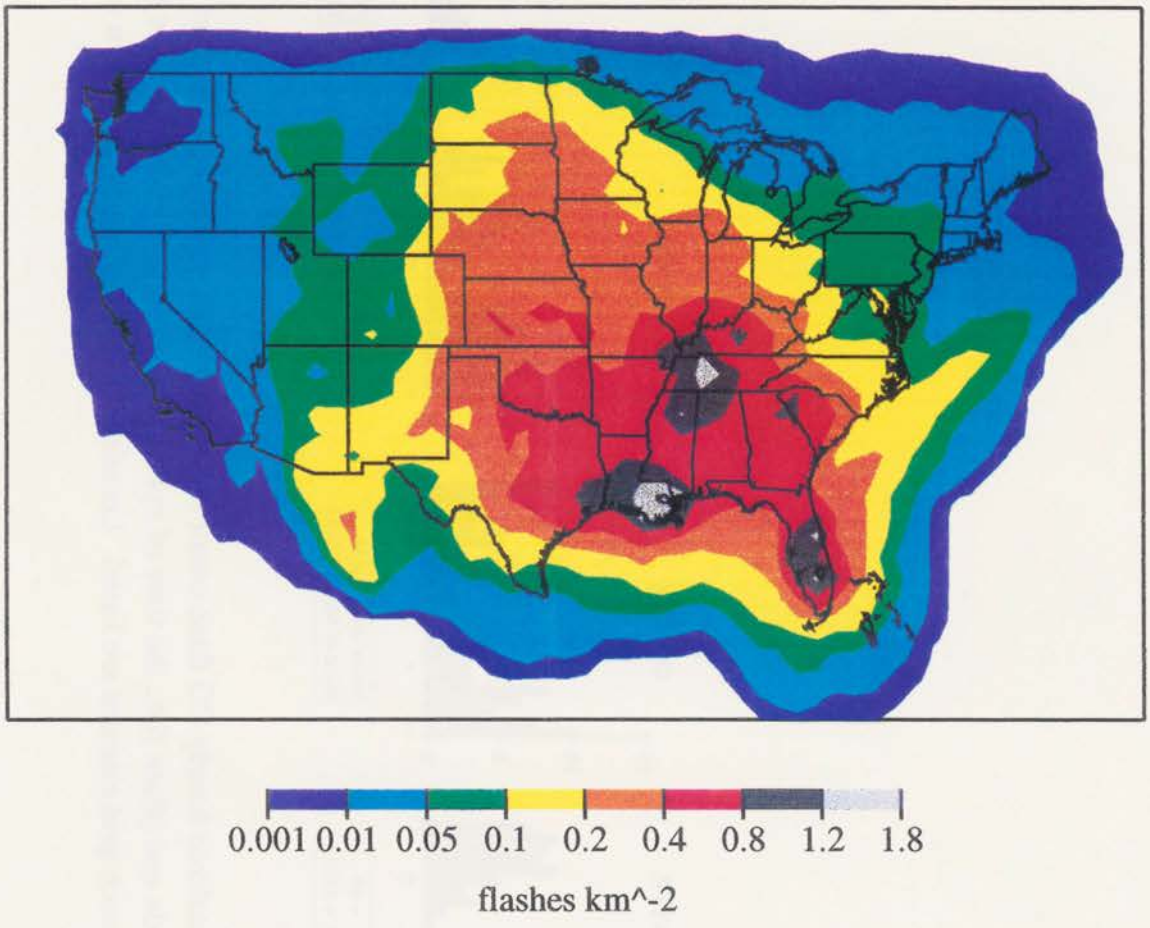

Figure 3.11 Annual positive CG flash density, averaged over 1995-97. Flash density values were not modified in order to account for detection efficiency values less than one.

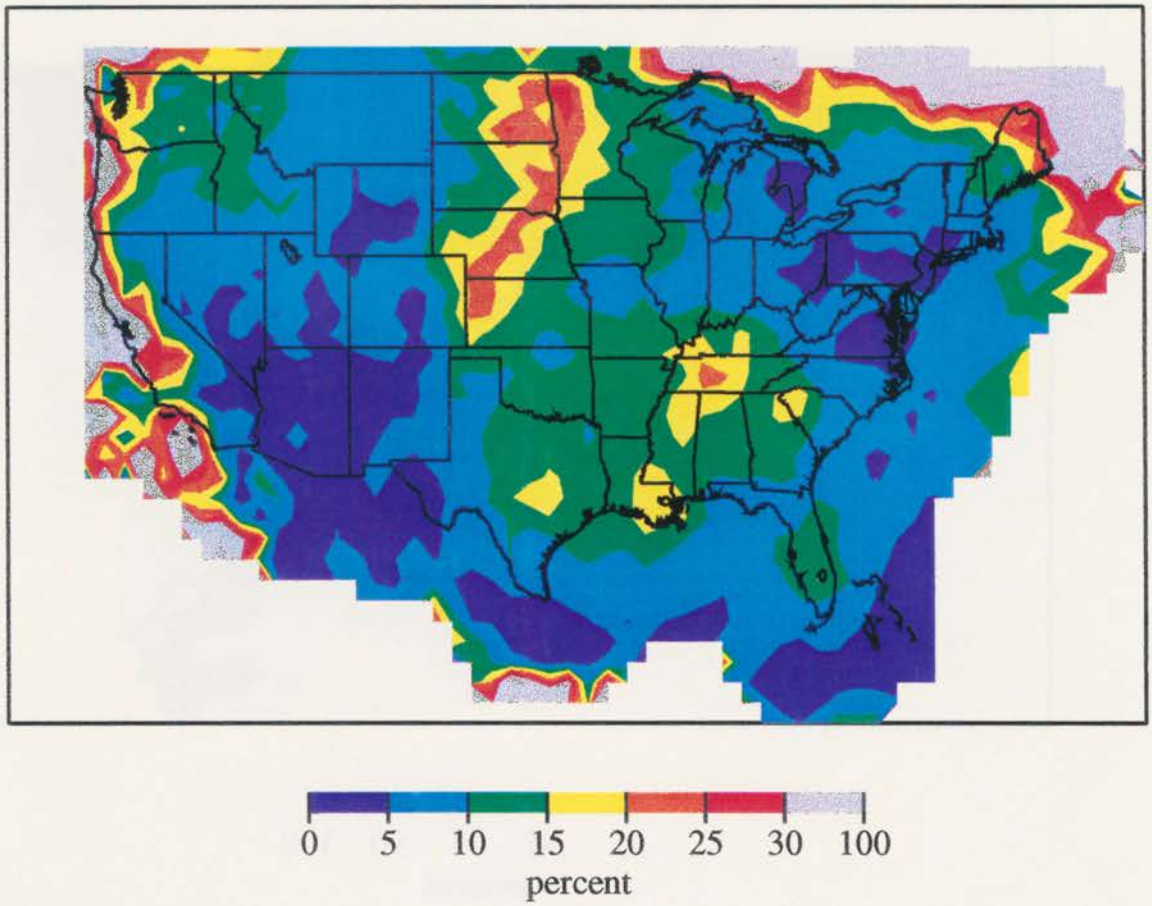

Figure 3.12 Annual percentage of positive polarity lightning, averaged over 1995-97.

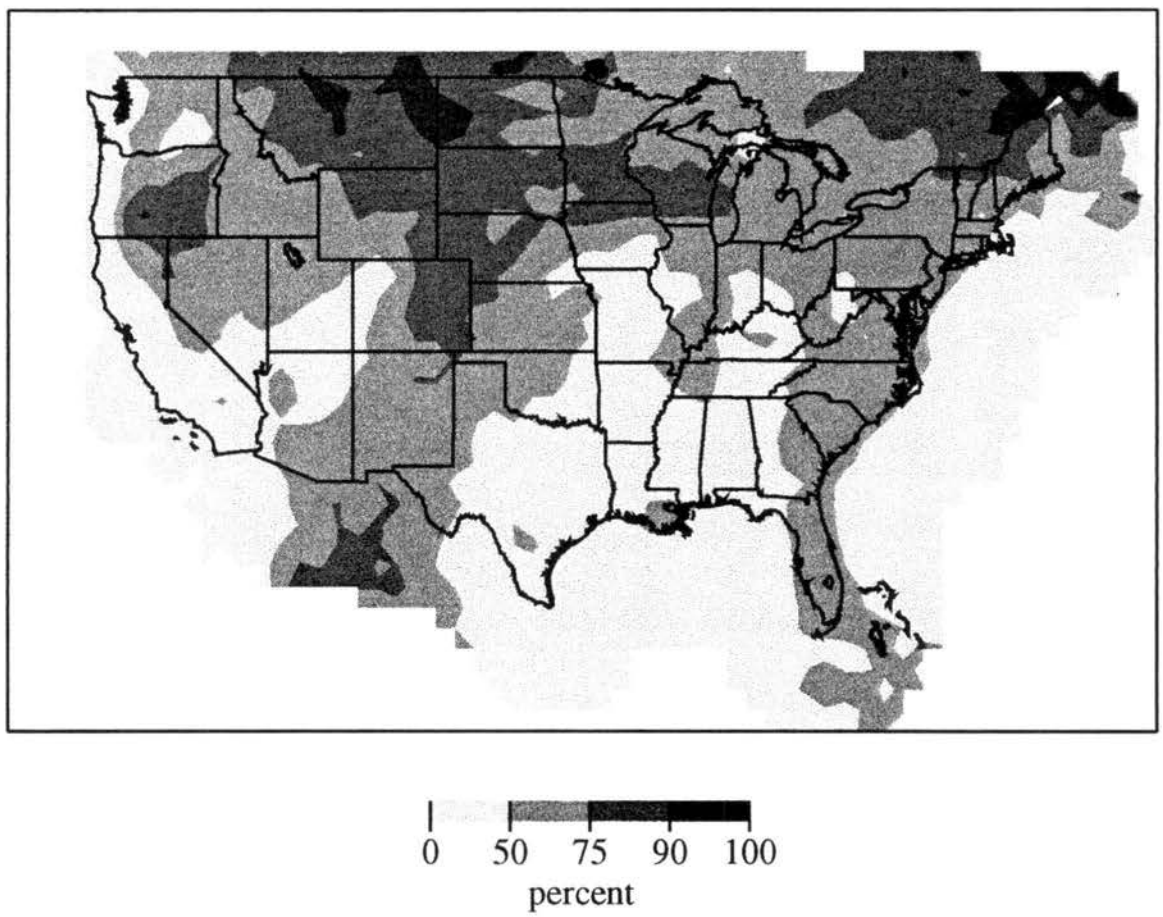

Figure 3.13 Percentage of positive cloud-to-ground lightning produced during June-August, averaged over 1995-97.

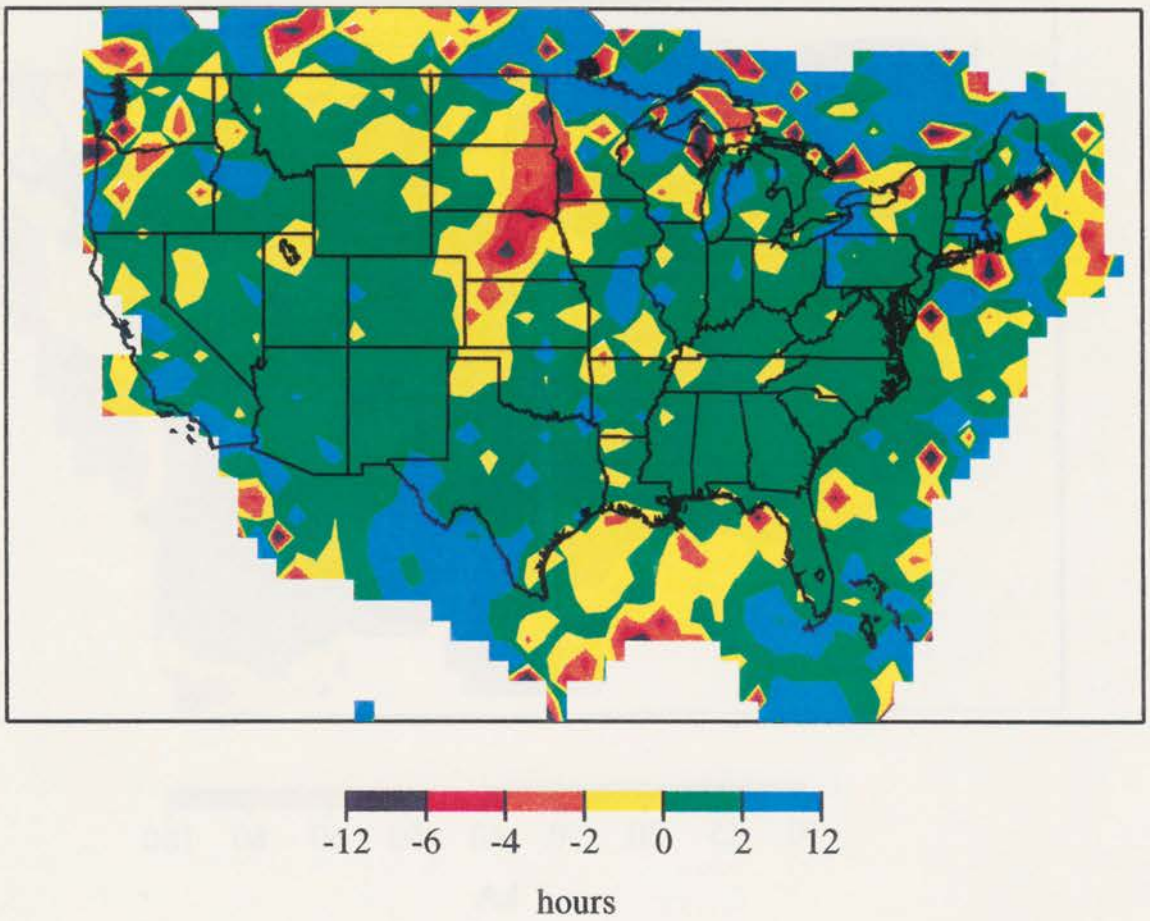

Figure 3.14 Time lag between the diurnal cycles of positive and negative CG lightning frequency for June-August 1994-96. Time lag values greater than zero indicate that the time of maximum positive CG lightning frequency occurred after the time of maximum negative CG lightning frequency.

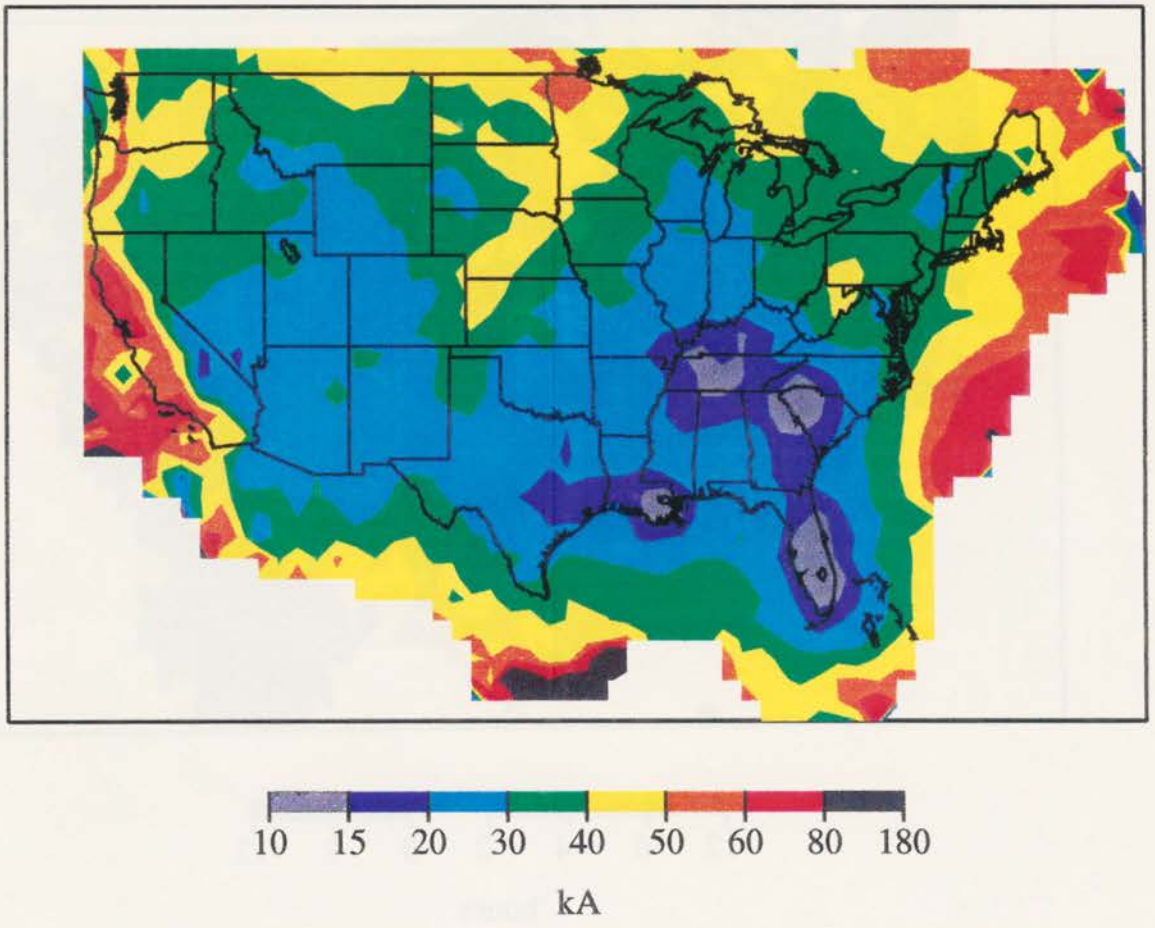

Figure 3.15 Annual mean positive peak current, averaged over 1995-97. Peak current values are given in kiloamps.

CHAPTER 4

CASE STUDIES

4.1 KFSD Case Study

4.1.1 Annual and Diurnal Variations

Figure 4.1 shows that the annual marches of monthly positive and negative CG flash count over the KFSD area exhibit an annual cycle with a strong summertime maximum; roughly 75% of positive and negative CG lightning is produced during summer. These observations indicate that the annual production of positive and negative CG lightning over the north-central U.S. are similar, as suggested in Figs. 3.6 and 3.13.

Figure 4.2 shows that the diurnal marches of hourly positive and negative CG flash count over the KFSD area are dissimilar. While both diurnal marches exhibit a diurnal cycle, maximum hourly positive CG flash count occurs roughly five hours before the maximum hourly negative CG flash count (i.e., 1800 LMT versus 2300 LMT). These observations suggest that the negative time lag observed over much of the north-central U.S. in Fig. 3.14 is due to the dominant production of positive (negative) CG lightning during the late afternoon and evening (the nocturnal period). We will show below that the negative time lag observed over the KFSD area is due to diurnal variations in convective type.

We observe significant diurnal variations in the percentage of positive polarity lightning, mean positive peak current, and mean negative multiplicity over the KFSD area during summer (Fig. 4.3). The diurnal marches of hourly percent positive polarity and hourly mean positive peak current exhibit a diurnal cycle with a late afternoon maximum and a morning minimum; positive polarity values and mean positive peak current values vary between 7 and 30% and 31 and 62 kA, respectively. The diurnal march of hourly mean negative multiplicity exhibits a diurnal cycle with a morning maximum and an early evening minimum; mean negative multiplicity values vary between 2.13 and 2.54. We will show below that these diurnal variations are due to diurnal variations in convective type.

4.1.2 Radar and Lightning Analysis

In this section, we examine the lightning statistics, positive cloud-to-ground lightning characteristics, and the radar echo characteristics of 21 convective events observed over the KFSD case study area during 1996. These 21 convective events produced roughly 75% of the positive and negative CG lightning observed over the KFSD area during 1996 (Table 4.1).

We examined the lightning statistics of the 21 convective events observed over the KFSD area during 1996 (Table B1) and found distinct differences between the lightning characteristics of evening events and nocturnal events[†]. Table 4.1 shows that evening

[†] The classification of evening events and nocturnal events is based on the time of maximum positive CG lightning production for each event. The time of maximum positive CG lightning production of evening events (nocturnal events) occurs between 1100 and 2300 CST (2300 and 1100 CST).

events are characterized by high percent positive polarity values (32%), high mean positive peak current values (54 kA), and low mean negative multiplicity values (2.04). In contrast, nocturnal events are characterized by low percent positive polarity values (10%), low mean positive peak current values (25 kA), and high mean negative multiplicity values (2.33). Table 4.1 also shows that evening events produced 53% of the positive CG lightning over the KFSD area during 1996 but only 27% of negative CG lightning; nocturnal events produced 47% of the positive CG lightning over the KFSD area during 1996 but only 25% of negative CG lightning. These observations are consistent with the diurnal variations observed in Fig. 4.3 and the negative time lag observed in Figs. 4.2 and 3.14. In addition, these observations suggest that the maximum in the percentage of positive polarity lightning and the maximum in mean positive peak current observed over the north-central U.S. in Figs. 3.12 and 3.15, respectively, are due to the significant production of high peak current positive CG lightning by evening events.

We examined the production of positive cloud-to-ground lightning by evening events and found some interesting results. Positive strike dominated storms were identified in 11 of 12 evening events at the time of maximum positive CG lightning production (Table 4.2). In fact, two or more PSD storms were observed in each of these 11 events at the time of maximum positive CG lighting production (a total of 46 PSD storms were observed). Our examination of CG plots over the lifecycle of evening events indicates that PSD storms dominated positive CG lightning production and contributed significantly to negative CG lightning production. For this reason, we attribute the lightning characteristics of evening events (i.e., high percent positive polarity values, high

positive peak current values, low negative multiplicity values) to PSD storms. These lightning characteristics have been documented in individual PSD storms (e.g., the Plainfield storm before polarity reversal; Seimon 1993). These observations suggest that the maxima observed over the north-central U.S. in Figs. 3.12 and 3.15 are due to PSD storms. We should note that our examination of CG plots over the lifecycle of nocturnal events indicated that PSD storms did not contribute significantly to the production of positive or negative CG lightning.

Bipolar lightning patterns were observed over the KFSD case study area in both evening events and nocturnal events. Our examination of CG plots and national radar summaries over the lifecycle revealed that three evening events and four nocturnal events exhibited bipolar lightning patterns (Table 4.2). The contribution of bipolar lightning to positive CG lightning production over the KFSD area was found to be small because most convective events propagated over the KFSD area (from west to east) before developing stratiform regions.

Evening events and nocturnal events exhibited similar radar echo characteristics at the time of maximum positive CG lightning production and at the maximum level of organization. Evening events and nocturnal events spanned a broad range of convective structures at the time of maximum positive CG lightning production and evening events and nocturnal events were frequently classified as MCSs with areally-extensive stratiform regions at their maximum level of organization (Table 4.2). These observations indicate that evening events and nocturnal events were both associated with MCSs at various

stages of development. However, we did observe differences between the radar echo characteristics of evening events and nocturnal events at the time of maximum positive CG lightning production. Evening events tended to exhibit cellular structures (i.e., isolated convective cells, line of cells, broken line) and linear organization more frequently than nocturnal events (Table 4.2). These observations indicate that evening events (and the production of positive CG lightning) tended to be associated with more formative stages of MCS development while nocturnal events (and the production of negative CG lightning) tended to be associated with more mature stages of MCS development. We believe that these observations are related to the timing and lightning production of severe storms and MCSs over the central U.S. Severe storms can be prolific producers of positive CG lightning (e.g., Stolzenburg 1994) and tend to occur during the late afternoon and early evening (e.g., Kelly et al. 1978; Kelly et al. 1985) and during the formative stages of MCSs (e.g., Maddox et al. 1986). In contrast, MCSs can be prolific producers of negative CG lightning and tend to occur during the nocturnal period (e.g., Goodman and MacGorman 1986).

Based on results from the KFSD case study, we propose that the three signals observed over the north-central U.S. in Figs. 3.12, 3.14, and 3.15 are 1) related to the climatological lifecycle of convective activity over the north-central U.S. and 2) represent areas over which PSD storms dominate positive lightning production. In the lee of the Rocky Mountains, diurnally- and topographically-forced ordinary thunderstorms dominate the production of positive CG lightning. Over the western Great Plains, these ordinary thunderstorms have either decayed or are organizing into MCSs. It is over this region and

during the formative stages of MCSs that PSD storms are able to dominate positive CG lightning production. Over the eastern Great Plains, MCSs have developed to the extent that the production of positive CG lightning by MCSs exceeds the production of positive CG lightning by PSD storms. While our hypothesis is consistent with climatological studies of thunderstorms, precipitation, severe weather, and MCSs over the central U.S. (e.g., Wallace 1975; McAnelly and Cotton 1989), more research on CG lightning activity over the central U.S. is needed to verify, disprove, or refine this hypothesis.

4.2 KEOX Case Study

4.2.1 Annual and Diurnal Variations

Figure 4.4 shows that the annual marches of positive and negative CG flash count over the KEOX case study area are dissimilar. While 68% of negative CG lightning is produced during summer, only 37% of positive CG lightning is produced during summer. These observations substantiate the differences in the summertime production of total and positive CG lightning depicted in Figs. 3.6 and 3.13.

The strong summertime production of negative CG lightning and the production of positive CG lightning throughout the year causes a significant annual variation in the percentage of positive polarity lightning. Figure 4.5 shows that the annual march of monthly percent positive polarity exhibits an annual cycle with a wintertime maximum; percent positive polarity values vary between 4% during summer to 25% during winter. We observe similar trends in the annual march of monthly mean positive peak current; mean positive peak current values vary between 19 kA in late summer and 48 kA in late

winter (Fig. 4.5). We will show below that these annual variations are due to the seasonal variation in convective type over the KEOX area.

Figure 4.6 shows that positive and negative CG lightning activity over the KEOX area during summer is modulated by the diurnal cycle with an afternoon maximum. Figure 4.6 also shows that positive CG lightning activity lags negative CG lightning activity by roughly an hour. These observations, including the positive time lag, are consistent with observations of CG lightning activity in diurnally-forced ordinary thunderstorms (e.g., Fuquay 1982) and diurnally-forced severe storms (e.g., Kane 1991).

4.2.2 Radar and Lightning Analysis

In this section, we examine the lightning statistics, positive cloud-to-ground lightning characteristics, and the radar echo characteristics of 25 convective events observed over the KEOX case study area during 1996. These 25 convective events produced roughly 55% (35%) of the positive (negative) CG lightning observed over the KEOX area during 1996 (Table 4.3).

We examined the radar echo characteristics of 25 convective events observed over the KEOX area during 1996 (Table B2) and found a strong seasonal variation in convective type. We found that events classified as MCSs occurred between November and May and that events not classified as MCSs (i.e., non-MCSs) occurred between April and September and were diurnally-forced with maximum CG lightning activity at 1500 LMT (Table 4.4). The seasonal variation in convective type can account for annual

variations in the percentage of positive polarity lightning and mean positive peak current observed over the KEOX area (Fig. 4.5). Table 4.3 shows that the percent positive polarity values and mean positive peak current values of MCSs (23% and 35 kA, respectively) are significantly greater than the percent positive polarity values and mean positive peak current values of non-MCSs (11% and 17 kA, respectively). The annual variation in the percentage of positive polarity lightning over the KEOX area can also be attributed to annual variations in vertical wind shear and cloud top height; increased vertical wind shear and decreased cloud top height during the cold season will tend to enhance the production of positive CG lightning (Clodman and Chisholm 1996).

Bipolar lightning patterns were observed over the KEOX case study area. Our examination of CG plots over the lifecycle of all 25 convective events indicates that almost all MCSs exhibited bipolar lightning patterns (Table 4.4). Bipolar lightning produced a significant portion of positive CG lightning over the KEOX area; most MCSs were mature and producing bipolar lightning as they propagated over the KEOX area (from west to east).

We identified only one positive strike dominated storm over the KEOX area in our examination of CG plots for all 25 convective events (Table 4.4). We believe that this number may significantly underestimate the actual number of severe storms that occurred during the time periods we examined. Results reported in Carey et al. (1997) indicate that PSD storms are a poor proxy for severe weather over the eastern U.S.

Table 4.1 Lightning statistics for the KFSD case study area: annual statistics for 1996, statistics for all 20 events sampled during 1996, and statistics for events classified as evening events (12) and as nocturnal events (9). Peak current values are given in kiloamps. See text for details.

Event Type	Total Flash Density (km^{-2})	Percent Positive Polarity	Positive			Negative		
			Flash Density (km^{-2})	Mean Peak Current	Mean Multi-plicity	Flash Density (km^{-2})	Mean Peak Current	Mean Multi-plicity
1996	1.86	19.1	0.36	43.8	1.12	1.50	24.1	2.19
All Events	1.38	19.8	0.27	44.9	1.12	1.11	23.6	2.23
Evening Events	0.59	32.2	0.19	53.9	1.14	0.40	23.5	2.04
Nocturnal Events	0.80	10.7	0.09	25.1	1.09	0.71	23.7	2.33

Table 4.2 Radar echo and positive cloud-to-ground lightning characteristics of 12 evening events and 9 nocturnal events sampled over the KFSD case study area during 1996. Convective type was determined at the time of maximum positive CG lightning production (TMP) for each event. See text for details.

Evening Events (12)
Convective Type
isolated convective cells (2)
line of cells (2)
broken line (4)
contiguous line (2)
LL/TS MCS (2)
Maximum Level of Organization
9 of 12 events were classified as MCSs (7 LL/TS MCSs)
Positive Cloud-to-Ground Lightning
11 of 12 events contained PSD storms at the TMP
3 of 12 events exhibited bipolar lightning patterns
Nocturnal Events (9)
Convective Type
broken line (3)
contiguous line (1)
cluster of cells (2)
LL/TS MCS (1)
MCS cluster (2)
Maximum Level of Organization
6 of 9 events were classified as MCSs (5 MCS clusters)
Positive Cloud-to-Ground Lightning
2 of 9 events contained PSD storms at the TMP
4 of 9 events exhibited bipolar lightning patterns

Table 4.3 Lightning statistics for the KEOX case study area: annual statistics for 1996, statistics for all 25 events sampled during 1996, and statistics for event classified as MCSs (12) and events not classified as MCSs (i.e., non-MCSs; 13). Peak current values are given in kiloamps. See text for details.

			Positive			Negative		
Event Type	Total Flash Density (km^{-2})	Percent Positive Polarity	Flash Density (km^{-2})	Mean Peak Current	Mean Multi-plicity	Flash Density (km^{-2})	Mean Peak Current	Mean Multi-plicity
1996	5.05	10.8	0.54	25.5	1.11	4.51	26.9	2.34
All Events	1.82	16.5	0.30	28.9	1.11	1.52	27.1	2.33
MCSs	0.88	22.5	0.20	35.2	1.11	0.68	28.5	2.19
Non-MCSs	0.94	11.0	0.10	16.9	1.11	0.84	25.9	2.44

Table 4.4 Radar echo and positive cloud-to-ground lightning characteristics of 12 MCS events and 13 non-MCS events sampled over the KFSD case study area during 1996. Convective type was determined at the time of maximum positive CG lightning production (TMP) for each event. See text for details.

MCS Events (12)
Convective Type
LL/TS MCS (10)
MCS cluster (2)
Temporal Variations
all events occurred between November and May
no significant diurnal variation
Maximum Level of Organization (MLO)
all events were classified at their MLO at the TMP
Positive Cloud-to-Ground Lightning
0 of 12 events contained PSD storms at the TMP
11 of 12 events exhibited bipolar lightning patterns
Non-MCS Events (12)
Convective Type
isolated convective cells (4)
short-lived line (3)
broken line (2)
contiguous line (4)
Temporal Variations
all events occurred between April and September
strong diurnal variation
maximum CG lightning activity at 1500 LMT
Maximum Level of Organization (MLO)
12 of 13 events were classified at their MLO at the TMP
one event was classified as an MCS cluster at its MLO
Positive Cloud-to-Ground Lightning
1 of 13 events contained PSD storms at the TMP
one event exhibited bipolar lightning patterns

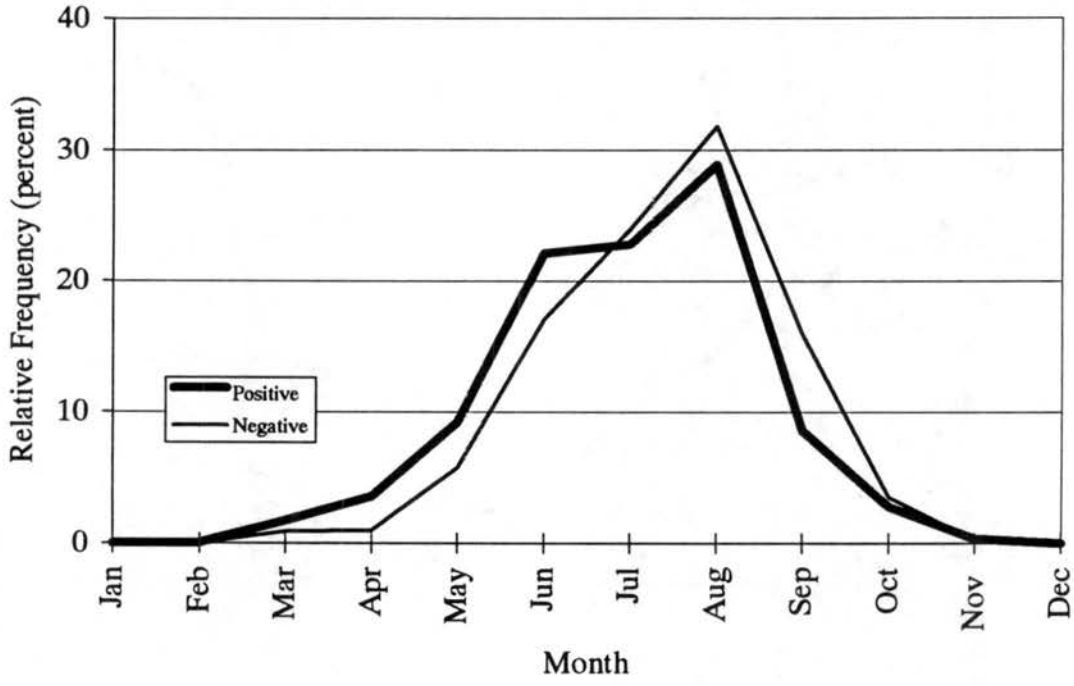

Figure 4.1 Annual marches of normalized monthly positive and negative CG flash count for KFSD, averaged over 1994–96.

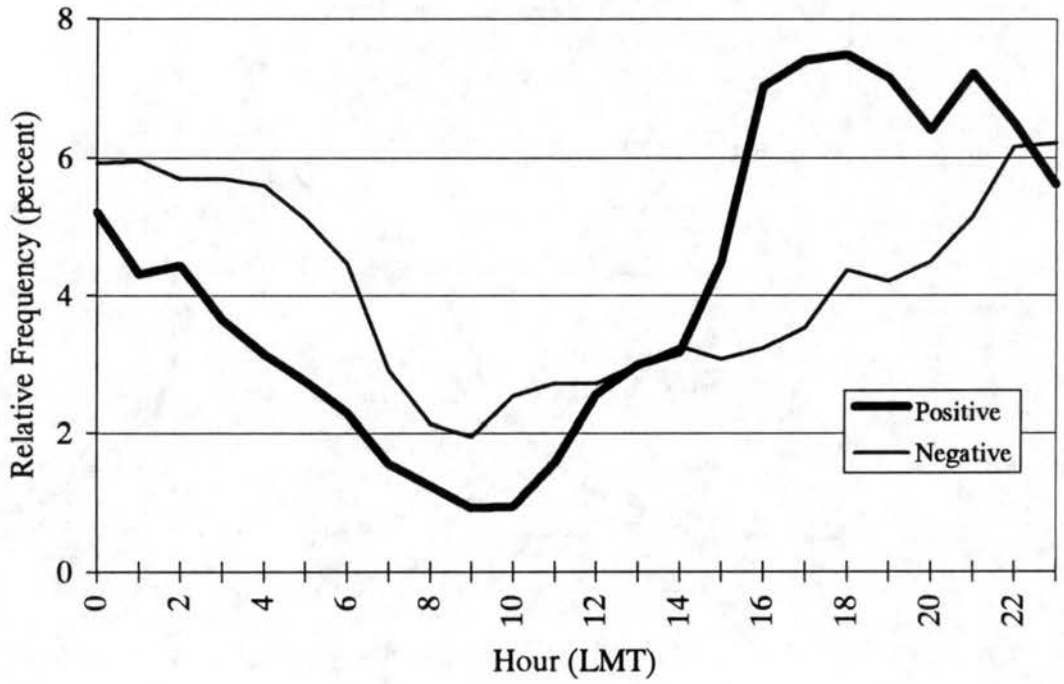

Figure 4.2 Diurnal marches of normalized hourly positive and negative CG flash count for KFSD, averaged over June–August 1994–96.

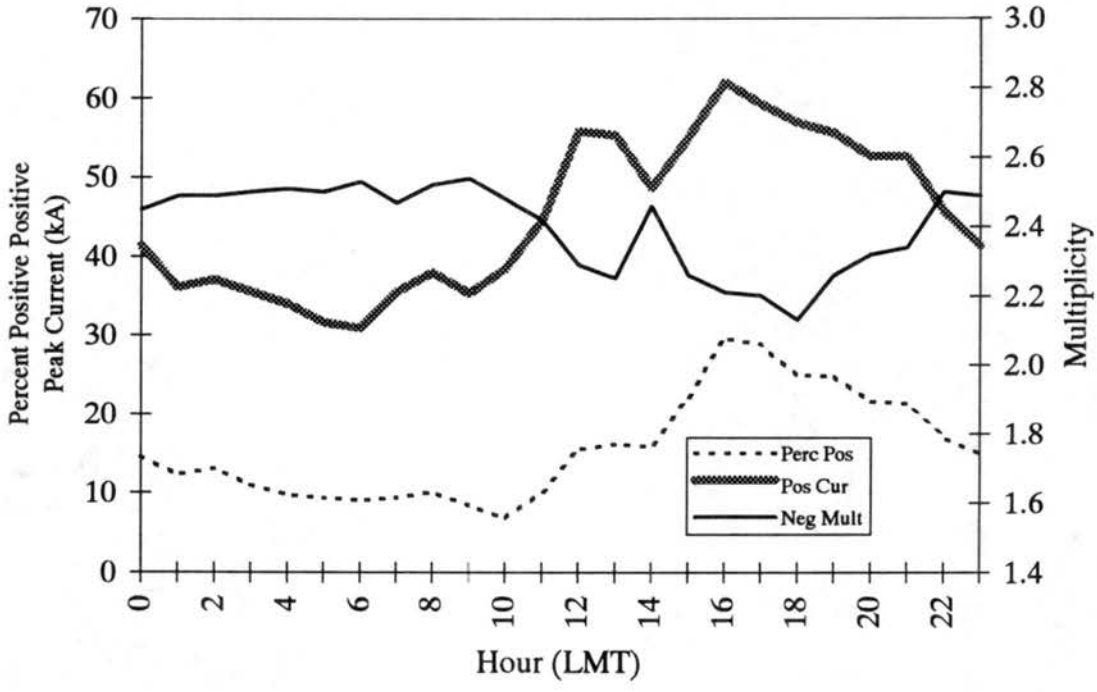

Figure 4.3 Diurnal marches of hourly percent positive polarity, hourly mean positive peak current, and hourly mean negative multiplicity for KFSD, averaged over June–August 1994–96.

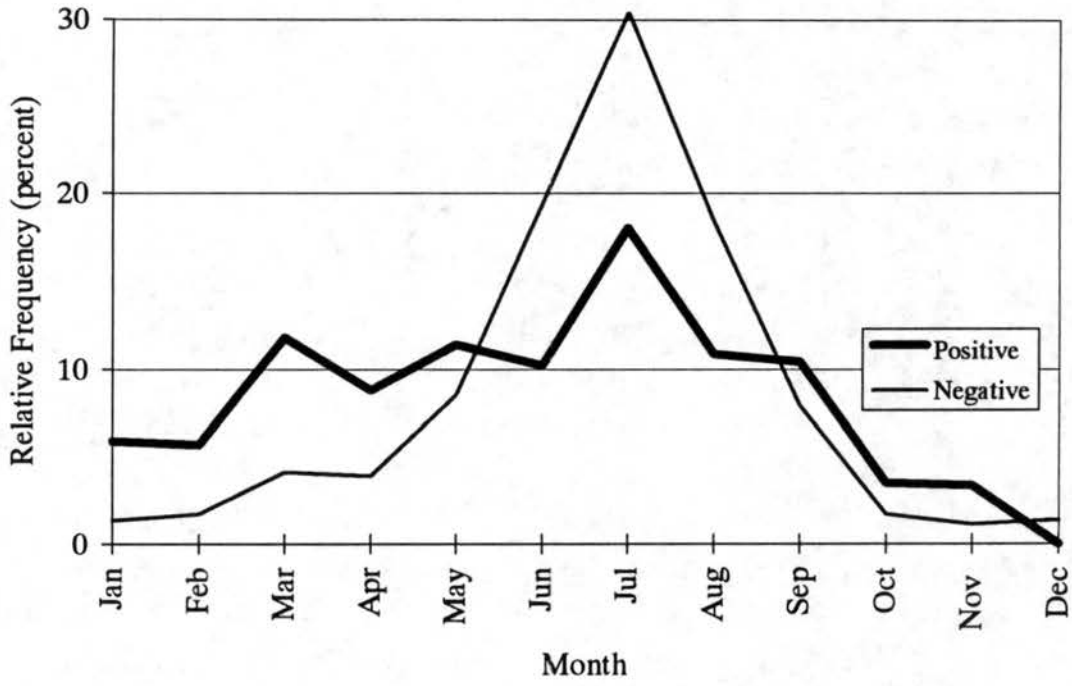

Figure 4.4 Annual marches of normalized monthly positive and negative CG flash count for KEOX, averaged over 1994–96.

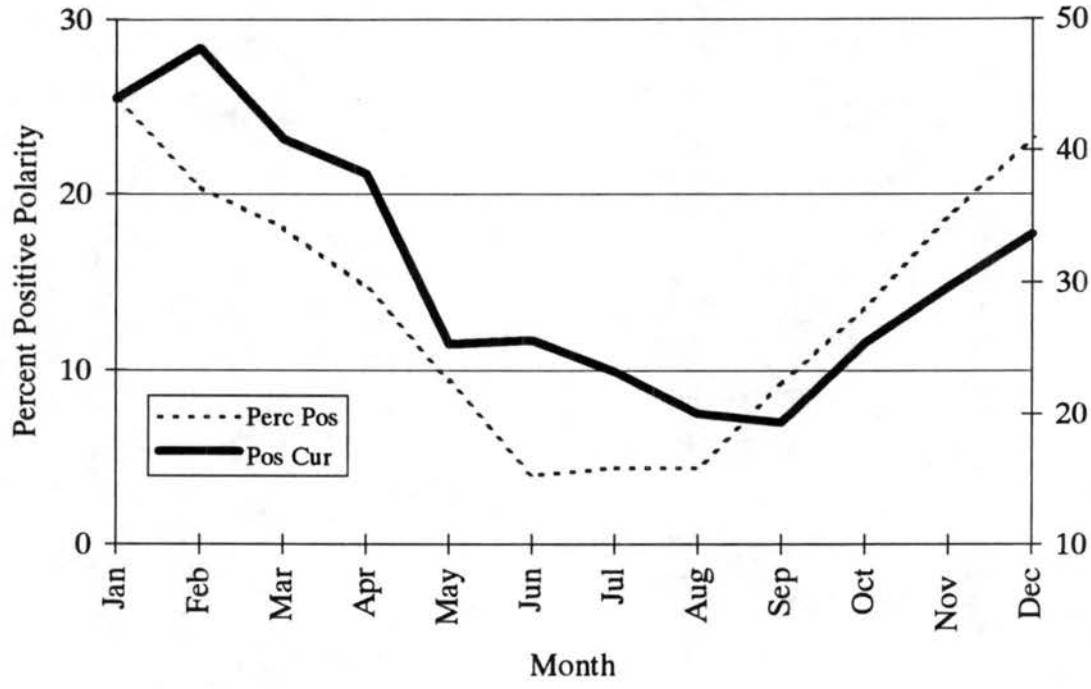

Figure 4.5 Annual marches of monthly percent positive polarity and monthly mean positive peak current for KEOX, averaged over 1994–96.

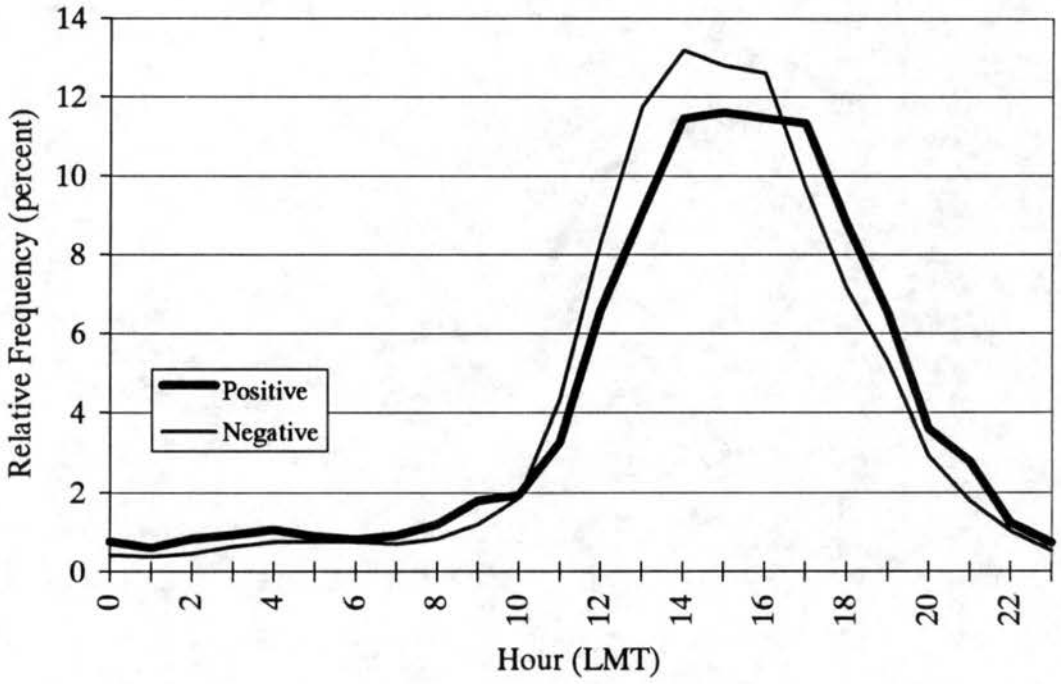

Figure 4.6 Diurnal marches of normalized hourly positive and negative CG flash count for KEOX, averaged over June–August 1994–96.

CHAPTER 5

CONCLUSIONS

We have documented the spatial and temporal variations of CG lightning activity over the contiguous U.S. from 1995–97. We have also examined the production of positive CG lightning over two case study areas located in the north-central U.S. and along the Gulf Coast. We summarize our main findings and make suggestions for future research.

1) Surface features such as elevated and depressed terrain, coastlines, and the Gulf Stream appear to control the location, magnitude, daily frequency, and timing of CG lightning activity. Maps of annual CG flash density, annual positive CG flash density, annual CG lightning days, and the normalized amplitude and phase of the diurnal cycle of CG lightning frequency during summer frequently show maximum located over elevated terrain in the western U.S. and over the Florida peninsula, the Gulf Coast, and the Gulf Stream.
2) Cumulative frequency distributions of daily CG flash count show a similar degree of skewness throughout the contiguous U.S.; 50% of cloud-to-ground lightning is produced on less than 15% of the days with cloud-to-ground lightning.

3) The majority of cloud-to-ground lightning is produced during summer over all areas in the contiguous U.S. with the exceptions of the south-central U.S. and the Pacific Coast.

4) Summertime cloud-to-ground lightning activity over the western and eastern U.S. is modulated by the diurnal cycle with an afternoon or early evening maximum.

5) Summertime cloud-to-ground lightning activity over the central U.S. is complex with significant longitudinal variations in daily activity. Daily CG lightning activity transitions from an afternoon regime over the western Great Plains to an afternoon-nocturnal regime over the eastern Great Plains and back to an afternoon regime over the lower Midwest and middle Mississippi Valley.

6) The percentage of positive polarity lightning reaches a minimum during summer over most areas in the contiguous U.S. with the exceptions of the northwestern and north-central U.S.

7) Three unique climatological signals are collocated over the north-central U.S.: a maximum in the percentage of positive polarity lightning, a maximum in mean positive peak current, and a region of negative time lag (i.e. negative CG lightning activity lagging positive CG lightning activity.

8) The production of positive cloud-to-ground lightning over the north-central U.S. is dominated by convective events which occur during summer and during the late afternoon and evening hours. These events comprise thunderstorms, some of which produce predominantly positive CG lightning and are likely severe (i.e. positive strike dominated storms).

9) Positive strike dominated storms exhibit unique lightning characteristics including high percent positive polarity values, high mean positive peak current values, and low mean negative multiplicity values.

10) Positive cloud-to-ground lighting is produced throughout the year over the Gulf Coast, by diurnally-forced convection during the warm season and by MCSs with areally-extensive stratiform regions during the cold season.

11) MCSs and diurnally-forced convection exhibit different lightning characteristics; MCSs (diurnally-forced convection) exhibit high (low) percent positive polarity values and high (low) mean positive peak current values.

12) A large population of low peak current positive CG flashes is observed over localized areas in the southeastern U.S. It is not known whether these flashes are real or false detections of intracloud lightning.

We believe that the most significant result of this study is our finding that positive strike dominated storms — which are usually severe —produced a significant portion of the positive CG lightning observed over the KFSD case study area during 1996. The implication of this result is that the three signals observed over the north-central U.S. in Figs. 3.12, 3.14, and 3.15 are caused by PSD storms. Results from our KFSD case study suggest that the location of these signals 1) is related to the timing, propagation, and lightning production of PSD storms and MCSs over the central U.S. and 2) represents an area over which PSD storms dominate positive lightning production. Clearly, more

research is needed to document the spatial and temporal distributions of PSD storms and to understand the nature of the signals observed over the north-central U.S.

We strongly feel that the identification of PSD storms in real-time using CG lighting data should be explored as a method for nowcasting severe weather. Scientific evidence is building that most PSD storms produce severe weather and that PSD storms produce a significant portion of severe weather over certain regions in the U.S. For example, Carey et al. (1997) found that 12, 37, 45% of large hail and tornado reports in the southern, central, and northern Great Plains, respectively, are accompanied by greater than 50% positive polarity lightning. Also, the association of PSD storms with severe weather outbreak conditions (MacGorman and Burgess 1994), long-track tornadoes (Perez et al. 1997), and F5 tornadoes (Seimon 1993) should provide further motivation for this research.

REFERENCES

Baldwin, J. L., 1973: *Climates of the United States*. U.S. Goverment Printing Office, Washington, D. C., 81.

Balling, R. C., Jr., 1985: Warm season nocturnal precipitation in the Great Plains of the United States. *J. Climate Appl. Meteor.*, **24**, 1383–1387.

Biswas, K. R., and P. V. Hobbs, 1990: Lightning over the Gulf Stream. *Geophys. Res. Lett.*, **17**, 941–944.

Blanchard, D. O., 1990: Mesoscale convective patterns of the southern High Plains. *Bull. Amer. Meteor. Soc.*, **71**, 994–1005.

Bluestein, H. B., and M. H. Jain, 1985: Formation of mesoscale lines of precipitation: severe squall lines in Oklahoma during the spring. *J. Atmos. Sci.*, **42**, 1711–1732.

——, G. T. Marx, and M. H. Jain, 1987: Formation of mesoscale lines of precipitation: Nonsevere squall lines in Oklahoma during the spring. *Mon. Wea. Rev.*, **115**, 2719–2727.

Branick, M. L., and C. A. Doswell III, 1992: An observation of the relationship between supercell structure and lightning ground-strike polarity. *Wea. Forecasting*, **7**, 143–149.

Brook, M., M. Nakano, P. Krehbiel, and T. Takeuti, 1982: The electrical structure of Hokuriku winter thunderstorms. *J. Geophys. Res.*, **87**, 1207–1215.

Carey, L. D., and S. A. Rutledge, 1997: Electrical and multiparameter radar observations of a severe hailstorm. *J. Geophys. Rev.*, accepted.

——, S. A. Rutledge, and B. A. Zajac, 1997: An investigation of the relationship between severe storm reports and positive cloud-to-ground lightning. *Eos, Trans., AGU*, **78**, Fall Meeting Suppl., No. 46.

Clodman, S., and W. Chisholm, 1996: Lightning flash climatology in the southern Great Lakes region. *Atmosphere-Ocean*, **32**, 345-377.

Cotton, W. R., and R. Anthes, 1991: *Cloud and Storm Dynamics*. Academic Press, 883 pp.

Court, A., and J. F. Griffiths, 1981: Thunderstorm climatology. *Thunderstorm Morphology and Dynamics*, University of Oklahoma Press, 9–39.

Cummins, K. L., E. A. Bardo, W. L. Hiscox, R. B. Pyle, and A. E. Pifer, 1995: A combined technology upgrade of the U.S. national network. *Presented at the Intl. Aerospace & Ground Conference on Lightning and Static Electricity*, Williamsburg, VA.

—, —, —, —, and —, 1995: A combined TOA/MDF technology upgrade of the U.S. national network. Proceedings, 10th International Conference on Atmospheric Electricity, Osaka, Japan, 288–292.

Curran, E. B., and W. D. Rust, 1992: Positive ground flashes produced by low-precipitation thunderstorms in Oklahoma on 26 April 1984. *Mon. Wea. Rev.*, **120**, 544–553.

Easterling, D. R., and P. J. Robinson, 1985: The diurnal variation of thunderstorm activity in the United States. *J. Climate Appl. Meteor.*, **24**, 1048–1058.

Engholm, C. D., E. R. Williams, and R. M. Dole, 1990: Meteorological and electrical conditions associated with positive cloud-to-ground lightning. *Mon. Wea. Rev.*, **118**, 470–487.

Fritsch, J. M., R. J. Kane, and C. R. Chelius, 1986: The contribution of mesoscale convective weather systems to the warm-season precipitation in the United States. *J. Climate Appl. Meteor.*, **25**, 1333–1345.

Fuquay, D. M., 1982: Positive cloud-to-ground lightning in summer thunderstorms. *J. Geophys. Res.*, **87**, 7131–7140.

Geertz, B., 1996: A radar-based survey of the characteristics of mesoscale convective systems in the southeastern USA. Preprints, 28th Conf. on Radar Meteorology, Amer. Meteor. Soc., Austin, Texas, 485–486.

Goodman, S. J., and D. R. MacGorman, 1986: Cloud-to-ground lightning activity in mesoscale convective complexes. *Mon. Wea. Rev.*, **114**, 2320–2328.

Graham, B. L., R. L. Holle, and R. E. Lopez, 1997: Lightning detection and data use in the United States. *Fire Management Notes*, **57**(2), 4–9.

Holle, R. L., A. I. Watson, R. E. Lopez, D. R. MacGorman, R. Ortiz, and W. D. Otto, 1994: The life cycle of lightning and severe weather in a 3–4 June 1985 PRE-STORM mesoscale convective system. *Mon. Wea. Rev.*, **122**, 1798–1808.

Houze, R. A., Jr., B. F. Smull, and P. Dodge, 1990: Mesoscale organization of springtime rainstorms in Oklahoma. *Mon. Wea. Rev.*, **118**, 613–654.

Kane, R. J., 1992: Correlating lightning to severe local storms in the northeastern United States. *Wea. Forecasting*, **6**, 3–12.

Kelly, D. L., J. T. Schaefer, R. P. McNulty, C. A. Doswell III, and R.F. Abbey, Jr., 1978: An augmented tornado climatology. *Mon. Wea. Rev.*, **106**, 1172–1183.

——, ——, and C. A. Doswell III, 1985: Climatology of nontornadic severe thunderstorm event in the United States. *Mon. Wea. Rev.*, **113**, 1997–2014.

Knapp, D. I., 1994: Using cloud-to-ground lightning data to identify tornadic thunderstorm signatures and nowcast severe weather. *Natl. Wea. Dig.*, **19**, 35–42.

Lopez, R. E., and R. L. Holle, 1986: Diurnal and spatial variability of lightning activity in northeastern Colorado and central Florida during the summer. *Mon. Wea. Rev.*, **114**, 1288–1312.

——, M. W. Maier, and R. L. Holle, 1991: Comparison of the signal strength of positive and negative cloud-to-ground lightning flashes in northeastern Colorado. *J. Geophys. Res.*, **96**, 22,307–22,318.

Lyons, W. A., 1996: Sprite observations above the U.S. High Plains in relation to their parent thunderstorm systems. *J. Geophys. Res.*, **101**, 29,641–29,652.

MacGorman, D. R., and D. W. Burgess, 1994: Positive cloud-to-ground lightning in tornadic storms and hailstorms. *Mon. Wea. Rev.*, **122**, 1671–1697

Maddox, R. A., C. F. Chappell, and L. R. Hoxit, 1979: Synoptic and meso-alpha scale aspects of flash flood events. *Bull. Amer. Meteor. Soc.*, **60**, 115–123.

——, K. W. Howard, D. L. Bartels, D. M. Rodgers, 1986: Mesoscale convective complexes in the middle latitudes. Ch. 17, *Mesoscale Meteorology and Forecasting*, P.S. Ray, Ed., 793 pp.

Maier, L. M., E. P. Krider, and M. W. Maier, 1984: Average diurnal variation of summer lightning over the Florida peninsula. *Mon. Wea. Rev.*, **112**, 1134–1140.

McAnelly, R. L., and W. R. Cotton, 1989: The precipitation life cycle of mesoscale convective complexes over the central United States. *Mon. Wea. Rev.*, **117**, 784–808.

Nielsen, K. E., R. A. Maddox, and S. V. Vasiloff, 1994: The evolution of cloud-to-ground lightning within a portion of the 10–11 June 1985 squall line. *Mon. Wea. Rev.*, **122**, 1809–1817.

Orville, R. E., R. W. Henderson, and L. F. Bosart, 1983: An east coast lightning detection network. *Bull. Amer. Meteor. Soc.*, **64**, 1029–1037.

——, R. A. Weisman, R. B. Pyle, R. W. Henderson, and R. E. Orville, Jr., 1987: Cloud-to-ground lightning flash characteristics from June 1984 through May 1985. *J. Geophys. Res.*, **92**, 5640–5644.

——, R. W. Henderson, and L. F. Bosart, 1988: Bipolar characteristics revealed by lightning location in mesoscale storm systems. *Geophys. Res. Lett.*, **15**, 129–132.

——, 1990a: Peak-current variations of lightning return strokes as a function of latitude. *Nature*, **342**, 6254, 149–151.

——, 1990b: Winter lightning along the East Coast. *Geophys. Res. Lett.*, **17**, 713–715.

——, 1991a: Lightning ground flash density in the contiguous United States—1989. *Mon. Wea. Rev.*, **119**, 573–577.

——, 1991b: Calibration of a magnetic direction finding network using measured triggered lightning return stroke peak currents. *J. Geophys. Res.*, **96**, 17,135–17,142.

——, 1994: Cloud-to-ground lightning flash characteristics in the contiguous United States: 1989–1991. *J. Geophys. Res.*, **99**, 10,833–10,841.

——, and A. C. Silver, 1997: Lightning Ground Flash Density in the contiguous United States: 1992-95. *Mon. Wea. Rev.*, **125**, 631–638.

Perez, A. H., L. J. Wicker, and R. E. Orville, 1997: Characteristics of cloud-to-ground lightning associated with violent tornadoes. *Wea. Forecasting*, **12**, 428–437.

Pierce, E. T., 1955: The development of lightning discharges. *Quart. J. Roy. Meteor. Soc.*, **81**, 229–240.

Rasmusson, E. M., 1971: Diurnal variation of summertime thunderstorm activity over the United States. Tech. Note 71-4, USAF-ETAC, 12 pp.

Reap, R. M., 1986: Evaluation of cloud-to-ground lightning data from the western United States for the 1983-84 summer seasons. *J. Climate Appl. Meteor.*, **25**, 785–799.

——, and D. R. MacGorman, 1989: Cloud-to-ground lightning: climatological characteristics and relationships to model fields, radar observations, and severe local storms. *Mon. Wea. Rev.*, **117**, 518–535.

——, and R. E. Orville, 1990: The relationships between network lightning locations and surface hourly observations of thunderstorms. *Mon. Wea. Rev.*, **118**, 94–108.

——, 1994: Analysis and prediction of lightning strike distribution associated with synoptic map types over Florida. *Mon. Wea. Rev.*, **122**, 1698–1715.

Rickenbach, T. M, 1996: Convection in TOGA COARE: horizontal scale and rainfall production. Ph.D. dissertation, Dept. Atmos. Science, Colorado State U., Fort Collins.

Riehl, H., 1954: *Tropical Meteorology*. McGraw-Hill Book Company, Inc., 392 pp.

Rust, W. D., W. L. Taylor, D. R. MacGorman, and R. T. Arnold, 1981: Research on electrical properties of severe thunderstorms. *Bull. Amer. Meteor. Soc.*, **62**, 1286–1293.

——, D. R. MacGorman, 1985: Unusual positive cloud-to-ground lightning in Oklahoma storms on 13 May 1983. Preprints, 14th Conference on Severe Local Storms, American Meteorological Society, Indianapolis, Indiana, 485–486.

Rutledge, S. A., and D. R. MacGorman, 1988: Cloud-to-ground lightning activity in the 10–11 June 1985 mesoscale convective system observed during the Oklahoma–Kansas PRE-STORM Project. *Mon. Wea. Rev.*, **116**, 1393–1408.

——, C. Lu, and D. R. MacGorman, 1990: Positive cloud-to-ground lightning in mesoscale convective systems. *J. Atmos. Sci.*, **47**, 2085–2100.

Seimon, A., 1993: Anomalous cloud-to-ground lightning in an F5 tornado-producing supercell thunderstorm on 28 August 1990. *Bull. Amer. Meteor. Soc.*, **74**, 189–203.

Schuur, T. J., B. F. Smull, W. D. Rust, and T. C. Marshall, 1991: Electrical and kinematic structure of the stratiform region of trailing an Oklahoma squall line. *J. Atmos. Sci.*, **48**, 825–842.

——, 1997: An observational and modeling study of mesoscale convective system electrification. Ph.D. dissertation, Dept. Atmos. Science, Colorado State U., Fort Collins.

Stolzenburg, M., 1994: Observations of high ground flash densities of positive lightning in summertime thunderstorms. *Mon. Wea. Rev.*, **122**, 1740–1750.

Toracinta, E. R., K. I. Mohr, E. J. Zipser, and R. E. Orville, 1996: A comparison of WSR-88D reflectivities, SSM/I brightness temperatures, and lightning for mesoscale convective systems in Texas. Part I: Radar reflectivity and lightning. *J. Appl. Meteor.*, **35**, 902–918.

Williams, E. R., 1989: The tripole structure of thunderstorms. *J. Geophys. Res.*, **94**, 13,151–13,167.

——, R. Zhang, and J. Rydock, 1991: Mixed phase microphysics and cloud electrification. *J. Atmos. Sci.*, **48**, 2195–2203.

Wallace, J. M., 1975: Diurnal variations in precipitation and thunderstorm frequency over the conterminous United States. *Mon. Wea. Rev.*, **103**, 406–419.

Watson, A. I., R. E. Lopez, and R. L. Holle, 1994a: Diurnal cloud-to-ground lightning patterns in Arizona during the Southwest monsoon. *Mon. Wea. Rev.*, **122**, 1716–1725.

——, ——, and ——, 1994b: Cloud-to-ground lightning and upper-air patterns during bursts and breaks in the southwest monsoon. *Mon. Wea. Rev.*, **122**, 1726–1739.

Wilson, C. T. R., 1920: Investigations on lightning discharges and on the electric field of thunderstorms. *Philos. Trans.* A, **221**, 73–115.

Winkler, J. A., B. R. Skeeter, and P. D. Yamamoto, 1988: Seasonal variations in the diurnal characteristics of heavy hourly precipitation across the United States. *Mon. Wea. Rev.*, **116**, 1641–1658.

APPENDIX A

The 1995 National Lightning Detection Network Upgrade, Low Peak Current Positive Cloud-to-Ground Lightning, and the False Detection of Intracloud Lightning

As discussed in Sec. 2a, the National Lightning Detection Network (NLDN) underwent a network-wide upgrade in 1995 in order to 1) increase the location accuracy of CG flashes and 2) increase the detection efficiency of low peak current CG flashes down to 5 kA (Cummins et al. 1995, 1996). Results from our analysis of all CG flashes detected the network (Table A1) indicate that the upgrade did succeed in increasing the detection efficiency of low peak current CG flashes. Mean positive current values decreased from 42 kA in 1994 to 31 kA in 1995; mean negative peak current values decreased from 33 kA in 1994 to 29 kA in 1995. While changes in the populations of positive and negative CG lightning were expected to result from the upgrade, the detection of a large population of low peak current positive CG flashes over localized areas in the southeastern U.S. was not expected. Figure A1 shows that a large number of positive CG flashes with peak current values less than 7 kA were detected over localized areas in the southeastern U.S. from 1995–97. The same map for 1994 shows no areas

with flash density values greater than 0.05 flashes km^{-2}. A quantitative comparison of Fig. A1 and with Fig. 15, the map of average annual positive CG flash density for 1995–97, indicates that these low peak current positive CG flashes account for 20 to 70% of the positive CG lightning over these areas. These observations raise concern about the validity of positive CG lightning data over the southeastern U.S. It has been suggested that low peak current positive CG flashes are not real but rather false detections of intracloud lightning (e.g., Lopez et al. 1991). Some researchers have suggest using a 7 kA peak current threshold for positive CG lightning in order to eliminate the false detection of intracloud lightning (P. Krehbiel and K. Cummins, personal communication, 1997). Unfortunately, this topic is without resolution; it is not known at this time whether these low current positive CG flashes are real or are false detections of intracloud lightning.

Table A1 shows significant interannual variability in mean peak current and multiplicity values since the 1995 NLDN upgrade. We do not know whether these interannual variations are due to subsequent network modifications or due to natural variability. We are inclined to believe that these interannual variations are due to network variability.

Table A1. Annual CG lightning statistics for 1994–97. Statistics were calculated using all flashes detected by the NLDN. Peak current values are given in kiloamps. "Below Thres." refers to a 7 kA peak current threshold. See text for details.

			Positive					Negative	
Year	Total Count ($\times 10^3$)	Percent Positive Polarity	Count ($\times 10^3$)	Count Below Thres. ($\times 10^3$)	Percent Below Thres.	Mean Peak Current	Mean Multiplicity	Mean Peak Current	Mean Multiplicity
1994	21,924	5.1	1,124	11	1.0	41.9	1.32	33.2	2.82
1995	19,273	8.5	1,642	118	7.2	30.7	1.14	29.2	2.37
1996	25,877	10.0	2,583	303	11.7	26.4	1.10	26.9	2.19
1997	26,817	10.2	2,729	653	23.9	21.3	1.11	22.3	2.22
Average 1995–97	23,865	9.63	2,297	358	15.6	25.3	1.11	25.9	2.25

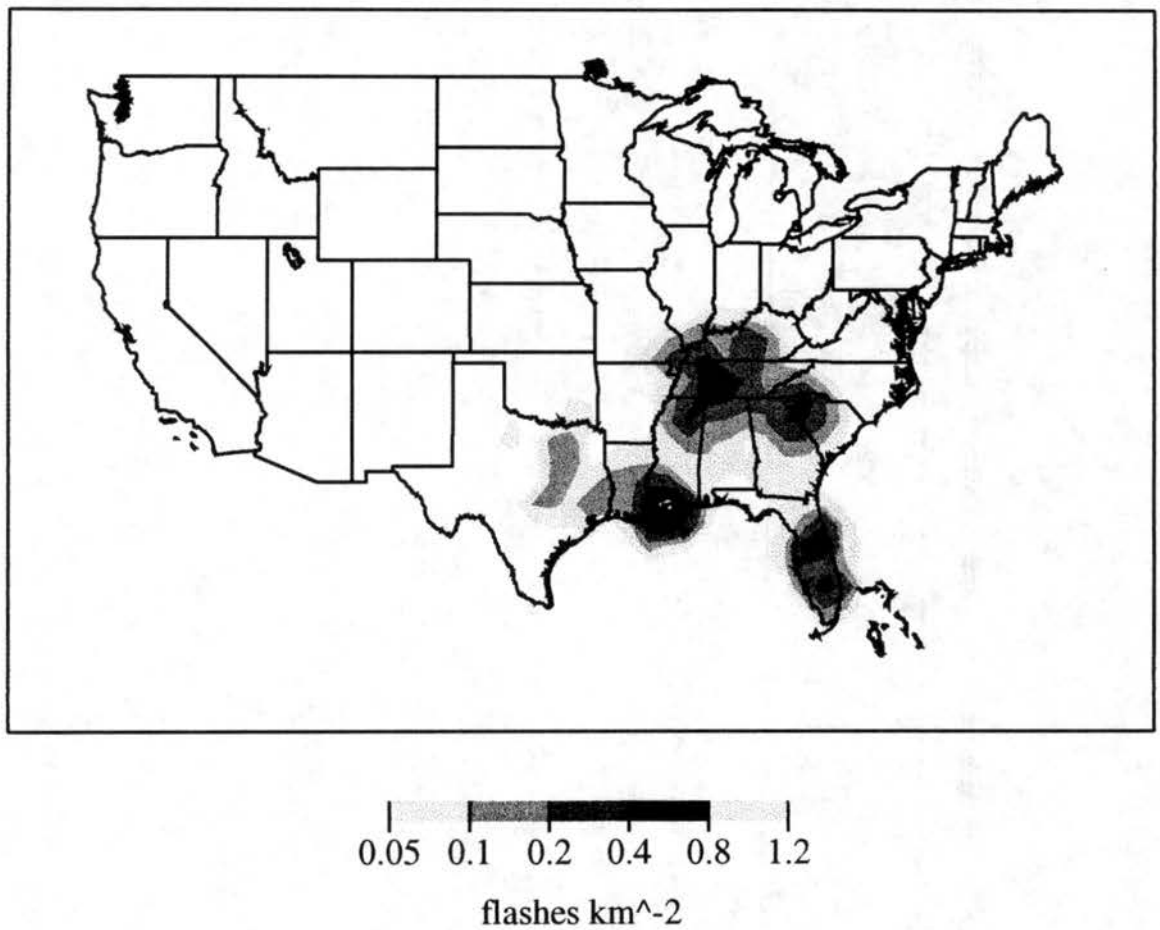

Figure A1 Annual flash density of positive CG flashes with peak current values less than 7 kA, averaged over 1995-97.

APPENDIX B

Lightning Statistics, Radar Echo Characteristics, and Positive Cloud-to-Ground Lightning Characteristics of Convective Events Sampled Over the KFSD and KEOX Case Study Areas

Tables B1 and B2 list the lightning statistics, radar echo characteristics, and positive cloud-to-ground lightning characteristics of the convective events sampled over the KFSD and KEOX case study areas during 1996, respectively. Tables B1 and B2 list the following information for each convective event:

1) Date and time of maximum positive CG lightning production
2) Lightning statistics over the lifecycle of each event
3) Radar echo classifications at the time of maximum positive CG lightning production (REC)
4) Maximum level of organizations (MLO; listed if different from REC)
5) Positive strike dominated storms at the time of maximum positive CG lightning production (PSD; Y/N)
6) Bipolar lightning patterns during the lifecycle of the convective event (BIPOLAR; Y/N)

7) Evening event or nocturnal event (EVE/NOCT; KFSD only)

The radar echo classification scheme used in this study, the time of maximum positive CG lightning production, maximum level of organization, PSD storms, and bipolar lightning patterns are described in Sec. 2d. The definition of an evening event and a nocturnal events is given in Sec. 4a.

Table B1-Part I. Lightning statistics, radar echo characteristics, and positive cloud-to-ground lightning characteristics for the 21 convective events sampled over the KFSD case study area during 1996. See text for details.

Date Time	Total Count	Percent Positive Polarity	Positive			Negative		
			Count	Mean Peak Current	Mean Multi-plicity	Count	Mean Peak Current	Mean Multi-plicity
				EVE/NOCT	REC	MLO	PSD	BIPOLAR
24 March 0415 UTC	1,882	63.4	1,193	63.6 evening	1.11 contiguous	689 MCS cluster	29.8 Y	1.43 N
19 May 0315 UTC	4,642	72.1	3,352	56.5 evening	1.09 broken line	1,290 LL/TS MCS	23.7 Y	1.57 N
1 June 0100 UTC	2,750	30.0	825	47.5 evening	1.11 line of cells	1,925 LL/TS MCS	20.5 Y	1.79 N
5 June 2300 UTC	1,612	69.0	1,112	46.5 evening	1.08 line of cells	500 LL/TS MCS	15.6 Y	1.13 N
19 June 1945 UTC	3,722	62.0	2,308	61.6 evening	1.17 isolated cells	1,414 ——	15.1 Y	1.22 N
20 June 0330 UTC	3,168	67.4	2,135	62.3 evening	1.19 isolated cells	1,033 MCS cluster	18.8 Y	1.49 N
20 June 1230 UTC	1,076	52.5	565	39.9 nocturnal	1.10 cluster of cells	511 MCS cluster	23.4 Y	2.14 N
21 June 0545 UTC	26,117	10.0	2,602	23.7 nocturnal	1.07 MCS cluster	23,515 ——	23.3 N	2.25 Y
1 July 0800 UTC	2,080	5.1	107	23.8 nocturnal	1.05 broken line	1,973 cluster of cells	19.3 N	2.05 N
1 July 2245 UTC	5,289	19.6	1,036	53.6 evening	1.10 broken line	4,253 ——	20.4 Y	2.07 N
6 July 1330 UTC	6,066	10.3	623	21.1 nocturnal	1.07 broken line	5,443 ——	22.4 N	2.59 N
17 July 0515 UTC	19,555	10.7	2,095	24.3 nocturnal	1.07 LL/TS MCS	17,460 ——	23.1 N	2.15 Y
4 August 1030 UTC	21,522	8.1	1,733	21.8 nocturnal	1.11 MCS cluster	19,789 ——	23.2 N	2.34 Y

Table B1-Part II.

Date Time	Total Count	Percent Positive Polarity	Positive			Negative		
			Count	Mean Peak Current	Mean Multi-plicity	Count	Mean Peak Current	Mean Multi-plicity
				EVE/NOCT	REC	MLO	PSD	BIPOLAR
5 August 0130 UTC	24,566	10.6	2,592	31.5 evening	1.09 LL/TS MCS	21,974 ——	27.6 N	2.37 Y
7 August 0030 UTC	12,314	50.6	6,232	60.5 evening	1.19 contiguous	6,082 LL/TS MCS	18.0 Y	1.54 Y
19 August 1215 UTC	5,703	15.0	855	18.7 nocturnal	1.07 contiguous	4,848 ——	28.3 N	2.74 N
22 August 0200 UTC	3,306	23.4	775	50.3 evening	1.14 broken line	2,531 LL/TS MCS	19.9 Y	1.71 N
26 August 0700 UTC	4,026	22.6	909	40.4 nocturnal	1.12 broken line	3,117 MCS cluster	25.9 Y	2.05 N
3 September 0245 UTC	1,248	43.5	543	41.2 evening	1.11 broken line	705 ——	20.5 Y	2.07 N
3 September 0600 UTC	13,839	8.8	1,215	22.4 nocturnal	1.09 cluster of cells	12,624 MCS cluster	25.1 N	2.59 Y
17 October 0115 UTC	9,157	17.7	1,617	43.8 evening	1.08 LL/TS MCS	7,540 ——	22.2 Y	2.05 Y

Table B2-Part I. Lightning statistics, radar echo characteristics, and positive cloud-to-ground lightning characteristics for the 25 convective events sampled over the KEOX case study area during 1996. See text for details.

Date Time	Total Count	Percent Positive Polarity	Positive			Negative		
			Count	Mean Peak Current	Mean Multiplicity	Count	Mean Peak Current	Mean Multiplicity
					REC	MLO	PSD	BIPOLAR
27 January 0145 UTC	7,320	32.5	2,376	37.0	1.12 LL/TS MCS	4,944 ——	29.4 N	2.07 Y
2 February 1700 UTC	4,997	40.9	2,042	48.0	1.16 LL/TS MCS	2,955 ——	32.0 N	2.12 Y
20 February 0015 UTC	7,942	25.6	2,032	47.0	1.10 MCS cluster	5,901 ——	31.7 N	2.03 Y
6 March 1115 UTC	9,808	21.4	2,096	21.9	1.12 MCS cluster	7,712 ——	32.4 N	2.48 Y
7 March 0500 UTC	8,467	23.4	1,983	28.1	1.10 LL/TS MCS	6,484 ——	25.0 N	2.17 Y
25 March 1530 UTC	11,356	15.6	1,769	45.5	1.10 LL/TS MCS	9,587 ——	29.8 N	2.03 Y
30 March 1115 UTC	8,264	20.7	1,713	49.1	1.08 LL/TS MCS	6,551 ——	34.0 N	2.11 Y
15 April 0530 UTC	11,996	20.0	2,397	45.4	1.07 LL/TS MCS	9,599 ——	26.7 N	1.99 Y
29 April 1345 UTC	1,566	23.2	363	24.0	1.22 contiguous	1,203 ——	23.2 N	2.67 N
29 April 2230 UTC	15,137	17.8	2,690	25.6	1.07 LL/TS MCS	12,447 ——	25.5 N	2.15 Y
24 May 2115 UTC	21,633	8.8	1,892	18.6	1.08 isolated cells	19,741 ——	22.0 N	2.16 N
28 May 1245 UTC	17,367	20.8	3,617	23.7	1.10 LL/TS MCS	13,750 ——	26.9 N	2.35 Y

Table B2-Part II.

Date Time	Total Count	Percent Positive Polarity	Positive			Negative		
			Count	Mean Peak Current	Mean Multi-plicity	Count	Mean Peak Current	Mean Multi-plicity
					REC	MLO	PSD	BIPOLAR
17 July 1900 UTC	17,344	7.6	1,312	16.1	1.13 short-lived line	16,032 ——	24.3 N	2.50 N
25 July 0045 UTC	10,147	5.8	583	20.9	1.07 broken line	9,564 ——	23.2 N	2.24 N
25 July 2045 UTC	13,376	8.3	1,114	25.6	1.11 short-lived line	12,262 ——	30.4 N	2.48 N
8 August 2345 UTC	13,922	8.0	1,113	15.4	1.11 isolated cells	12,809 ——	26.2 N	2.40 N
9 August 2200 UTC	17,531	5.3	932	16.9	1.12 isolated cells	16,599 ——	24.4 N	2.46 N
3 September 0315 UTC	4,566	22.7	1,035	14.3	1.11 contiguous	3,531 MCS cluster	27.9 N	2.87 Y
3 September 2230 UTC	4,815	15.8	762	12.2	1.08 isolated cells	4,053 ——	26.0 N	2.67 N
16 September 1830 UTC	6,170	16.3	1,005	15.4	1.11 short-lived line	5,165 ——	34.2 N	2.81 N
16 September 2315 UTC	4,089	37.7	1,541	12.9	1.19 contiguous	2,548 ——	22.1 N	2.69 N
17 September 0615 UTC	1,760	43.6	767	18.4	1.13 broken line	993 ——	36.5 Y	2.97 N
17 September 2030 UTC	1,600	40.1	641	13.9	1.06 contiguous	959 ——	31.8 N	2.51 N
8 November 0300 UTC	4,636	22.6	1,033	13.9	1.13 LL/TS MCS	3,587 ——	25.3 N	2.68 N

Table B2-Part III.

Date Time	Total Count	Percent Positive Polarity	Positive Count	Positive Mean Peak Current	Positive Mean Multiplicity	Negative Count	Negative Mean Peak Current	Negative Mean Multiplicity
					REC	MLO	PSD	BIPOLAR
1 December	3,260	32.2	1,051	39.7	1.18	2,209	29.0	2.43
1230 UTC					LL/TS MCS	——	N	Y